UNIVERSIDADE DE LISBOA
FACULDADE DE CIÊNCIAS
QUÍMICA E BIOQUÍMICA

Importance of Anoctamins for Calcium Signalling in Different Cellular Localizations

Ana Fragoso Amado Faria Fonseca

Mestrado em Bioquímica
Bioquímica Médica

Dissertação orientada por:
Prof. Dr. med. Karl Kunzelmann, Prof. Dr. Margarida Amaral

2016

ACKNOWLEDGEMENTS/AGRADECIMENTOS

I would first like to offer my sincerest gratitude to my supervisors, Prof. Karl Kunzelmann and Prof. Margarida Amaral, who provided me the wonderful opportunity to conduct my thesis research at the University of Regensburg, when I least expected, opening a new project for me to work on. I want to thank Prof. Karl Kunzelmann for his immense knowledge and Prof. Margarida for her support.

I am particularly grateful for the incredible help given by Prof. Rainer Schreiber during this whole year, for all his meaningful advices, constructive suggestions, vast expertise and a lot of patience. I also want to thank Ji, for helping me every time I needed.

A special thanks goes to Inês for her enthusiastic encouragement and positivity in the laboratory, for all the great microscopy tricks she taught me in the 'dark room' and also for showing how to throw a great party! I also want to thank all the girls in the lab for their support: Kip for always being so kind and for teaching me how to write my name in *thai*!, Gam for her kindness also, pointing out her particular sense of humor ('nope!'), Robbie for her great friendship and comfort (a big hug from your 'Anina'!), and finally Joana, who we met later on, but was also a good friend and nice companion for all the coffees and when biking late. I want to truly thank you all for everything, all days and nights we spent together, all the wonderful moments we shared! During the everyday life but also for all the cheerful dinners and parties! This was such an incredible experience which all of you helped turning even greater!

Assistance provided by all our technicians Briggitte, Patricia, Tini, Susi and Silvia, was truly appreciated, who would ease our lives and brighten up our days!

Um obrigada enorme á minha família por todo o apoio, motivação e pensamento positivo! Aos meus pais e à minha irmã, pelo amor incondicional, boa disposição e jantares em família! Às minhas avós, aos meus tios e aos meus primos pelo carinho, alegria e entusiasmo! Muito obrigada a todos por me acompanharem nesta etapa e por me ajudarem a crescer!

Obrigada Filipa pela tua amizade inabalável, por me teres incentivado a agarrar esta oportunidade, por me apoiares todos os dias, por todos os momentos incríveis que partilhamos onde quer que estivéssemos, por todas as aventuras, cervejas, músicas, companhia e muitas gargalhadas! Á Ana por todo o carinho e por ter sempre uma palavra amiga para dizer! Obrigada a todos os meus amigos que me apoiaram ao longo deste ano, que mesmo estando longe me puseram sempre um sorriso na cara!

This was a really valuable experience, with all the ups and downs of life itself, for which I want to thank everyone involved, not only in scientific and technical terms but also for helping me become a better person and a better scientist! Thank you everyone!

SUMMARY

Calcium signalling is a ubiquitous cellular mechanism responsible for the regulation of numerous biological processes. Ca^{2+} acts as a second messenger capable of activating a particular family of proteins named Ca^{2+}-activated chloride channels (CaCCs), of which anoctamins (ANOs/TMEM16) constitute the main components.

Anoctamins are expressed in several cells and their absence is related to numerous diseases, however their precise function is not fully understood. Curiously, it was recently suggested that these channels might modulate intracellular Ca^{2+} signalling. Indeed, ANO1 supports Ca^{2+}-dependent Cl^- secretion in the intestine by facilitating [Ca^{2+}] increase, acting as a counterion channel or tethering the endoplasmic reticulum (ER) to the plasma membrane (PM). Similar PM-ER contacts were reported for the yeast anoctamin homologue Ist2 and ANO1 in dorsal root ganglia. The ANO4 function is still unknown, but in this work there is evidence that this channel might alter the ER store filling.

The primary cilium is a small hair-like structure that protrudes from the cell membrane, specialized in several signalling pathways, including Ca^{2+} signalling. This organelle is virtually present in every mammalian cell, developing when cells enter a quiescent differentiated state. Remarkably, anoctamins were found in this compartment, where they might play important roles. Particularly, ANO6 is involved in apoptosis-dependent cyst lumen formation in MDCK cells, being highly expressed in apoptotic epithelial cells from human polycystic kidneys. Moreover, ANO1 Cl^- currents in the primary cilium are extremely important to promote ciliogenesis.

Genetically encoded Ca^{2+} indicators for optical imaging (GECOs) offer great advantages towards common Ca^{2+} dyes, since they allow better spatial and temporal resolution of the fluorescence signals. Therefore, two different domain targeting GECOs were used to study the effect of anoctamins in compartmentalized Ca^{2+} signalling close to the PM or the primary cilium. ANO1 and ANO4 overexpressing cells were stimulated with different compounds and measured either with a global cytosolic Ca^{2+} dye (Fura-2) or with a PM-targeted green fluorescent protein (GFP)-based Ca^{2+} indicator (PM-GCaMP2). ANO1 increased the Ca^{2+} response close to the PM, similarly to Ist2 and nhTMEM16 overexpressing cells, whereas ANO4 decreased the intracellular Ca^{2+} response. Additionally, cell lines stably expressing ciliary-targeting GECOs were developed and initial ciliary Ca^{2+} measurements were performed, using different channel inhibitors. Cellular localization studies revealed that the sensor is present in the primary cilium, but also in the PM or other intracellular membranes. The sensor was able to detect ciliary and cytosolic Ca^{2+} changes simultaneously, however the inhibitors did not allow a clear understanding of the signalling processes.

This work gives new insights on Ca^{2+} modulation by anoctamins in different microdomains, namely the PM and primary cilium. It is possible that some of these channels act as tethering proteins increasing Ca^{2+} on the membrane, while others might induce Ca^{2+} leakage from the ER or inhibit the sarco-endoplasmic ATPase (SERCA) pump. Still, in the primary cilium their role so far is not well understood and further studies are welcomed.

Key words: Ca^{2+} signalling; anoctamins (ANOs); microdomains; primary cilium; genetically encoded Ca^{2+} indicators for optical imaging (GECOs).

RESUMO

A sinalização pelo cálcio (Ca^{2+}) é um mecanismo celular ubíquo, responsável pela regulação de inúmeros processos biológicos. Tais mecanismos incluem respostas rápidas a processos como a contração, secreção e fertilização, enquanto uma regulação por resposta mais prolongada pode induzir a morte celular por apoptose ou necrose. Este ião executa a sua função reguladora, atuando como um mensageiro secundário quando mobilizado de fontes internas, o retículo endoplasmático (RE) e o sarcoplasmático (RS), ou do meio exterior, através do influxo de Ca^{2+} para a célula.

As células mantêm um apertado controlo dos níveis de Ca^{2+}, sendo que a concentração intracelular em repouso é cerca de 100 nM, ao passo que a concentração extracelular pode atingir os 2 mM. Estas são ativadas por um estímulo, como por exemplo o nucleótido trifosfato de adenosina (ATP), aumentando o Ca^{2+} no citosol para ~1 µM. De forma simplificada, o ATP ativa a via do inositol 1,4,5-trifosfato/diacilglicerol (IP_3/DAG), através da ligação a recetores acoplados a proteínas G (GPCRs), como o recetor purinérgico $P2Y_2$, que levam à libertação de IP_3 e DAG após clivagem do fosfatidilinositol 4,5-bisfosfato (PIP_2) na membrana. Consequentemente, o IP_3 difunde até aos respetivos recetores no retículo endoplasmático, promovendo a libertação de Ca^{2+} das reservas internas.

A homeostase do Ca^{2+} é mantida por diversos componentes, nomeadamente, canais responsáveis pelo influxo de Ca^{2+} sensíveis à despolarização da membrana, a recetores ou à diminuição do conteúdo em Ca^{2+} das reservas ('*stores*') do RE. O reabastecimento destas reservas é um processo importante denominado '*store-operated* Ca^{2+} *entry*' (SOCE), que envolve as proteínas 'st*romal*-i*nteracting* m*olecule 1*' (STIM1) e Orai1, bem como canais de potencial transitório ativados por recetor (TRP). A interação entre estes componentes permite a entrada de Ca^{2+} na célula, após a sua libertação para o citosol devido à ação dum determinado estímulo. O excesso de Ca^{2+} no citoplasma é removido para o meio extracelular pela bomba ATPase de Ca^{2+} da membrana plasmática (PMCA) e canais de antiporte de sódio (Na^+)/Ca^{2+} (NCX), mas também é reposto no retículo pela ação da ATPase de Ca^{2+} sarco-endoplasmática (SERCA).

A ação do Ca^{2+} tem a capacidade de ativar uma família particular de proteínas, os canais de cloreto (Cl^-) ativados pelo cálcio ('*Ca^{2+}-activated Cl^- channels*' – CaCCs), dos quais as anoctaminas são os principais componentes. As anoctaminas constituem uma família de dez proteínas (ANO1-10/TMEM16A-K), das quais alguns membros são canais aniónicos relativamente não seletivos. Estas são expressas em vários tipos de células, tais como neurónios, células epiteliais, oócitos e células do músculo esquelético e liso. As anoctaminas participam em muitos processos fisiológicos, incluindo a secreção de Cl^-, excitação neuronal e cardíaca, bem como na regulação de volume celular. Até à data apenas a ANO1, -2 e -6 demonstraram verdadeiramente mediar correntes CaCC, sendo que a ANO6 constitui também uma scramblase ativada por Ca^{2+}. A sua função exata é ainda incerta, mas devido ao número crescente de doenças associadas a mutações nos genes das anoctaminas, estas têm despertado o interesse dos investigadores.

Recentemente, foi determinada a estrutura cristalina de um homólogo das anoctaminas do fungo *Nectria haematococca* (nhTMEM16), revelando que estas são constituídas por homodímeros de 10 hélices-α transmembranares em cada subunidade. Esta descoberta permitiu o desenvolvimento de um modelo estrutural das anoctaminas, onde é proposto que o poro seja formado parcialmente de proteína e lípidos.

Curiosamente, foi sugerido recentemente que estes canais, para além de serem ativados pelo Ca^{2+}, poderão também desempenhar um papel de moduladores da sinalização de Ca^{2+} intracelular.

Esta nova propriedade das anoctaminas foi recentemente reportada em murganhos transgénicos condicionais para ANO1 no intestino, onde se observou que a secreção de Cl^- dependente do Ca^{2+} se encontrava ausente e a sinalização pelo Ca^{2+} estava muito reduzida. Neste órgão, é possível que a ANO1 auxilie na sinalização de Ca^{2+}, atuando como um canal de contra iões ('*counterion channel*'), facilitando o influxo ou a libertação de Ca^{2+} ao equilibrar as cargas aquando do transporte de Cl^-. Alternativamente, a ANO1 poderá desempenhar uma função de ancoragem ('*tethering*') do RE à membrana plasmática (MP), ativando canais de potássio (K^+) ativados pelo Ca^{2+}. Esta sugestão resulta de funções de ancoragem terem sido reportadas para a proteína de levedura Ist2, homóloga das anoctaminas, a qual estabelece pontos de contacto entre a MP e o RE, bem como para a ativação preferencial da ANO1 através da libertação de Ca^{2+} em gânglios da raiz dorsal. A função da ANO4 é ainda desconhecida, mas neste trabalho apresentam-se evidências que suportam uma possível função na modulação da reposição dos níveis de Ca^{2+} no RE.

O cílio primário é uma estrutura semelhante a um pequeno cabelo que se estende a partir da membrana celular, especializado em diversas vias de sinalização, incluindo a sinalização de Ca^{2+} e vias de desenvolvimento embrionário. Este organelo está presente virtualmente em todas as células de mamíferos, tanto epiteliais, por exemplo células do túbulo renal, como não epiteliais, nomeadamente, condrócitos, fibroblastos e neurónios. O cílio primário possui um citoesqueleto constituído por vários microtúbulos e desenvolve-se quando as células entram num estado diferenciado quiescente. Este processo tem o nome de ciliogénese, durante o qual canais e recetores são transportados para a membrana ciliar.

Neste organelo, a sinalização de Ca^{2+} constitui uma via central responsável pela sensação mecânica ('*mechanosensation*'), que ocorre no epitélio do túbulo renal. Os cílios detetam o fluxo de urina que provoca a sua deflexão, induzindo um aumento de Ca^{2+}. A pressão causada pelo movimento de fluidos permite a entrada de Ca^{2+} no cílio, levando a um aumento de Ca^{2+} nas células adjacentes através do mecanismo de libertação de Ca^{2+} induzida pelo Ca^{2+} ('*Ca^{2+}-induced Ca^{2+}-release*' – CICR). Além destas proteínas, também se acumulam diversos canais TRP no cílio primário, bem como GPCRs, o que indica que este organelo constitui uma potencial plataforma para comunicação entre diferentes vias.

Durante muito tempo, o cílio primário foi considerado como uma estrutura rudimentar, mas a sua importância na sinalização é atualmente reconhecida devido à descoberta de diversas doenças relacionadas com defeitos no cílio. A doença do rim poliquístico é a ciliopatia mais estudada, responsável pela formação de grandes quistos cheios de líquido no túbulo renal. Esta é causada por mutações em moléculas de sinalização existentes no cílio, perturbando o processo de sensação mecânica, o que leva a uma morfogénese do tecido renal desregulada. Para além disso, mutações que provocam a formação de cílios curtos podem resultar numa rápida duplicação celular e consequente desenvolvimento de cancro.

Interessantemente, foram também encontradas anoctaminas neste compartimento celular, onde poderão desempenhar papéis importantes. Particularmente, a ANO6 está envolvida na formação do lúmen de quistos dependente da apoptose em células MDCK, sendo altamente expressa em células epiteliais apoptóticas de rins poliquísticos humanos. Além disso, a ANO1 também se localiza no cílio primário e

é extremamente importante para a ciliogénese. As correntes de Cl^- mediadas por este canal promovem a ciliogénese possivelmente através da regulação do potencial de membrana, regulação osmótica ou regulação de proteínas pelo Cl^-.

Os indicadores de Ca^{2+} geneticamente codificados para imagiologia ótica ('*Genetically encoded Ca^{2+} indicators for optical imaging*' – GECOs) oferecem grandes vantagens em comparação com as sondas de Ca^{2+} comuns, uma vez que permitem uma melhor resolução espacial e temporal dos sinais de fluorescência. Portanto, dois GECOs específicos para diferentes domínios foram usados no presente trabalho para estudar o efeito das anoctaminas na sinalização de Ca^{2+} compartimentalizada perto da MP ou do cílio primário.

A ANO1 e ANO4 foram sobreexpressas em células HeLa e HEK293, nas quais foram efetuadas medições da concentração de Ca^{2+} intracelular ($[Ca^{2+}]_i$) com uma sonda de Ca^{2+} global (Fura-2), bem como da concentração de Ca^{2+} próximo da MP ($[Ca^{2+}]_P$) com um indicador de Ca^{2+} específico de membrana (PM-GCaMP2), constituído pela proteína fluorescente verde ('*Green Fluorescent Protein*' – GFP). Estas células foram estimuladas com diferentes compostos, observando-se um aumento da $[Ca^{2+}]_P$ quando a ANO1 é sobreexpressa, de forma semelhante à sobreexpressão da Ist2 e da nhTMEM16. Por outro lado, a sobreexpressão da ANO4 diminuiu a $[Ca^{2+}]_i$.

Adicionalmente, foram desenvolvidas linhas celulares que expressam de forma estável GECOs específicos para o cílio primário e foram realizados estudos iniciais sobre os mecanismos de Ca^{2+} neste organelo, usando inibidores para diferentes canais, incluindo para as anoctaminas. Estudos de localização intracelular revelaram que o sensor está presente no cílio primário, mas também na MP e noutras membranas intracelulares. O sensor permitiu detetar alterações de Ca^{2+} no cílio e no citosol simultaneamente, no entanto os inibidores não permitiram uma compreensão clara dos processos de sinalização.

Este trabalho proporcionou novos conhecimentos acerca da modulação de Ca^{2+} pelas anoctaminas em diferentes microdomínios, nomeadamente na MP e no cílio primário. É possível que algumas destas proteínas desempenhem funções de ancoragem ('*tethering*'), aumentando a $[Ca^{2+}]_P$, enquanto outras poderão induzir o esvaziamento ('*leakage*') de Ca^{2+} do RE ou inibir a bomba ATPase de Ca^{2+} sarco-endoplasmática (SERCA). No entanto, apesar dos esforços realizados, a compreensão da sua função no cílio primário é ainda incerta e novos estudos serão necessários para a total compreensão do papel das anoctaminas nestes processos.

Palavras-chave: Sinalização de Ca^{2+}; anoctamina (ANO); microdomínios; cílio primário; Indicadores de Ca^{2+} geneticamente codificados para imagiologia ótica (GECOs).

INDEX

INDEX OF TABLES AND FIGURES

Main figures:

Appendix figures:

Appendix table:

ABBREVIATIONS

%	Percentage
$[Ca^{2+}]$	Ca^{2+} concentration
$[Ca^{2+}]_{cilium}$	Primary cilium Ca^{2+} concentration
$[Ca^{2+}]_{cyt}$	Cytoplasmic Ca^{2+} concentration of ciliated cells
$[Ca^{2+}]_{i}$	Intracellular Ca^{2+} concentration
$[Ca^{2+}]_{o}$	Extracellular Ca^{2+} concentration
$[Ca^{2+}]_{P}$	Ca^{2+} concentration close to the Plasma Membrane
⌀	Diameter
µg	Microgram (10^{-6} g)
µL	Microlitre (10^{-6} L)
µm	Micrometre (10^{-6} m)
µM	Micromolar (10^{-6} M)
5-HT	5-Hydroxytryptamine = serotonin
5HT6	5-Hydroxytryptamine (serotonin) receptor isoform 6
a.u.	Arbitrary Unit
ACA	N-(p-Amylcinnamoyl)anthranilic Acid
ANO	Anoctamin (from anion+octa)
ANOVA	Analysis Of Variance
ATP	Adenosine Triphosphate
ATPase	Adenosine Triphosphatase
bp	Base Pairs
BSA	Bovine Serum Albumin
Ca^{2+}	Calcium ions
CaCC	Ca^{2+}-Activated Cl^- Channel
CaM	Calmodulin
cAMP	cyclic Adenosine Monophosphate
CaV	Voltage gated Ca^{2+}-selective channels
CCD	Charge-Coupled Device
CCH	Carbachol
CD8	Cluster of Differentiation 8
cDNA	complementary DNA
CFTR	Cystic Fibrosis Transmembrane conductance Regulator
CICR	Ca^{2+}-induced Ca^{2+} release
Cl^-	Chloride ions
CPA	Cyclopiazonic Acid
cpEGFP	circularly permuted Enhanced GFP
cpGFP	circularly permuted GFP
CRAC	Ca^{2+}-release activated Ca^{2+}
CTS	Ciliary Targeting Sequence
d	Day
DAG	Diacylglycerol
DF	Dilution Factor
DIC	Differential Interference Contrast
DMEM	Dulbeco's Modified Eagle Medium

DMEM:F-12	Dulbecco's Modified Eagle Medium: Nutrient Mixture F-12
DNA	Deoxyribonucleic acid
DRG	Dorsal Root Ganglia
EDTA	Ethylenediamine Tetraacetic Acid
EGFP	Enhanced Green Fluorescent Protein
EGTA	Ethylene Glycol Tetraacetic Acid
ER	Endoplasmic Reticulum
F-12	Ham's F12 Nutrient Mixture
FBS	Fetal Bovine Serum
Fura-2 AM	Fura-2 acetoxymethyl (AM) ester Ca^{2+} indicator
g	Gram
G-418	Geneticin
GCaMP	GFP-based Ca^{2+} sensitive protein
GECO	Genetically Encoded Ca^{2+} sensor for Optical imaging
GFP	Green Fluorescent Protein
GPCR	G-Protein-Coupled Receptor
Gq	G protein
h	Hour
H^+	Protons
HEK293	Human Embryonic Kidney cell line
HeLa	Henrietta Lacks cervical cancer immortal cell line
Hh	Hedgehog protein/pathway
hTERT RPE-1	human Telomerase Reverse Transcriptase immortalized Retinal Pigment Epithelial cell line
IFT	Intraflagellar Transport
IgG	Immunoglobulin G
IP_3	Inositol 1,4,5-Triphosphate
IP_3R	Inositol 1,4,5-Triphosphate Receptor
K^+	Potassium ions
K_d	Dissociation constant
L	Litre
m	Metre
M	Molar
M13	Myosin light chain kinase M13 fragment
MDCK M2	Madin-Darby Canine Kidney cell line
mg	Milligram (10^{-3} g)
min	Minute
mL	Millilitre (10^{-3} L)
MLCC20	N-terminal 20 amino acids from neuromodulin
mM	Millimolar (10^{-3} M)
mm	Millimitres (10^{-3} m)
ms	Millisecond (10^{-3} s)
Na^+	Sodium ions
NCKX	Na^+/Ca^{2+}-K^+ exchanger
NCX	Na^+/Ca^{2+} exchanger
NFA	Niflumic Acid
nhTMEM16	*Nectria haematococca* transmembrane protein 16
nM	Nanomolar (10^{-9} M)

nm	Nanometres (10^{-9} m)
Ø FBS	Serum free media
ºC	Degree Celsius
Orai1	Ca^{2+}-release activated Ca^{2+} protein 1
$P2Y_2$	Purinergic GPCR purinoceptor 2
PBS	Phosphate Buffered Saline
PC	Polycystin
PCP	Planar Cell Polarity pathway
PFA	Paraformaldehyde
PIP_2	Phosphatidylinositol 4,5-bisphosphate
PKD	Polycystic Kidney Disease
PLA_2	Phospholipase A2
PLC	Phospholipase C
PM	Plasma Membrane
PMCA	Plasma Membrane Ca^{2+}-ATPase
PM-GCaMP2	Plasma Membrane targeted GFP-based Ca^{2+} sensitive protein
PS	Phosphatidylserine
R	Fluorescence ratio measured with Fura-2
Rmax	Maximum Fluorescence ratio at saturating [Ca^{2+}]
Rmin	Minimum fluorescence ratio in the absence of Ca^{2+}
ROC	Receptor-Operated Channels
rpm	rotations per minute
RT	Room Temperature
RTK	Receptor Tyrosine-Kinases
RyR	Ryanodine Receptors
s	Second
SCAN	Small-conductance Ca^{2+}-Activated Nonselective cation current
SEM	Standard Error of the Mean
SERCA	Sarco-Endoplasmic Reticulum Ca^{2+}-ATPase
Sf_2/Sb_2	Quotient between the fluorescence intensity of free and Ca^{2+}-bound Fura-2 measured at 380 nm
Smo	Smoothened protein
SOC	Store-Operated Channels
SOCE	Store-Operated Ca^{2+} Entry
SR	Sarcoplasmic Reticulum
STIM1	*st*romal-*i*nteracting *m*olecule 1
TA	Tannic Acid
TMEM16	Transmembrane protein 16
TRP	Transient Receptor Potential
UV-Vis	Ultraviolet-Visible
v/v	volume/volume
V-ATPase	Vacuolar H^+-ATPase
VGCC	Voltage-Gated Ca^{2+} Channels
V_m	Membrane potential
VOC	Voltage-Operated Channels
w/v	weight/volume
Wnt	Wingless pathway
XeC	Xestospongin C

1. INTRODUCTION

1.1. Calcium signalling machinery

Born from the stars, like any other element, calcium stands out because of its ubiquitous role in cell signalling[1,2]. Calcium ions (Ca^{2+}) are versatile intracellular messengers responsible for the regulation of a diversity of cellular processes[2]. These mechanisms include short-term responses such as contraction and secretion, as well as fertilization, proliferation and development. Long-term regulation can result in cell death trough necrosis and apoptosis[1–3].

Cells maintain a tight balance between their intracellular and extracellular Ca^{2+} levels. At rest, the intracellular Ca^{2+} concentration ($[Ca^{2+}]_i$) is around 100 nM, while the extracellular level can reach approximately 2 mM[1,2]. Upon stimulation, for example through hormones, neurotransmitters or depolarization, this level can rise to ~1 µM, activating the cells[2,3]. The elevated $[Ca^{2+}]$ triggers several cellular pathways[2], being fundamental to understand the regulation of Ca^{2+} signalling mechanisms.

The control of diverse cellular responses by Ca^{2+} is achieved by a vast collection of signalling molecules, that comprise the Ca^{2+} signalling toolkit (Figure 1.1). These components can be combined in different ways to generate signals with distinct spatial and temporal profiles, and also for crosstalk with other signalling pathways[2].

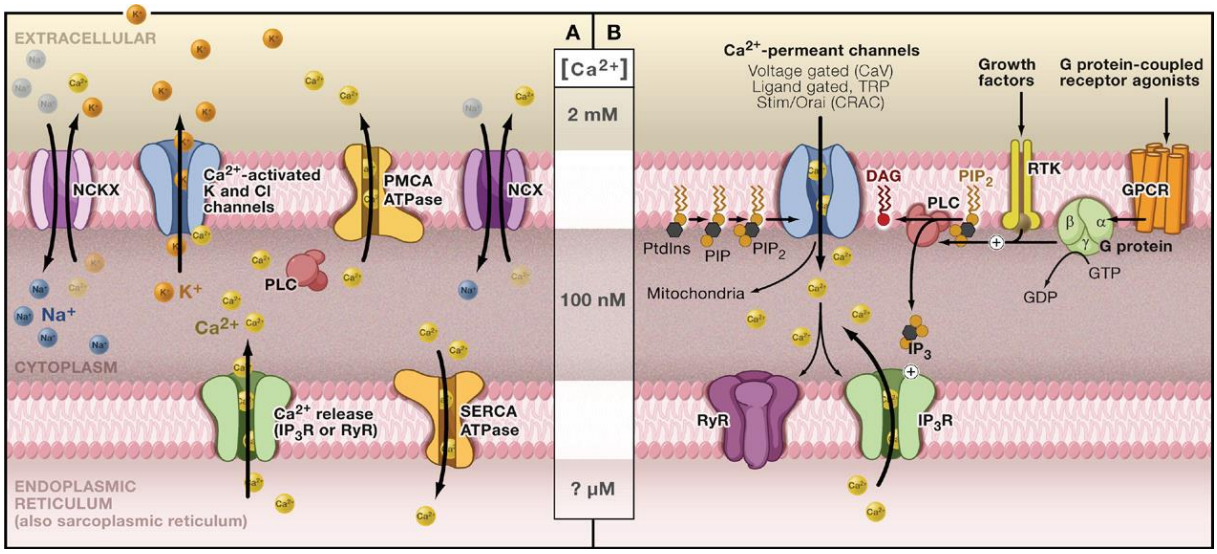

Figure 1.1 – Components of the Ca^{2+} signalling machinery. (A) In resting cells, Ca^{2+} is maintained at a low level ($[Ca^{2+}]_i$ ~100 nM) via PMCA and SERCA, that pump Ca^{2+} to the outside or to the ER/SR, respectively. In parallel, NCX and NCKX, trade Na^+ ions for Ca^{2+} ions. Intracellular Ca^{2+} can hyperpolarize cells by activating K^+ or Cl^- channels, which decreases the activity of voltage gated Ca^{2+}-selective channels (CaV), increasing the driving force across Ca^{2+}-permeant channels. **(B)** In excitable cells, plasma membrane ion channels are activated by voltage, as well as extra- or intracellular ligand binding. When open, the $[Ca^{2+}]_i$ rises to ~1 µM and can trigger more release from the ER, primarily by RyR. Activation can also occur through binding of agonists to GPCRs, for instance ATP to $P2Y_2$ receptors, or growth factors to RTKs. This triggers PLC activation, that cleaves PIP_2 into IP_3 and DAG. IP_3 later diffuses to IP_3R, liberating Ca^{2+} from internal stores. GPCRs act through Gq proteins, whereas RTKs dimerize upon ligand binding, autophosphorilate and interact with other proteins to activate PLC. Retrieved from Clapham, 2007 [1].

Cell stimulation triggers the signalling through the generation of various Ca^{2+} mobilizing signals from internal and external sources of Ca^{2+}. The endoplasmic reticulum (ER) or the equivalent organelle from muscle cells, sarcoplasmic reticulum (SR), constitute the internal Ca^{2+} stores. Release of Ca^{2+} from these stores is driven by two main channels: inositol 1,4,5-triphosphate receptors (IP_3R) and ryanodine

receptors (RyR). These channels are principally activated by Ca^{2+}, an autocatalytic process known as Ca^{2+}-induced Ca^{2+} release (CICR)[2]. Additionally, RyR can be activated by membrane depolarization, while IP_3R are specifically activated by the second messenger inositol 1,4,5-triphosphate (IP_3)[2–5].

Ca^{2+} mobilizing signals are generated when stimuli, bind to cell surface receptors, such as G-protein-coupled receptors (GPCRs)[2]. For example, when the agonist adenosine triphosphate (ATP) binds to a purinergic GPCR ($P2Y_2$)[6,7], G proteins (Gq) stimulate phospholipase C (PLC) to cleave the membrane bound phosphatidylinositol 4,5-bisphosphate (PIP_2) into IP_3 and diacylglycerol (DAG). This leads to IP_3 diffusion through the cytosol that reaches the IP_3R and releases Ca^{2+} [2,8]. Additionally, growth factor binding to receptor tyrosine-kinases (RTK) can also activate PLC to generate IP_3, initiating the Ca^{2+} signalling pathway[1].

Moreover, there are several plasma membrane (PM) channels that supply Ca^{2+} into the cytoplasm, through external Ca^{2+} entry. These include voltage-operated channels (VOCs), activated by membrane depolarization; receptor-operated channels, (ROCs), activated by extracellular ligands; and store-operated channels (SOCs), activated by store depletion. The activity of these channels leads to an intracellular Ca^{2+} rise[2].

Replenishing of internal stores is mediated by SOCs in a process termed store-operated Ca^{2+} entry (SOCE). The SOC machinery is composed by the *st*romal-*i*nteracting *m*olecule 1 (STIM1) and Orai1 proteins, which are critical subunits of the Ca^{2+}-release activated Ca^{2+} (CRAC) channels, also known as CRAC modulators[1,9–11]. The decrease in the ER [Ca^{2+}] is sensed by STIM1, that translocates to ER-PM junctional areas and associates with the Orai1 proteins, mediating Ca^{2+} entry across the PM[9]. Additionally, transient receptor potential (TRP) channels, facilitate receptor-induced Ca^{2+} influx and are also able to interact with the STIM1/Orai1 complex[1,9].

Finalized the signalling functions, the cellular resting state is restored via different pumps and exchangers that remove Ca^{2+} from the cytoplasm. Plasma membrane Ca^{2+}-ATPases (PMCA) pumps, accompanied by Na^+/Ca^{2+} exchangers (NCX) and Na^+/Ca^{2+}-K^+ exchangers (NCKX), extrude Ca^{2+} out of the cell, while sarco-endoplasmic reticulum ATPases (SERCA) pumps return it to the ER[1,2,12] (Figure 1.1).

1.2. Anoctamins – Calcium-activated chloride channels as calcium modulators

Calcium-activated chloride channels (CaCCs) are relatively non-selective anion channels characterized by activation through increases in the cytosolic [Ca^{2+}]. These channels are found in numerous cell types, including neurons, various epithelial cells, olfactory and photoreceptors, cardiac, smooth and skeletal muscle cells, leukocytes and oocytes[13,14].

CaCCs participate in many important physiological processes, including epithelial fluid secretion, sensory transduction, membrane excitability of neurons and cardiac muscle, regulation of vascular tone and oocyte fertilization[13,14]. Channel activation occurs through a $[Ca^{2+}]_i$ rise in the range of 0.2-5 µM that can come from either Ca^{2+} influx or Ca^{2+} store release. This increase can result from direct Ca^{2+} binding to the channel or it can occur indirectly via Ca^{2+} binding to enzymes or proteins[13]. Activation

can be achieved experimentally by stimulation of cells with Ca^{2+} mobilizing agonists, through Ca^{2+} ionophores such as ionomycin, by loading of cells with Ca^{2+}-containing pipette solutions and by adding Ca^{2+} to the bath solution in excised inside out patches[14].

CaCC possess a characteristic biophysical fingerprint that comprises a half-maximal [Ca^{2+}] for activation in the submicromolar range; anion-selectivity with a permeability sequence resembling the Eisenman type I sequence and a relatively poor selectivity towards cations; and time- and voltage-dependent currents with kinetics varying according to the Ca^{2+} levels[13,14].

1.2.1. Anoctamins

Anoctamins constitute a family of ten transmembrane proteins (ANO1-10/TMEM16A-K)[15–18], which function is yet not fully understood. It is speculated that all members form Ca^{2+}-activated Cl^- channels (CaCCs)[15], although only ANO1 and ANO2 are now truly considered to produce CaCC currents[19–21], as well as ANO6, that possesses another particular function as a Ca^{2+}-activated lipid scramblase[22]. This family of channels are also relatively permeable to cations[16].

These proteins are widely expressed in numerous tissues and their CaCC activity is key for several cellular processes, for example neural excitability in nociceptive sensory neurons, Cl^- secretion in airways, fluid transport in various glands, as well as olfaction and cell volume regulation[15]. Because of these central functions, mutations in the anoctamin genes have been shown to be involved in an increasing number of diseases[15,18]. The resulting pathologies include forms of muscular dystrophy, cerebellar ataxia and impaired blood clotting in a rare bleeding disorder called Scott syndrome.

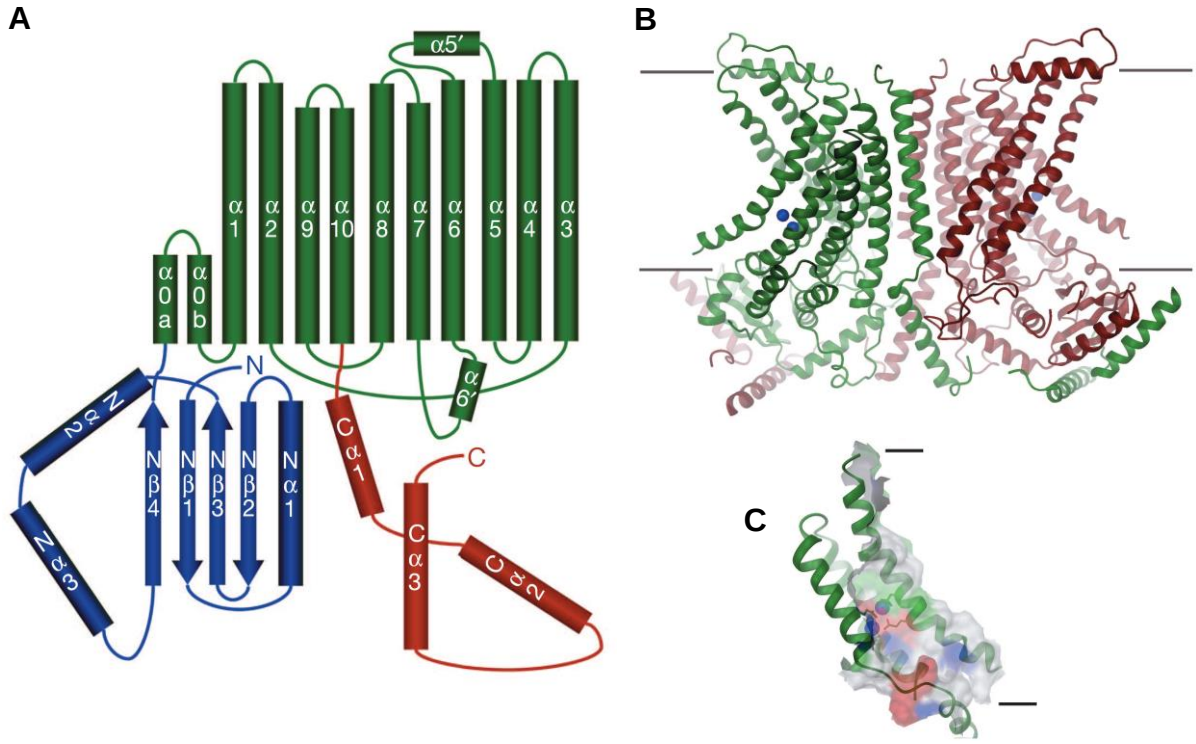

Figure 1.2 – Model of nhTMEM16 crystallographic structure. (A) Subunit topology, showing the ten transmembrane α-helices (green) and the N- and C-termini (blue and red, respectively). **(B)** Ribbon representation of the dimer within the membrane with bound Ca^{2+} ions (blue spheres). **(C)** Detail of the Ca^{2+} binding site. Adapted from Brunner *et al.*, 2014 [25].

Furthermore, upregulation of some anoctamins is linked to different types of cancer, for instance breast and prostate cancers, but also to other disorders like asthma[15,17,18].

For many years the molecular identity of CaCCs remained unknown, until 2008 when three independent groups identified ANO1 as the major component of this type of channels[20,23,24]. More recently, Brunner *et al.*[25], determined the crystal structure of the anoctamin fungal homologue from *Nectria haematococca*, nhTMEM16 (Figure 1.2). This protein operates as a Ca^{2+}-activated scramblase and consists of a homodimer with ten transmembrane α-helices in each subunit. The monomers contain a cavity exposed to the lipid bilayer, harbouring a conserved Ca^{2+} binding site in the hydrophobic core of the membrane[25]. Remarkably, this allowed Whitlock and Hartzell[26] to develop a model of the TMEM16 pore, that they hypothesize to be composed not only of protein but partly of lipids. These authors propose that anoctamins evolved from ancestral phospholipid scramblases that suffered structural changes to become Cl^- channels[26].

1.2.2. Calcium and anoctamins in membrane microdomains

Anoctamins are distributed in different intracellular regions[16,27], depending on which they may play different roles. Interestingly, recent studies indicate that the broad function of anoctamins is tightly related to their cellular localization and that, besides being activated by Ca^{2+}, these channels might also modulate intracellular Ca^{2+} signalling[27].

This has been reported in an intestinal-specific mouse knockout model for ANO1, where this channel was found to support Ca^{2+}-dependent Cl^- secretion. Electrolyte secretion in the intestinal epithelia can be activated by an increase in intracellular cyclic adenosine monophosphate (cAMP) or Ca^{2+}, promoting the opening of apical Cl^- channels[28]. Carbachol (CCH) is a cholinomimetic drug that can simulate the effect of the neurotransmitter acetylcholine, inducing the IP_3 pathway and increasing $[Ca^{2+}]_i$. Elevation of Ca^{2+} levels then triggers transient intestinal Cl^- secretion[29].

Schreiber *et al.*[28], observed that ANO1 is primarily expressed in the basolateral compartment of mouse intestinal epithelial cells. Furthermore, mice deficient for ANO1 in the intestine demonstrated a reduced CCH-induced Ca^{2+} response, which is consistent with the idea that this channel assists Cl^- secretion by facilitating $[Ca^{2+}]_i$ increase. Then, Ca^{2+} is capable of activating basolateral K^+ channels, increasing the driving force for apical Cl^- secretion, that occurs mainly through Cystic Fibrosis Transmembrane conductance Regulator (CFTR). The authors propose three possible mechanisms for the regulatory effect of ANO1 in Ca^{2+} signalling:

1) ANO1 may be localized in the ER, operating as a counterion channel and facilitating Ca^{2+} release by IP_3R.
2) ANO1 could support the activation of basolateral Ca^{2+} activated K^+ channels, tethering the basolateral ER to the PM.
3) or ANO1 could control Ca^{2+} influx indirectly, by facilitating Ca^{2+} store emptying, or as a Cl^- bypass channel[28].

Remarkably, the Ist2 protein is an anoctamin homologue from yeast identified as tethering protein. Ist2 is localized in the cortical ER and binds specific phosphoinositide lipids from the PM. The recruitment

of the ER to the PM by Ist2 occurs via its flexible C-terminus polybasic domain, comprising a cortical sorting signal, that extends from the cytosol and connects to the PM[30,31].

It was shown that anoctamins need high concentrations of Ca^{2+} for activation under physiological conditions. However, such increases in the Ca^{2+} levels are unlikely to occur in the whole cytosol, but in isolated compartments[27,32]. With this in mind, Jin and co-workers[32] discovered a preferential coupling of ANO1 to sources of intracellular Ca^{2+} signals in dorsal root ganglia (DRG) neurons. This are nociceptive sensory neurons that exhibit strong CaCC currents probably mediated by ANO1. The group was able to determine that ANO1 is selectively activated by GPCR-induced Ca^{2+} release from the ER, but not by influx through voltage-gated Ca^{2+} channels (VGCC). This is achieved by tethering of PM domains containing ANO1 and GPCRs to juxtamembrane regions of the ER though interaction with IP_3R, that are separated from the VGCCs[32].

These studies give exciting information concerning the involvement of anoctamins in compartmentalized Ca^{2+} signalling and possibly acting as tethering proteins, however a lot of questions are still unresolved and need further investigation.

1.3. Primary cilium – a specialized signalling compartment

1.3.1. Primary cilia structure and ciliogenesis

The primary cilium, as first designated by S. Sorokin[33], is an extension of the plasma membrane that acts as a solitary antenna[34,35]. Over the past century, this structure has been underestimated and regarded as rudimentary, gaining interest again as several diseases have been found to be cilia related[36].

The cilium is a conserved structure formed by a microtubule cytoskeleton called axoneme, organized in a ring of 9 doublet microtubules. It derives from a mother centriole, comprising the basal body, and is surrounded by the ciliary membrane. Primary cilia can be distinguished from motile cilia by the absence of an additional central pair of microtubules, as well as motor proteins[37].

The process of assembly and growth of cilia is called ciliogenesis and occurs during cell differentiation[37]. This takes place when cells become confluent and reach a stationary phase[35]. After successful cell division, a cell enters growth arrest in G_0 phase and starts to differentiate[35,38]. During this phase, centrioles are available for cilium formation, making ciliogenesis and mitosis mutually exclusive processes, existing a constant balance between the two mechanisms[38]. In order to re-enter the cell cycle, cells resorb their primary cilium and liberate the centrosome[35,38]. This process allows centrosome duplication and formation of the mitotic spindle during chromosomal segregation. Typically, ciliogenesis occurs either through the absence of proliferative stimuli or by cell polarization[38].

The development of the cilium occurs via intraflagellar transport (IFT)[37]. In this process, materials are transported into, along and out of the cilium, accounting for the assembly of axonemal proteins and delivery of receptors and channels to the ciliary membrane[35,37]. The primary cilium starts to grow when a Golgi-derived vesicle encapsulating a mother centriole docks to the cell membrane[36,37,39]. Fusion of additional vesicles and continuous IFT promotes the extension of the cilium and maturation of the axoneme[35,37,39]. IFT involves several motor proteins, including kinesin and dynein, that are necessary

for the anterograde and retrograde transport, respectively[35]. The former carries cargo outwards the cilium and the latter transports components back to the cell body[37,40] (Figure 1.3).

1.3.2. Signalling in the primary cilium – Calcium and development pathways

Given the features of the primary cilium, it has long been described as a specialized sensory organelle that is able to detect several chemical and mechanical stimuli[41–43]. Also, due to the regulated transport of molecules inside the cilium[39], it is natural to think that it is involved in multiple signalling pathways[38,42].

Ca^{2+} ions constitute one of the major components of primary cilia signalling, acting as secondary messengers during signal transduction in different pathways[36,38,42]. These ions are of great importance in mechanosensation, particularly in renal tubule epithelia[34,40,42]. Here, primary cilia are associated with fluid flow sensing which causes bending of the cilium[44] and induces Ca^{2+} signalling[45,46]. The shear force caused by fluid movement opens a protein complex formed by polycystin 1 and 2 (PC1 and PC2) that allows Ca^{2+} to move inside the cilium, elevating the cytosolic Ca^{2+} levels[42,47]. More specifically, PC1 acts as a receptor for cell interaction and regulates PC2, which shares homology and associates with TRP channels, functioning as an ion channel[40,48].

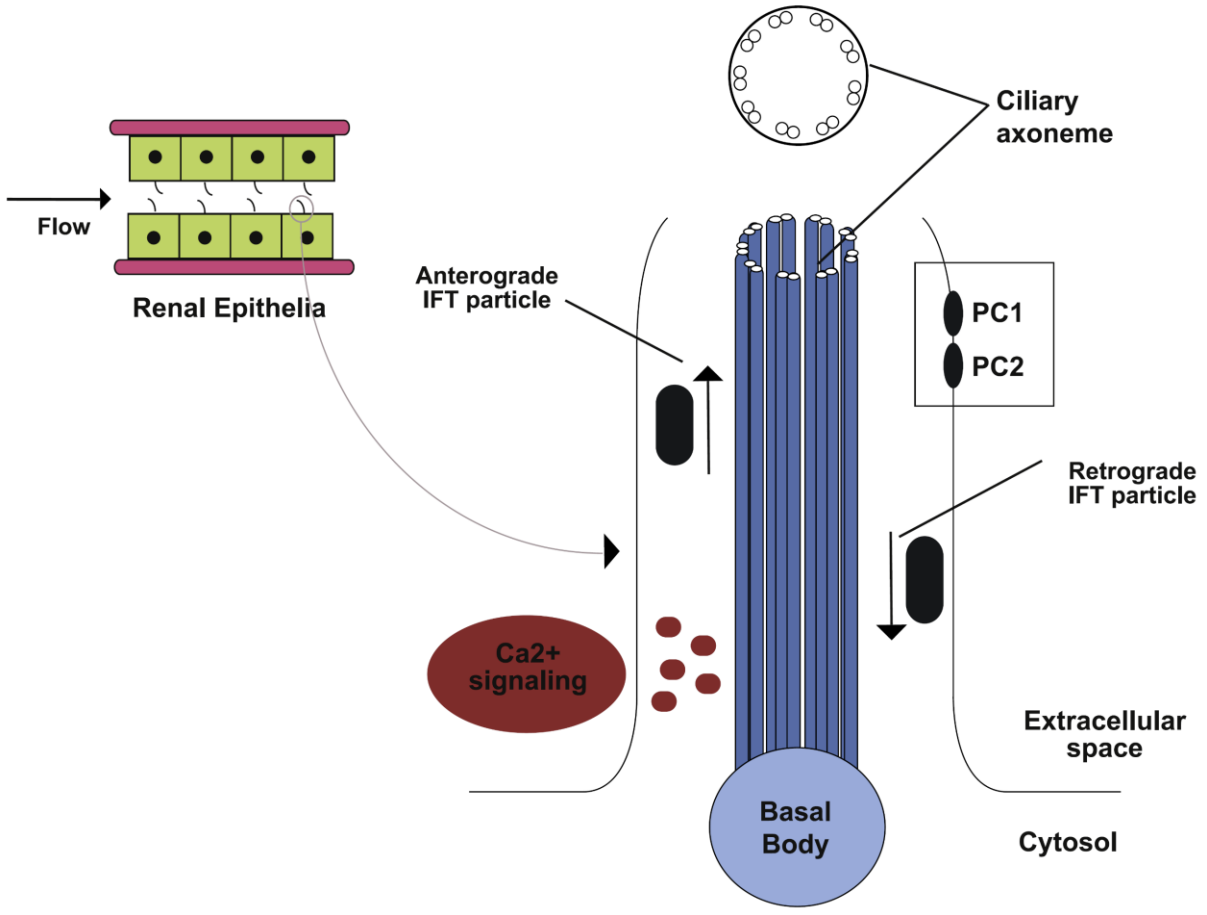

Figure 1.3 – Primary cilium structure and function. Schematic representation of the primary cilium structure showing the axoneme constituted by 9 microtubule pairs, protruding from the centriole derived basal body. This is the base for IFT, where proteins are transported via particle complexes along the cilium. PC1 and PC2 are located at the cilium and are proposed to interact in a Ca^{2+} signalling process susceptible to fluid flow. Renal tubular epithelium is illustrated in the upper left, where primary cilia are required as mechanosensors. Adapted from Lee and Somlo, 2014 [40].

The local Ca^{2+} increase through these channels triggers intraorganeollar Ca^{2+} increase in adjacent cells through CICR[45,47], which makes these proteins essential for the primary cilium as a mechanosensor[40,47]. Subsequent signal transduction leads to a number of effects in downstream processes[47], such as reabsorption of water and solutes like $NaHCO_3$, aiding in the maintenance of the glomerular tubular balance[8] (Figure 1.3).

Along with these proteins, several TRP channels accumulate inside the primary cilium, conducting Ca^{2+} ions. These channels possess multiple modes of activation, including receptor ligands, intracellular second messengers, fluid stress, swelling and even temperature or voltage, which contribute for cilium sensitivity. Consequently, the particular properties of this organelle may regulate the activity of the TRP channels, enabling specific local Ca^{2+} signalling[34].

Additionally, the primary cilium is enriched with several proteins involved in other signalling pathways, including GPCRs, for example 5-hydroxytryptamine (5-HT; serotonin) receptor isoform 6 (5HT6) and Smoothened (Smo). This indicates that the signalling strength in the primary cilium might be more robust, compared to the remaining cellular membrane. Alternatively, this compartment might constitute a specialized platform for enhanced molecular crosstalk among signalling pathways[34].

The Ca^{2+} signalling in the primary cilium is not only dependent on TRP channel activity but also on purinergic receptors[34,49,50]. Purinergic Ca^{2+} signalling is a well-known mechanism occurring in the cytoplasm[6,7]. However, its role in the primary cilium is not completely understood[34]. In this regard, Su *et al.*[49] observed that cytosolic ATP-induced Ca^{2+} signals are followed by a local Ca^{2+} increase in the cilium, propagating from the ciliary base to the tip. In a different way, it was reported that bending of the kidney cilium induces ATP release, stimulating the paracrine activation of P2Y receptors and resulting in Ca^{2+} increase. Consequently, Ca^{2+} opens apical K^+ channels, facilitating K^+ excretion. Also, ATP inhibits transport of ions and water, eliciting an auto- and paracrine diuretic response[50].

Intriguingly, this year, Delling and colleagues[51] stated that primary cilia are not Ca^{2+}-responsive mechanosensors, calling into question earlier findings[40,47]. The authors report the lack of Ca^{2+} increases in the primary cilium, upon physiological and higher levels of fluid flow. With this observations, they conclude that mechanosensation in primary cilia must occur through processes other than Ca^{2+} signalling[51]. Nevertheless, there is still a lot to be understood in this field.

The primary cilium is also involved in other types of signalling, being of great importance for embryonic development and tissue homeostasis. The most studied mechanisms with evidence for a primary cilium function in this early stages are the Hedgehog (Hh) and Wingless (Wnt) pathways[39]. Studies revealed that components of these pathways localize in primary cilia and that mutations in IFT proteins lead to defects in signal transduction. Perturbations on Hh pathway result in abnormal neural tube patterning and severe polydactyly[39,52]. On the other hand, Wnt signalling relates to cilia through mechanosensation induced Ca^{2+} increase. In this case, cilia defective cells have an overactivity of the non-canonical or planar cell polarity (PCP) pathway that can lead to polarized tissue defects, resulting in the formation of cysts[38,52].

In addition to the referred pathways, primary cilia also play a substantial role in several other mechanisms, such as cell migration, growth and proliferation, and regulation of organ size[37,38].

1.3.3. Relevance in disease – Ciliopathies and cancer

Sensibly all mammalian cells can develop primary cilia, an organelle that evolved into a versatile tool for numerous cellular functions. They are present in epithelial cells, for example from the kidney tubule, as well as in nonepithelial cells like chondrocytes, fibroblasts and neurons. Defects on primary cilia in these broad range of cells lead to a variety of diseases termed ciliopathies and account for the several organ systems affected[37,53].

Undoubtedly, the most studied cilia-related disease is the polycystic kidney disease (PKD). This disease is characterized by the formation of large fluid filled cysts along the kidney tubule, caused by dedifferentiation and proliferation of the epithelial cells, with consequent loss of organ function[8,37,47]. Evidence suggests that mutations in components of the primary cilium that disrupt the signalling mechanisms are the probable cause for the disease[8,37]. This disorder is one of most frequent hereditary nephropathies, being responsible for most cases of kidney failure[48].

Polycystic kidney diseases are caused by mutations in PC1 and PC2 proteins, which are expressed in the primary cilium of kidney epithelium, and disrupt the mechanosensation function of this organelle. In fact, it was shown that loss or dysfunction of these proteins did not result in increased Ca^{2+} influx upon physiological fluid flow. This might lead to PKD due to compromised fluid sensing, which normally regulates tissue morphogenesis[47].

Additionally, the revolutionary finding of Pazour *et al.*[54], revealed that lack of an essential component of the IFT lead to the formation of short primary cilia, ultimately resulting in PKD. This suggests that IFT is critical for ciliary assembly, indicating that cilia have a crucial role in the kidneys[54].

Mouse models have been extensively used to study PKD[55], however they can also be used to investigate other ciliopathies. These include the formation of cysts and fibrosis in other organs, such as the liver and pancreas, abnormal formation of the left-right body axis, retinal degradation, cognitive defects and obesity[40,52,53,55].

Since primary cilia can regulate cell cycle progression, they are also related to cancer development. In fact, cells with mutations that result in absent or shortened cilia are prone to initiate rapid cell duplication. Additionally, it was shown that some tumor suppressor proteins are associated with ciliogenesis, which can result in ciliary loss in early tumorigenic events. Moreover, cells that inherit more than two centrosomes might develop an aberrant number of cilia, which distorts the normal ciliary signalling. Centrosomal abnormalities are a common feature of human cancers, relating primary cilia to this disease[38].

1.3.4. Anoctamins in the primary cilium

Anoctamins were recently shown to be present in primary cilia, where they might also play a role. In particular, ANO6 was found on primary cilia from renal tubular cells as an important protein involved in cystogenesis. In this study, Forschbach *et al.*[56], reported that although ANO6 was not essential for ciliogenesis nor cyst expansion *in vitro*, knockdown of ANO6 resulted in impaired cyst lumen formation in a three-dimensional cyst model from MDCK cells. Additionally, the absence of ANO6 reduced

apoptosis and removal of epithelial cells from the lumen was incomplete. Furthermore, the authors showed that this channel is highly expressed in apoptotic epithelial cells from human polycystic kidneys, hence its functional relevance in cyst formation[27,56].

In a different study, Ruppersburg and Hartzell[57], showed for the first time an association between ANO1 and primary cilia. They observed that ANO1 is located in the primary cilium and that pharmacological blocking or silencing of the channel leads to impaired ciliogenesis. Therefore, the authors propose that ANO1 Cl^- currents are required for the genesis or maintenance of primary cilia by three possible mechanisms:

1) regulation of the apical membrane potential (V_m), which could affect ciliogenic Ca^{2+} signalling. Ciliary PKD/TRP channels could promote Ca^{2+} influx and activate ANO1, which then might control the Ca^{2+} driving force and open probability of VGCCs by altering V_m;
2) ANO1 could regulate the hydrodynamic and osmotic forces that promote ciliary extension. Membrane trafficking and cytoskeletal assembly might not be enough to form the cilium, thus osmotic pressure may be required to produce an initial cellular bleb into which ciliary components could traffic and assemble;
3) the Cl^- ion might act as a protein regulator. Cl^- is spatially and temporally dynamic, therefore, local Cl^- gradients in the periciliary region could regulate protein function in a compartmentalized fashion[57].

In addition, it was found that ANO1 contributes to proton (H^+) secretion and protein reabsorption in kidney proximal tubules. This is likely to occur through flow dependent regulation of H^+ secretion by the vacuolar H^+-ATPase (V-ATPase) and activation of ANO1. The H^+ secretory function of the V-ATPase depends on Cl^- and can be activated by intracellular Ca^{2+} increase. Moreover, since bending of the primary cilium causes paracrine release of ATP elevating intracellular Ca^{2+}, it is possible that this results in the parallel activation of the V-ATPase and ANO1[50,58].

Given these observations is it possible that anoctamins also play a role modulating Ca^{2+} signalling in the primary cilium? It is certainly a question worth investigating, that can open new paths for discovery, possibly related to ciliopathies.

1.4. Domain targeting calcium indicators

1.4.1. PM-GCaMP2

A green fluorescent protein (GFP)-based high signal-to-noise Ca^{2+} probe (GCaMP) was previously developed[59] and can be targeted to specific domains or proteins. This sensor has high affinity for Ca^{2+} which enables its improved signal over background ratio[59].

The indicator consists of a circularly permuted enhanced GFP (cpEGFP) connected to the M13 fragment of myosin light chain kinase (M13) by its N-terminus. This peptide is a target sequence for calmodulin (CaM), that was fused to the C-terminus of cpEGFP. Binding of Ca^{2+} to CaM induces a Ca^{2+}-CaM-M13 interaction that causes a conformational change in cpEGFP, altering its fluorescence intensity[59]. Designed and random mutations in GCaMP gave rise to improved sensors[60,61], notably GCaMP2[61].

In order to generate a membrane targeted Ca^{2+} sensor, a signal peptide from neuromodulin was fused to GCaMP2 in the M13 N-terminus[62]. The signal sequence consists of the N-terminal 20 amino acids from neuromodulin (MLCC20)[63] and its addition results in post-translational palmitoylation of the protein, enabling the attachment of the sensor to the cytosolic side of the PM[62,63] (Figure 1.4).

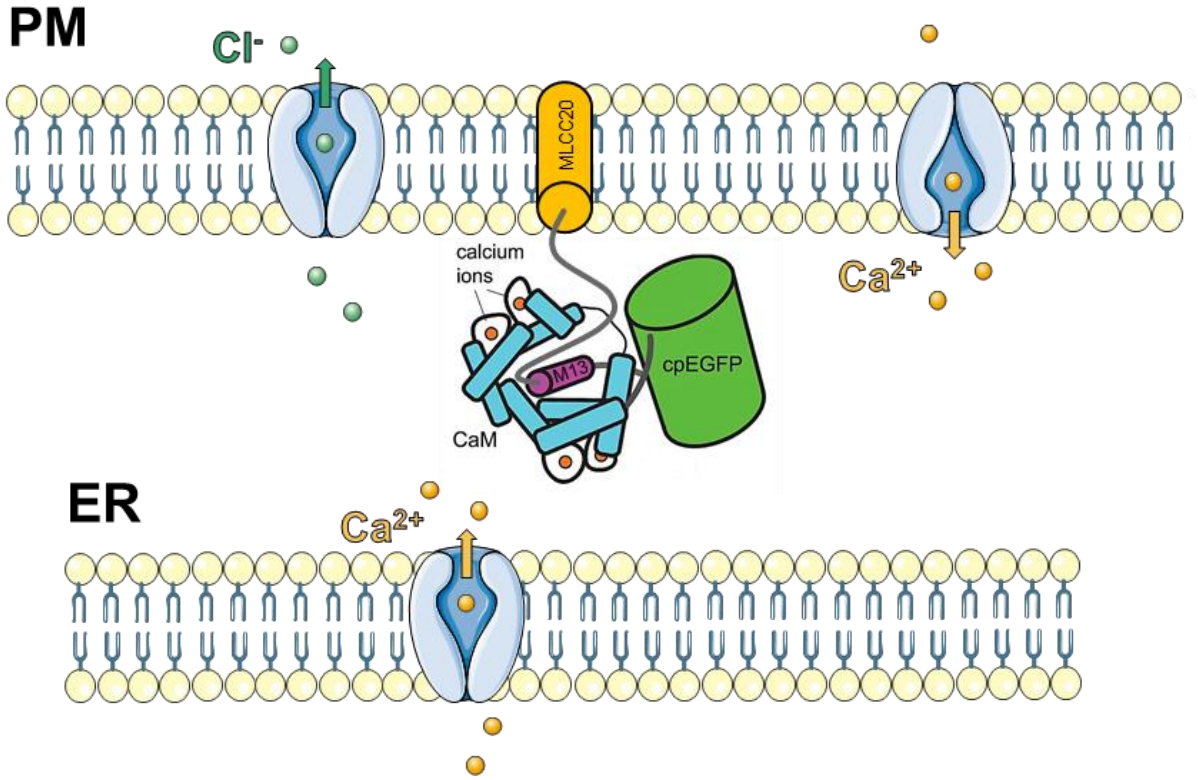

Figure 1.4 – Schematic representation of the PM-GCaMP2 sensor inserted in the membrane. The signal sequence from neuromodulin (MLCC20) targets the Ca^{2+} indicator to the PM, which in turn consists of a myosin light chain kinase fragment (M13) fused to a circularly permuted EGFP (cpEGFP) protein and calmodulin (CaM), located N to C terminally. This probe is sensitive to Ca^{2+} changes that might result from Ca^{2+} influx or Ca^{2+} release from the stores, possibly activating nearby Cl^- channels. The GCaMP representation (centre) was adapted from Akerboom *et al.*, 2012 [60].

1.4.2. Ciliary-GECOs

The reduced dimensions of the primary cilium make the interpretation of the real ciliary signals frequently difficult[34,49]. Electrophysiological approaches have been proposed[64], although patch-clamping of the ciliary membrane can be challenging. Additionally, common Ca^{2+} indicator dyes often lead to signal saturation of the entire cytosol, being unable to dissect the local ciliary Ca^{2+} transients[34,49].

These obstacles led to the development of cilium-targeted genetically encoded Ca^{2+} indicators for optical imaging (GECOs), which are attached to the cilium through ciliary targeting sequences (CTS). This sequences include peptides and proteins that are expressed in the primary cilium, for example 5HT6 or Smo, allowing the monitoring of cilia specific Ca^{2+} signalling[34,41,49].

There are several sensors available, among which 5HT6-mCherry-GECO1.0 and SMO-Cherry-GECO1 constitute interesting tools[41,49]. They possess a CTS, consisting of either 5HT6 or Smo protein, fused to an mCherry protein, which allows the visualization of the primary cilium independently of the $[Ca^{2+}]$. 5HT6 is a serotonin receptor observed to accumulate in the primary cilium[34], whereas Smo is a protein involved in Hh signalling[52], also localized in this organelle. The Ca^{2+}-sensitive part is similar to the

GCaMP indicators and consists of a skeletal muscle light-chain kinase (M13), a circularly permuted GFP (cpGFP) and CaM fused to mCherry[49] (Figure 1.5).

With these new sensors, investigators were able to determine that the basal ciliary [Ca^{2+}] level is around 580 nM in human retinal pigment epithelial (hRPE) cells, which is about five times higher than in the cytosol. Interestingly, they also state that ciliary Ca^{2+} can rise dramatically without significantly change the global cytoplasmic Ca^{2+}, which opposes to the previous hypothesis where Ca^{2+} influx through PC channels induce a cytosolic Ca^{2+} increase[34,41].

In a similar method, using a hRPE cell line stably expressing enhanced green fluorescent protein (EGFP) tagged to Smo protein (SMO-EGFP), the authors could visualize the primary cilium and record ciliary currents. Patch clamp experiments revealed that the ciliary membrane possess a high number of channels, comparable to the channel density of other intracellular organelles like mitochondria. Taken together, these findings suggest that the primary cilium possess a high dynamic level of Ca^{2+} compared to the cytoplasm, which the researchers propose to be maintained through constitutive activity of a TRP channel complex[34,65].

In conclusion, these new probes constitute a great tool to investigate the underlying signalling mechanisms occurring in the primary cilium.

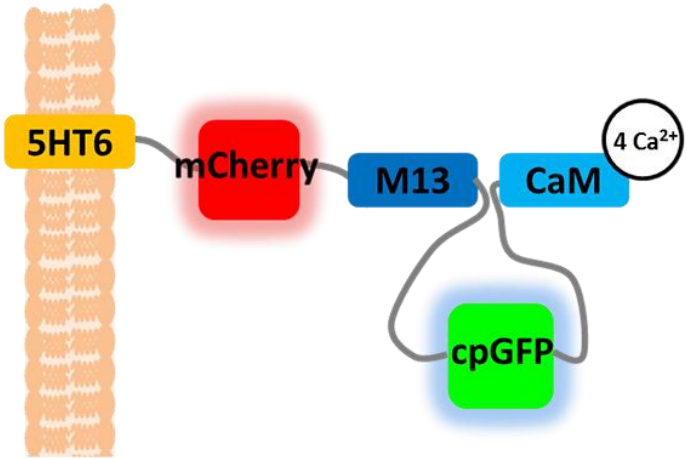

Figure 1.5 – 5HT6-mCherry-GECO1.0 targets primary cilia and detects ciliary Ca^{2+} changes. Schematic representation of 5HT6-mCherry-G-GECO1.0, containing an mCherry protein, a skeletal muscle light-chain kinase (M13), a circularly permuted GFP (cpGFP) and calmodulin (CaM), fused to the CTS. This sequence allows the sensor to be bounded to the ciliary membrane and is composed of the full-length 5-hydroxytryptamine (serotonin) receptor isoform 6 (5HT6). Only the Ca^{2+} bound conformation is represented. Retrieved from Su *et al.*, 2013 [49], supporting information.

2. OBJECTIVES

As new findings about Ca^{2+} modulation by anoctamins in different cellular localizations were emerging, it was of interest to look deeper into this matter. Particularly, ANO1 and ANO4 were observed to affect Ca^{2+} levels in close proximity of the PM, having possible functions regulating Ca^{2+} in this region and in the ER. Therefore, the Ca^{2+} levels were measured in cells overexpressing ANO1 and ANO4 using two different Ca^{2+} indicators: Fura-2 for measurements of intracellular Ca^{2+} concentration ($[Ca^{2+}]_i$) and PM-GCaMP2 for measurements of the Ca^{2+} concentration near the PM ($[Ca^{2+}]_P$).

Additionally, anoctamins were found to be expressed in another subcellular compartment, the primary cilium, an important sensory organelle involved in Ca^{2+} signalling. In order to address the importance of these channels in primary cilia, additional objectives were established, more specifically:

- To generate stably expressing cell lines with ciliary Ca^{2+} sensors using hTERT RPE-1 and MDCK M2 cells transfected with 5HT6-mCherry-GECO1.0 or SMO-Cherry-GECO1.
- To investigate the Ca^{2+} signalling activation in the primary cilium using different agonists like ATP and serotonin (5-HT).
- To determine the origin of the Ca^{2+} signalling in this region, through store depletion experiments with CPA (SERCA pump inhibitor) and IP_3 receptor and TRP channel inhibitors.
- To examine the involvement of anoctamins in this process, using anoctamin inhibitors: CaCC-A01, niflumic acid (NFA) and tannic acid (TA).

3. MATERIALS AND METHODS

3.1. Cell Culture

Cells were grown in 25 or 75 cm^2 culture flasks (as appropriate) in an incubator with a humidified atmosphere of 5% CO_2, at 37 ºC. Cell culture procedures were performed inside laminar-flow hoods using aseptic techniques, sterile equipment and solutions. Cell culture reagents were purchased from Gibco® – Life Technologies™, except where noted.

3.1.1. Mammalian cell lines and culture conditions

HeLa[66], HEK293[67] and MDCK M2[68] cell lines were cultured in Dulbeco's Modified Eagle Medium (DMEM) 1x supplemented with 10% Fetal Bovine Serum (FBS). For MDCK M2 cells stably overexpressing SMO-Cherry-GECO1 (SMO-GECO) or 5HT6-mCherry-GECO1.0 (5HT6-GECO), the media was further supplemented with 500 µg/mL Geneticin (G-418; Capricorn Scientific, Ebsdorfergrund, Germany).

hTERT RPE-1[69] cells (RPE) were cultured in Dulbecco's Modified Eagle Medium: Nutrient Mixture F-12 (DMEM:F-12) supplemented with 10% FBS and 0,01 mg/mL Hygromicin B. For RPE 5HT6-GECO cells, the media was further supplemented with 500 µg/mL G-418.

Media changes and cell passages were performed every 2-3 days (d), as necessary. HEK293 and HeLa cells were splitted from 25 cm^2 culture flasks, whereas MDCK M2 and RPE cells were splitted from 75 cm^2 culture flasks. To subculture cells, the media from the flasks was previously aspirated and 3-5 mL of phosphate buffered saline (PBS) buffer solution were added to rinse cells, except for MDCK M2 cells that were incubated for 5 min with PBS supplemented with 1 mM Ethylenediamine tetraacetic acid (EDTA; Ambion® – Life Technologies™). PBS was then removed, 1-2 mL Trypsin-EDTA were added and cells were incubated for ~3-5 min at 37 ºC. Trypsin was deactivated by the addition of 5-6 mL media and cells were subsequently centrifuged at 25 000 rotations per minute (rpm) for 3 min. Supernatant was then removed and cells were ressuspended in 7 mL media.

For the experiments cells were seeded in 12-well plates containing 18 mm ⌀ round glass-coverslips (A. Hartenstein, Würzburg, Germany) coated with a collagen/fibronectin mixture, except for HeLa cells that do not need coating media. Coating media consists of a mixture of F-12 (Ham) Nutrient Mixture 1x media, human fibronectin (1 mg/mL, PromoCell, Heidelberg, Germany), collagen (PureCol® – Advanced BioMatrix), bovine albumin and Penicillin-Streptomycin. Before plating, cells were counted in a hemocytometer using Trypan blue stain 0,4% to distinguish live cells from dead cells. HEK293 and HeLa cells were seeded at ~$5x10^{-4}$ cells/mL, while MDCK M2 and RPE cells were seeded at ~$2x10^{-5}$ cells/mL. After splitting, cells were transferred to new culture flasks with fresh media in 1:5 or 1:10 dilutions.

3.1.2. Transient transfections

All transient transfections were performed using Lipofectamine® 3000 transfection reagent (Invitrogen – Life Technologies™), according to manufacturer's instructions, in the absence of antibiotics. This procedure is termed lipofection and consists on a highly efficient liposome mediated Deoxyribonucleic

acid (DNA)-transfection technique. It makes use of cationic lipids that form DNA complexes spontaneously and are then able to fuse with the plasma membrane, allowing the uptake and expression of the DNA[70]. Experiments were performed 48-72h after transfection.

For single cell fluorescence $[Ca^{2+}]_i$ measurements, cells were grown on glass-coverslips and were co-transfected with different complementary DNA (cDNA). For ATP and store depletion experiments, HEK293 and HeLa were co-transfected with cDNA encoding either human ANO1, ANO4 or empty pcDNA3.1 vector (mock) along with cDNA encoding cluster of differentiation 8 (CD8) co-receptor. The latter was transfected in a proportion of 1:4 in order to have ANO cDNA in excess. In a different experiment with ATP and the Orai1-inhibitor, HEK293 cells were co-transfected with cDNA encoding either ANO4 or mock and cDNA encoding $P2Y_2$ receptor, using cells transfected only with mock cDNA as a negative control.

The membrane localized fluorescent Ca^{2+} indicator MLCC20-GCaMP2 (PM-GCaMP2) has a PM targeting sequence MLCC20 fused to the high signal to noise Ca^{2+} sensor protein GCaMP2[61–63], that enables $[Ca^{2+}]_P$ measurements. For single cell fluorescence $[Ca^{2+}]_P$ measurements, cells were grown on glass-coverslips and were co-transfected with different cDNA. For ATP and store depletion experiments, HeLa cells were co-transfected with cDNA encoding either ANO1, ANO4 or mock with MLCC20-GCaMP2 cDNA. The latter was transfected in a proportion of 1:4 in order to have ANO cDNA in excess. For purinergic stimulation experiments of ANO homologues, HEK293 cells were co-transfected with cDNA encoding either Ist2, nhTMEM16 or mock and MLCC20-GCaMP2 plasmid, with an excess of ANO homologues cDNA in a 1:4 ratio.

3.2. Generation of stable expressing cell lines with ciliary calcium sensors

Stable transfection allows long-term introduction of DNA into cells, in contrast to transient transfection, in which introduced DNA persist in cells only for a few days. Normally, stably transfected cells incorporate the transfected DNA into their genome and pass it to their progeny.

In order to generate stable expressing cells, it is necessary to have an efficient DNA delivery system and a way to select the cells which incorporated the DNA. This is achieved using selectable markers on the DNA construct used for transfection, applying the appropriate selective pressure afterwards. In this case, a neomycin resistance gene was used as a marker, which confers resistance to the G-418 antibiotic. Cultivation under selective medium induces death of non-transfected cells, surviving only the cells expressing the resistance gene.

3.2.1. Killing curve

In the first place, a killing curve was made to determine the right concentration of antibiotic for the selection of stably transfected cells (Appendix I – Killing curve, Figure A I). For this process, MDCK M2 and RPE cells were seeded at ~$1x10^{-5}$ cells/mL in a 12-well plate. The next day, the media was changed to media with increasing amounts of G-418 in duplicate wells, from 0 µg/mL (control) to 1000 µg/mL, as shown in the following scheme (Figure 3.1).

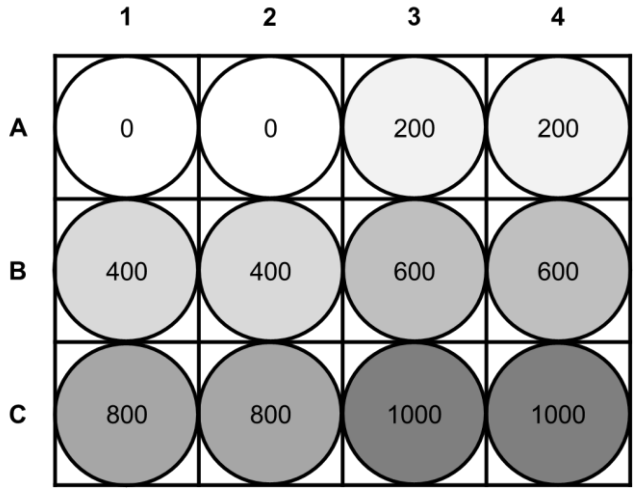

Figure 3.1 – Scheme of the G-418 titration for determination of working selection concentration. Increasing amounts of G-418 (0-1000 µg/mL) were added to duplicate wells of cells seeded in a 12-well plated at ~$1x10^{-5}$ cells/mL. Visual toxicity was accessed to determine the optimal concentration required for antibiotic selection.

3.2.2. Stable transfections

For stable transfection of MDCK M2 and RPE an electroporation system was used, Neon® Transfection System (Invitrogen™), as these cells are difficult to transfect. Electroporation uses high-voltage electric impulses to introduce DNA into cells. These pulses cause transient structural changes in the membrane lipid bilayers, inducing reversible pore formation that enables material flow[71,72]. The transfection was carried out according to the company's protocol, using either 5HT6-mCherry-GECO1.0 (5HT6-GECO) or SMO-Cherry-GECO1 (SMO-GECO) plasmid, in media without antibiotics. After 24h of transfection, live cells were observed under the microscope for transfection efficiency (Appendix II – Transfection Efficiency, Figure A II-IV). 5HT6-GECO and SMO-GECO are sensitive Ca^{2+} indicators with a CTS, that enable local ciliary Ca^{2+} measurements[41,49].

3.2.3. Selection and expansion of transfected cells

The selection was initiated 48h after transfection, using the optimal antibiotic concentration [G-418] = 500 µg/mL. Non-transfected cells were used as a negative control for the selection process. Cell death starts after approximately 2d after selection. The media was changed every 2-3d until the cells from the negative control were all dead, which occurs after approximately 10-14d after the beginning of the selection process. Then, the cells were maintained in selection media and appropriate media changes were performed until they reached confluence. At this point, the cells were harvested and used for experiments as a polyclonal cell line.

In parallel, generation of a monoclonal line was attempted, using a limiting dilution method. This process consists in seeding cells at < 1 cell/well in a 96-well plate, in order to isolate the selected cells and expand them from single cells. Alternatively, cells were seeded sparsely but not at a limiting dilution, allowing the formation of colonies. Afterwards, colonies evolving from a single cell were picked with a pipette and transferred to another culture plate for monoclonal expansion.

3.3. Molecular Biology

3.3.1. Plasmid cDNA

All transient and stable transfections were performed with cDNA, using the plasmids described on Appendix III – cDNA plasmids, Table A I.

3.4. Functional analysis – Calcium signalling measurements

All cell fluorescence measurements with the different Ca^{2+} indicators were performed continuously on an inverted microscope Axiovert S100 (Zeiss, Germany) with a Fluar x40/1.30 oil objective (Zeiss, Germany) and a high speed polychromator system (VisiChrome, Visitron Systems, Germany). Control of experiment and imaging acquisition were performed using the software package Meta-Fluor (Universal imaging, USA). All compounds used in the experiments were purchased from Sigma-Aldrich® (except where noted) and dissolved in Ringer solution (mM: NaCl 145; KH_2PO_4 0,4; $K_2HPO_4 \cdot 3H_2O$ 1,6; D-(+)-glucose 5; $MgCl_2 \cdot 6H_2O$ 1; Ca-D-gluconate$\cdot 1H_2O$ 1,3; pH 7,4).

3.4.1. Fura-2 AM measurements

Transiently transfected HEK293 and HeLa cells (see section 3.1.2 Transient transfections) and MDCK M2 stably expressing 5HT6-GECO (see section 3.2.2 Stable transfections) were loaded with 2 µM Fura-2 AM ester (Biotium) in Ringer solution with 0,02% Pluronic® F-127 (Molecular Probes®, Invitrogen™) for 1h at room temperature (RT). Incubation allows cleavage of the ester group by endogenous esterases, entrapping the dye within the cell membrane which becomes fluorescent.

Cells expressing CD8 were incubated for ~1 min with Dynabeads CD8 (Invitrogen™, Thermo Fisher Scientific) before the measurements, in order to recognize the transfected cells. After loading, the coverslips were mounted in a culture chamber and perfused continuously with Ringer solution at a rate of ~8 mL/min at 37 ºC.

For live-cell fluorescence imaging of intracellular Ca^{2+}, Fura-2 was excited at 340/380 nm, and the emission was recorded between 510±40 nm using a CCD-camera (CoolSnap HQ, Visitron Systems, Germany). To determine the $[Ca^{2+}]_i$ from the 340/380 nm fluorescence ratio, after background subtraction, the following equation was used:

$$[Ca^{2+}]_i = K_d \left[\frac{(R - Rmin)}{(Rmax - R)} \times \frac{Sf_2}{Sb_2}\right]$$

Equation 3.1 – Equation for $[Ca^{2+}]_i$ determination from Fura-2 ratiometric fluorescence measurements. R is the fluorescence ratio measured, Rmin is the minimum fluorescence ratio in the absence of Ca^{2+} and Rmax is the maximum fluorescence ratio at saturating $[Ca^{2+}]$; Sf_2/Sb_2 is the quotient between the fluorescence intensity of free and Ca^{2+}-bound Fura-2 measured at 380 nm[73].

To calculate the Rmin, Rmax and the constant Sf_2/Sb_2, a calibration of $[Ca^{2+}]_i$ was made, perfusing cells with Ringer containing 1 µM ionomycin[74] (LKT Laboratories, Inc.), 5 µM nigericin (Biotrend®, Köln, Germany) and 10 µM monensin (Calbiochem®, Darmstadt, Germany), followed by Ringer with 5 mM Ethylene Glycol Tetraacetic Acid (EGTA; Roth®, Karlsruhe, Germany), in order to equilibrate

intracellular and extracellular Ca^{2+} in intact loaded cells. The dissociation constant (K_d) of the Fura-2•Ca^{2+} complex used was 224 nM, as described in the literature[73].

Functional analysis of $[Ca^{2+}]_i$, was performed using several compounds. HEK293 were stimulated with ATP and also the effect of the Orai1-inhibitor YM-58483[75] (Tocris Bioscience) was evaluated in these cells. HeLa cells were also stimulated with ATP and store depletion was induced using cyclopiazonic acid[76] (CPA; Calbiochem®, Darmstadt, Germany) or ionomycin[74].

3.4.2. PM-GCaMP2 measurements

Transfected HEK293 and HeLa cells (see section 3.1.2 Transient transfections) were mounted and perfused as described above. PM-GCaMP2 was excited at 405/485 nm, and the emission was recorded between 535±12,5 nm using a CCD-camera. The $[Ca^{2+}]_P$ changes are given in arbitrary ratiometric units.

Functional analysis of $[Ca^{2+}]_P$, was also performed using ATP and CPA in HeLa and HEK293 cells.

3.4.3. Ciliary-GECOs measurements

Stably transfected MDCK M2 5HT6-GECO cells (see section 3.2.2 Stable transfectionsStable transfection) were grown to confluence in glass coverslips and serum starved for 4-6d, in selective media without FBS, to induce cilium formation[38]. Afterwards, the cells were mounted and perfused as described above. The mCherry part of this fluorescent indicator is used as a primary cilium marker independent of the $[Ca^{2+}]$. Therefore, before each experiment, a photo was taken exciting the 5HT6-GECO at 560 nm, and recording the emission between 620±30 nm using a CCD-camera. To measure the ciliary Ca^{2+} changes, 5HT6-GECO was excited at 405/485 nm, and the emission was recorded between 535±12,5 nm using a CCD-camera. The $[Ca^{2+}]_{cilium}$ and $[Ca^{2+}]_{cyt}$ changes are given in arbitrary fluorescence intensity units.

Initially, fluorescence intensity changes from MDCK M2 5HT6-GECO cells were also measured with an Axiovert 200M fluorescence microscope (Zeiss, Göttingen, Germany). The variations on the fluorescence intensity correspond to $[Ca^{2+}]$ changes.

Functional analysis of $[Ca^{2+}]_{cilium}$ and $[Ca^{2+}]_{cyt}$, was also performed using several compounds. MDCK M2 5HT6-GECO cells were stimulated with either ATP or 5-HT[77] hydrochloride. The effect of two different TRP channel inhibitors, SKF 96365[78,79] hydrochloride (SKF; Tocris Bioscience) and N-(p-amylcinnamoyl)anthranilic acid[80] (ACA) was evaluated; as well as two different IP_3 and RyR inhibitors, Xestospongin C[81] (XeC; Cayman Chemical Company, Hamburg, Germany) and Dantrolene[82]; and three anoctamin inhibitors: CaCC inhibitor[83,84] (CaCC-A01; Tocris Bioscience), niflumic acid[18] (NFA) and tannic acid[85] (TA). Additionally, cells were also perfused with CPA and ionomycin.

3.5. Protein analysis – Immunocytochemistry

For immunocytochemistry, MDCK M2 stably expressing either 5HT6-GECO or SMO-GECO and RPE stably expressing 5HT6-GECO, were grown on coated glass coverslips and serum starved for 4-6d.

First, the cells were shortly rinsed with PBS containing Ca^{2+} (PBS^{+}), followed by fixation with 4% (w/v PBS) Paraformaldehyde (PFA; Merck) for 10 min at RT. Cells were washed 3 times with PBS to remove the excess fixing solution and were permeabilized with 0,5% (v/v PBS) Triton-X 100 for 10 min at RT. A second rinse was performed for 3 times with PBS, followed by 40 min incubation at RT with 1% (w/v) of filtered bovine serum albumin (BSA) in PBS (1% BSA/PBS).

The primary antibodies rabbit anti-GFP (Invitrogen®, Molecular Probes™) and mouse anti-acetylated tubulin were incubated with a dilution factor (DF) of 1:300 in 1% BSA/PBS for 1h at 37 ºC. The anti-GFP antibody was used to detect the GFP part of the ciliary Ca^{2+} indicator and was examined for co-localization with anti-acetylated tubulin, which is used as a primary cilium marker since it detects acetylated tubulin that accumulates in the cilium. The excess of primary antibodies was washed for 3 times with PBS and cells were incubated with the secondary antibodies Alexa Fluor 488 conjugated Donkey anti-rabbit IgG (Invitrogen®, Molecular Probes™) and Alexa Fluor 660 conjugated Goat anti-mouse IgG (Invitrogen®, Molecular Probes™) in 1% BSA/PBS, DF 1:500. Alternatively, for MDCK M2 SMO-GECO cells a secondary antibody Alexa Fluor 546 conjugated Donkey anti-mouse IgG (Invitrogen®, Molecular Probes™) was used instead of the A660 antibody. Nuclei were stained with Hoechst 33342 in 1% BSA/PBS (DF 1:200, Invitrogen®, Molecular Probes™). Nuclear and secondary antibody staining were done in the dark for 1h at RT.

A final washing step was performed for 3 times with PBS before mounting the cells in glass slides with Dako fluorescent mounting medium (Dako, Eching, Germany). The next day, cells were examined with an Axiovert 200M fluorescence microscope (Zeiss, Göttingen, Germany), equipped with ApoTome and Axio-Vision (Zeiss, Jena, Germany).

3.6. Spectral analysis – Absorbance measurements

The inhibitors used were examined for possible fluorescence artifacts by measuring the absorbance of the inhibitor solutions. The absorbance measurements were performed using a NanoDrop 2000 UV-Vis Spectrophotometer (Thermo Scientific) and analysed with the NanoDrop 2000/2000c software (Thermo Scientific). First, the instrument was cleaned and the blank was set using distilled water. Then 1 µL of each inhibitor solution was placed in the device and UV-Vis specters were traced.

3.7. Statistical Analysis

To compare two different samples, paired or unpaired Student's *t*-test was used as appropriate. When more than two samples were compared, analysis of variance (ANOVA) was performed using the software package Origin (OriginLab Corporation, USA). Results with p-value < 0.05 were considered significant.

4. RESULTS

4.1. Insights on [Ca^{2+}] modulation by ANO1 and ANO4 in close proximity to the PM and the ER

The signalling cascades mediated by Ca^{2+} are known to play a central role in several cellular processes[2], being of great importance to investigate potential Ca^{2+} modulators. The Ca^{2+}-activated Cl^- channels ANO1 and ANO4 are possible candidates, since recent findings from our group revealed that the presence of these channels induced different Ca^{2+} responses[27].

Therefore, in order to assess how these proteins change the [Ca^{2+}] in different subcellular localizations, various Ca^{2+} indicators were used. In these regard, $[Ca^{2+}]_i$ changes were measured using the global cytosolic Ca^{2+}-sensor Fura-2, while PM localized Ca^{2+} signals were recorded with a PM targeted GCaMP2 (PM-GCaMP2).

4.1.1. Overexpression of ANO4 but not of ANO1 reduces $[Ca^{2+}]_i$ inside the stores in HeLa cells

It has been shown in a previous study that ANO1 is capable of supporting Ca^{2+} signalling in mouse intestine[28]. Also, last year, Inês Cabrita showed in her Master thesis that anoctamins change the ATP-induced Ca^{2+} response, among which ANO4 decreased intracellular Ca^{2+} signalling. This could be due to reduced [Ca^{2+}] inside the stores. Thus, to evaluate this question, [Ca^{2+}] inside the stores was detected indirectly by measurement of cytosolic Ca^{2+} concentration ($[Ca^{2+}]_i$) upon store depletion in the presence or absence of ANO1 or ANO4.

For this purpose, an overexpressing cellular system was used where ANO1 and ANO4 were each co-expressed with cluster of differentiation 8 (CD8) co-receptor in HeLa cells. The expression of the CD8 co-receptor allows the identification of the transfected cells after incubation with Dynabeads CD8 for ~1 min. $[Ca^{2+}]_i$ was measured with the Ca^{2+} indicator Fura-2 AM ester, that remains inside the cell and fluoresces after intracellular esterases cleave the ester group.

The influence of these channels on the Ca^{2+} concentration ([Ca^{2+}]) inside the stores was determined by measurements of intracellular Ca^{2+} concentration ($[Ca^{2+}]_i$) with different store depletion protocols. In the first experiment (Figure 4.1 A, C), the cells were stimulated with 100 µM ATP in the absence of extracellular Ca^{2+} (0 mM $[Ca^{2+}]_o$) and were further treated with 10 µM CPA[76] (SERCA pump blocker), in order to completely deplete the intracellular store. ATP induces a transient increase of $[Ca^{2+}]_i$ (peak), due to ER store release, which is normally followed by a plateau, representing the Ca^{2+} influx. However, the plateau could not be observed, since the extracellular Ca^{2+} was removed.

The Ca^{2+} turnover in the ER occurs through diffusion of Ca^{2+} to the cytoplasm according to a concentration gradient and SERCA activity, that pumps Ca^{2+} back into the ER[1]. Addition of CPA inhibits SERCA, resulting in a relatively slow Ca^{2+} leak from the ER to the cytosol. The extracellular Ca^{2+} was subsequently restored (1 mM $[Ca^{2+}]_o$) and an influx of Ca^{2+} through SOCE was observed. ANO1 overexpression caused only a $[Ca^{2+}]_i$ decrease following extracellular Ca^{2+} removal, while ANO4 overexpression led to decreased $[Ca^{2+}]_i$ peaks upon ATP and CPA stimulation.

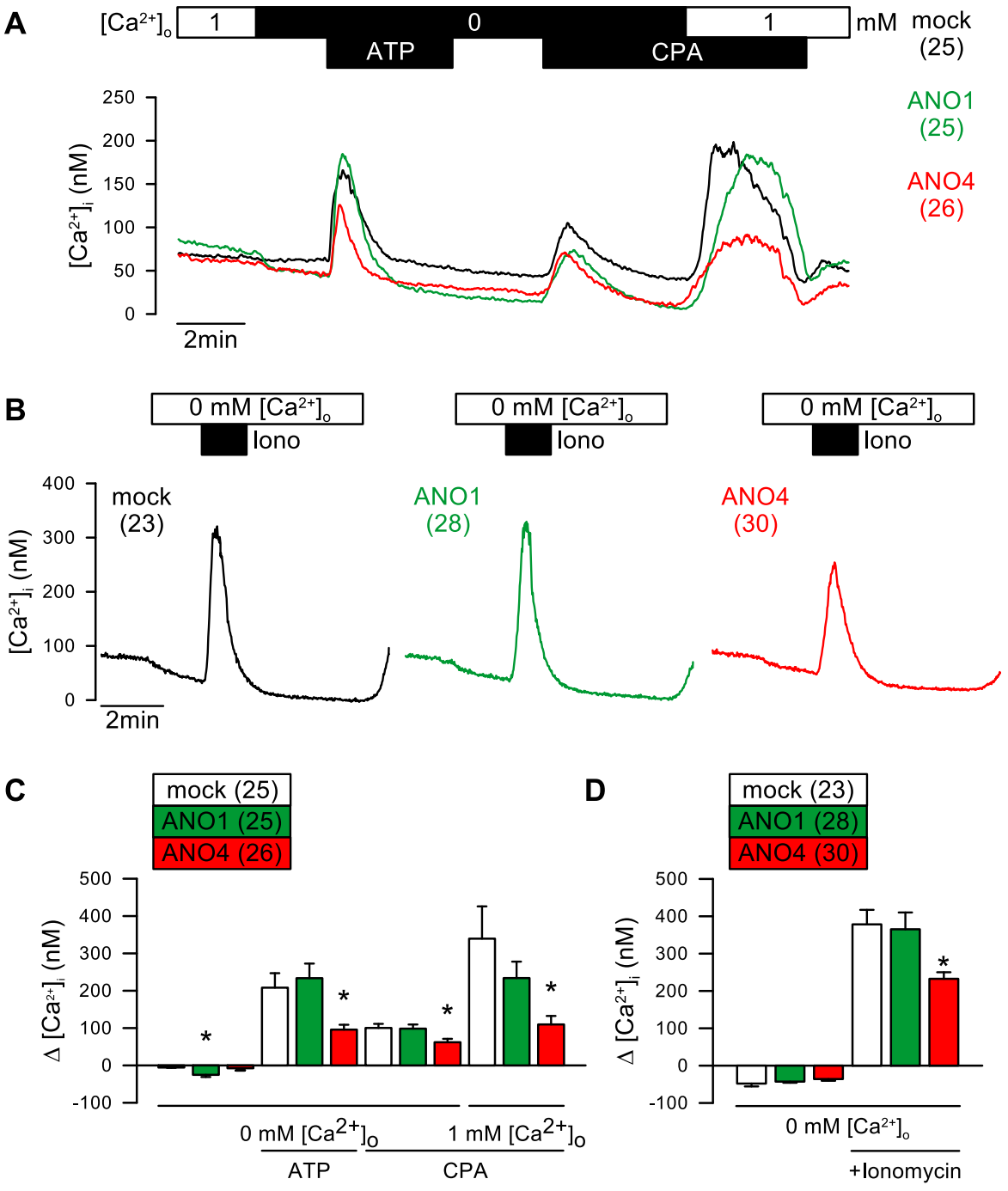

Figure 4.1 – ANO4 decreases the [Ca^{2+}] release from the ER store in HeLa cells. Original mean tracings of $[Ca^{2+}]_i$ upon ER store depletion in mock, ANO1 and ANO4 overexpressing HeLa cells. **(A)** The cells were stimulated with 100 µM ATP in the absence of extracellular Ca^{2+}, followed by addition of 10 µM CPA. Subsequently, the extracellular Ca^{2+} was restored in the presence of CPA, revealing a Ca^{2+} influx. **(B)** Effect of 1 µM ionomycin (Iono) in the absence of extracellular Ca^{2+}. Summary of **(C)** the extracellular free Ca^{2+} effect, which leads to a significant $[Ca^{2+}]_i$ decrease in ANO1 overexpressing cells, and store depletion effect with ATP and CPA, showing a significant $[Ca^{2+}]_i$ decrease in ANO4 overexpressing cells; and **(D)** the extracellular free Ca^{2+} effect, leading to a slight decrease in the $[Ca^{2+}]_i$, and subsequent ionomycin-induced Ca^{2+} increase. The results indicate that the store content from ANO4 overexpressing cells is significantly lower than ANO1 overexpressing cells. Values represent mean ± SEM; * ANOVA to mock, $p < 0.05$; (n) = number of cells.

These results suggest that ANO4 might decrease the Ca^{2+} stored in the ER, however, according to this, it was expected a stronger influx through SOCE after extracellular Ca^{2+} restitution or a higher baseline in ANO4 overexpressing cells.

To resolve this problems, store depletion was induced with 1 µM of ionomycin under extracellular free Ca^{2+} condition (Figure 4.1 B, D). Ionomycin is a Ca^{2+}-selective ionophore that transports Ca^{2+} ions across bilipidic membranes[74], increasing $[Ca^{2+}]_i$. Removal of Ca^{2+} led to a slight decrease in the $[Ca^{2+}]_i$, and subsequent ionomycin stimulation revealed a significantly smaller peak in ANO4 overexpressing cells. Therefore, together these results suggest that ANO4 overexpressing cells have a lower $[Ca^{2+}]$ inside the ER store.

4.1.2. Overexpression of ANO4 reduces Ca^{2+} signalling in $P2Y_2$ co-expressing HEK293 cells and increases Ca^{2+} influx by activation of Orai1.

To complement the ionomycin experiments, the effect of ANO4 overexpression in the $[Ca^{2+}]$ inside the intracellular stores was evaluated in HEK293 cells co-expressing the purinergic $P2Y_2$ receptor. This receptor was overexpressed in order to enhance the purinergic pathway. Additionally, an Orai1 inhibitor was used to examine if CRAC channels were activated by store depletion (SOCE).

$[Ca^{2+}]_i$ was measured with the Ca^{2+} sensor Fura-2 and cells were subjected to the action of the specific Orai1 inhibitor YM-58483. This is a very potent inhibitor of store operated Ca^{2+} influx channels which blocks SOCE[75]. The effect of 5 µM YM-58483 on basal $[Ca^{2+}]_i$ was determined and purinergic stimulation with 100 µM ATP was assessed (Figure 4.2). Cells overexpressing $P2Y_2$ alone were used as a second control to distinguish the effect of ANO4 overexpression. The results indicate that the basal cytosolic Ca^{2+} is significantly enhanced in ANO4 overexpressing cells (Figure 4.2 A, C) and that this augmented $[Ca^{2+}]_i$ is sensitive to the Orai1 inhibitor YM-58483 (Figure 4.2 A, D). Overexpression of $P2Y_2$ enhanced the effect of ATP on $[Ca^{2+}]_i$, and was significantly reduced by overexpression of ANO4 in $P2Y_2$ transfected cells (Figure 4.2 B, E).

These data are in agreement with the previous results, suggesting a reduced $[Ca^{2+}]$ inside the ER store and activation of Orai1 by SOCE in ANO4 overexpressing cells.

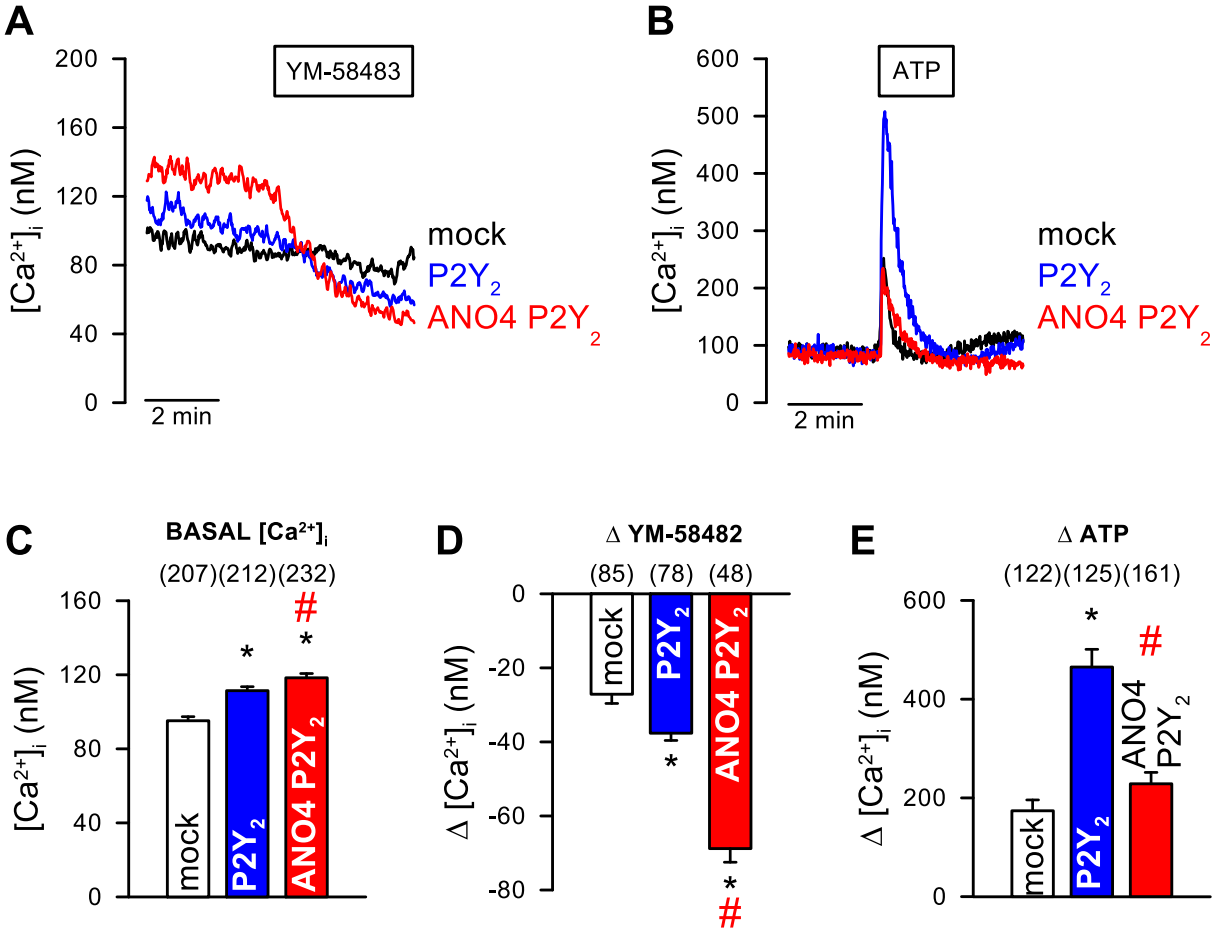

Figure 4.2 – Ca^{2+} modulation by ANO4 and Orai1-inhibitor effect in HEK293 cells. Original recordings of $[Ca^{2+}]_i$ from mock and $P2Y_2$ overexpressing cells and ANO4 $P2Y_2$ co-expressing HEK293 cells **(A)** upon 5 µM YM-58482 (Orai1-inhibitor) treatment and **(B)** purinergic stimulation with 100 µM ATP. Summary of **(C)** the basal $[Ca^{2+}]_i$, showing a significantly higher baseline when $P2Y_2$ is overexpressed or co-expressed with ANO4; **(D)** the YM-58482 effect, that results on a significant decrease on basal $[Ca^{2+}]_i$; **(E)** and 100 µM ATP stimulation effect, showing a significant increase for $P2Y_2$ overexpressing cells, that is significantly reduced by ANO4 overexpression. Values represent mean ± SEM; * ANOVA to mock; # unpaired *t*-test $P2Y_2$ vs. ANO4 $P2Y_2$, $p < 0.05$; (n) = number of cells.

4.1.3. ATP-induced $[Ca^{2+}]_P$ changes in the absence of extracellular Ca^{2+} in ANO1 and ANO4 overexpressing HeLa cells

To study $[Ca^{2+}]$ changes in close proximity to the PM ($[Ca^{2+}]_P$), a membrane targeted fluorescent Ca^{2+} indicator PM-GCaMP2 was co-expressed with ANO1 and ANO4 (see 1.4.1 PM-GCaMP, Figure 4.3).

Removal of external Ca^{2+} caused a decrease on the basal $[Ca^{2+}]_P$, but ANO1 and ANO4 overexpression groups were not different from the control. Purinergic stimulation with 100 µM ATP in the presence of extracellular Ca^{2+} (data not shown) and under extracellular free Ca^{2+} condition led to a transient increase of $[Ca^{2+}]_P$ in mock transfected cells, suggesting induction of Ca^{2+} release from the ER store by ATP. Overexpression of ANO1 caused an enhanced $[Ca^{2+}]_P$ peak, while ANO4 overexpression led to a reduced $[Ca^{2+}]_P$ peak. This data suggest that ANO1 induces a greater $[Ca^{2+}]_P$ increase close to the PM, while ANO4 decreases this concentration.

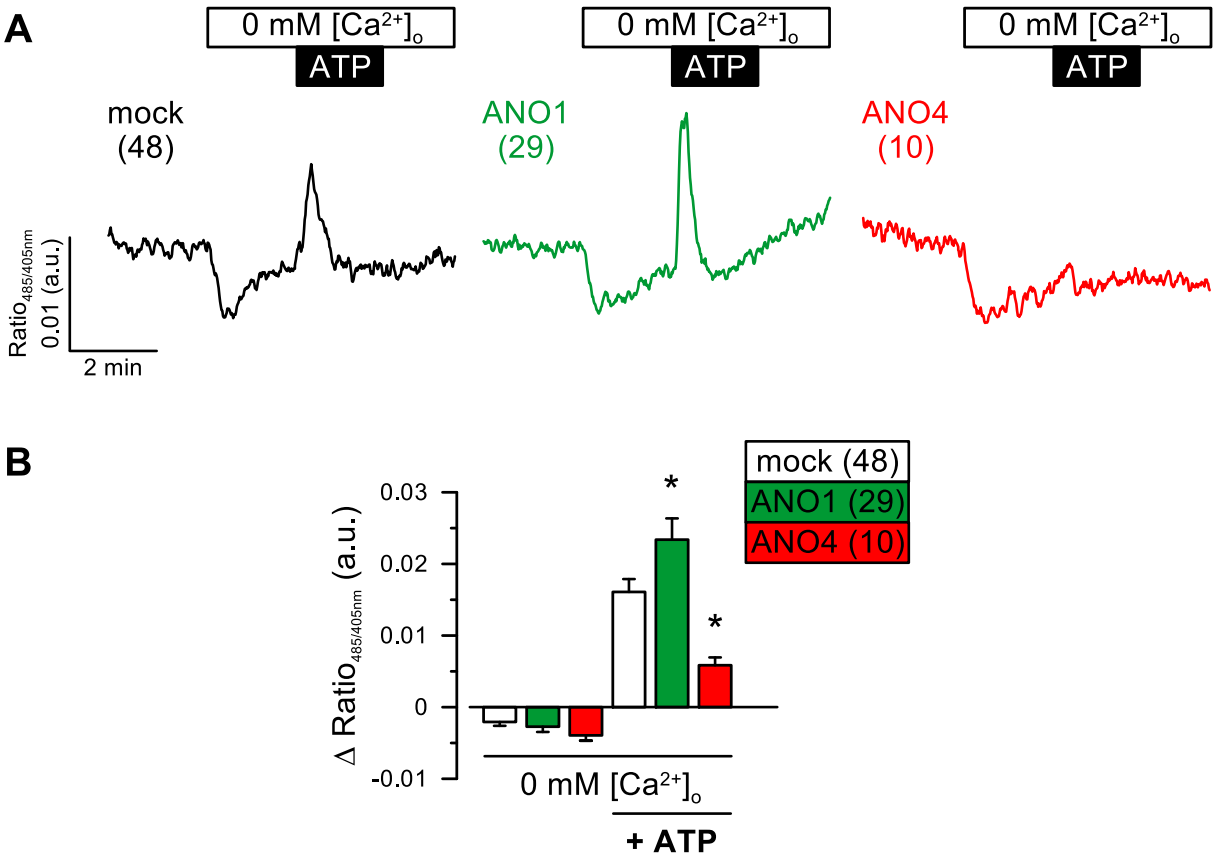

Figure 4.3 – ANO1 and ANO4 induce different changes on $[Ca^{2+}]_P$ measured with PM-GCaMP2 in HeLa cells. (A) Original mean tracings of $[Ca^{2+}]_P$ from HeLa cells co-expressing PM-GCaMP2 with either mock, ANO1 or ANO4 upon purinergic stimulation with 100 µM ATP in the absence of extracellular Ca^{2+}. **(B)** Summary of the extracellular free Ca^{2+} effect alone and after ATP stimulation, revealing a significant $[Ca^{2+}]_P$ increase and decrease in ANO1 and ANO4 overexpressing cells, respectively. Values represent mean ± SEM; * ANOVA to mock, $p < 0.05$; (n) = number of cells.

4.1.4. ATP-induced $[Ca^{2+}]_P$ changes in Ist2 and nhTMEM16 overexpressing HEK293 cells

The function of ANO1 on compartmentalized Ca^{2+} signalling was studied by comparison with the effects of two ANO homologues, Ist2 and nhTMEM16. Ist2 corresponds to the yeast homologue, that was described as a tethering protein[30,31], whereas nhTMEM16 is the fungal homologue, which possesses scramblase activity[25], functions that can be related to ANOs.

Thus, changes of $[Ca^{2+}]_P$ were measured by co-expressing the PM-GCaMP2 sensor with Ist2 or nhTMEM16 in HEK293 cells. The cells were stimulated with 10 µM ATP and a transient $[Ca^{2+}]_P$ increase was observed that was significantly higher in Ist2 and nhTMEM16 overexpressing cells (Figure 4.4).

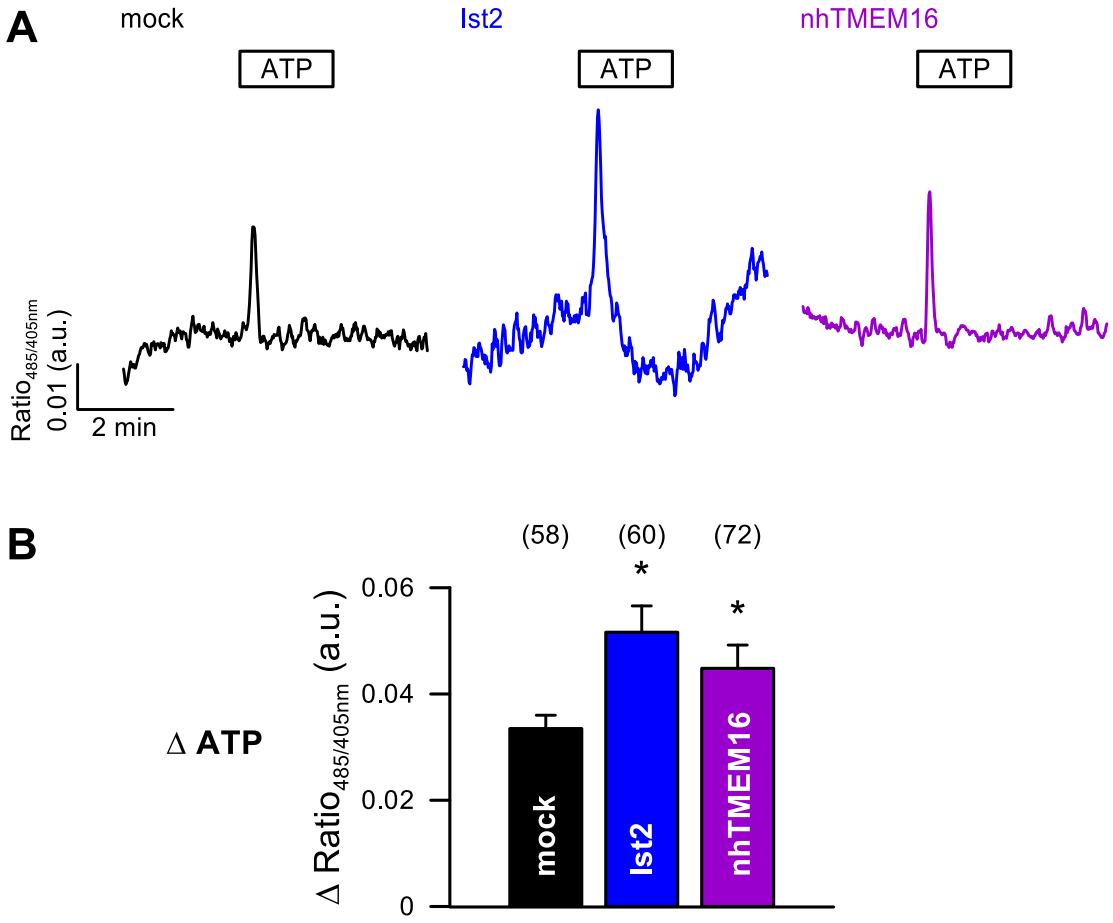

Figure 4.4 – ANO homologues enhance intracellular Ca^{2+} close to the PM. (A) Original recordings of HEK293 cells co-expressing either mock, Ist2 or nhTMEM16 with PM-GCaMP2, after purinergic stimulation with 10 µM ATP. **(B)** Summary presenting significant increase of $[Ca^{2+}]_P$ when the ANO homologues Ist2 and nhTMEM16 are overexpressed. Values represent mean ± SEM; * ANOVA to mock, $p < 0.05$; (n) = number of cells.

4.2. Ca^{2+} signalling in the primary cilium and influence of ANOs

4.2.1. Generation of stably expressing ciliary-GECO cell lines

In order to measure intracellular Ca^{2+} changes in the primary cilium, it was necessary to develop a system capable of efficiently detecting variations in the level of Ca^{2+} in this particular region. This was essential because transient expression is often difficult and expression might be lost while culturing cells without FBS (Ø FBS) to induce growth arrest. Normally, it is necessary around 4d to induce the formation of primary cilia (Figure 4.5).

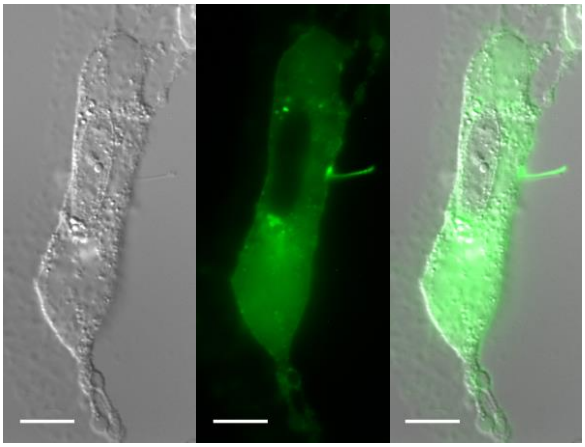

Figure 4.5 – Transient expression of 5HT6-GECO in RPE cells after serum starvation. Live cell fluorescence imaging of RPE cells transiently overexpressing 5HT6-GECO after 3d Ø FBS. The fluorescence intensity is brighter in the primary cilium, indicating that the sensor is expressed in this location due to the 5HT6 CTS. Bars indicate 10 µm.

In this regard, MDCK M2 and RPE cells were chosen as suitable working tools to study this sensory organelle, as they can easily develop primary cilia under resting conditions. Therefore, this cells were used to generate stable cell lines encoding a Ca^{2+} sensor with a ciliary targeting sequence (CTS). This sequence derives from proteins known to localize to primary cilia, allowing the sensor to be expressed in this location.

With this in mind, two cDNA plasmids were used to transfect these cell lines, namely 5HT6-mCherry-GECO1.0 (5HT6-GECO) and SMO-Cherry-GECO1 (SMO-GECO). These constructs are composed of a Ca^{2+} sensor (GECO) fused to a mCherry protein, that acts as a fluorescent marker independent of $[Ca^{2+}]$, and the 5HT6 or Smo proteins, respectively, that comprise the CTS[49] (see 1.4.2 Ciliary-GECOs). The GECO sensor belongs to the family of genetically encoding Ca^{2+} sensors for optical imaging, which are modified GCaMPs with higher sensibility. 5HT6 corresponds to the 5HT6 receptor, a serotonin receptor known to be highly expressed in the cilium[34], as well as Smo protein, which is involved in Hh signalling[52].

Primary cilia develop when cells are in the absence of proliferation stimuli, which can be achieved by serum starvation[38]. Therefore, subsequent Ca^{2+} signalling experiments in the primary cilium were performed after 4-6d of cultivation in serum free media (Ø FBS).

The expression of the ciliary Ca^{2+} sensors in stably transfected cells was confirmed by immunostaining against acetylated tubulin (red/magenta), a ciliary marker, and GFP (green), to detect the GECO part of the inserted construct (Figure 4.6). Ciliary expression of the SMO- and 5HT6-GECO constructs is shown by co-localization of both signals (in yellow, merge panels). These results suggest that both cell lines express the sensor not only in the cilium but also in the plasma membrane, and possibly membranes from internal organelles. Besides, it is possible to observe that the expression of this protein is not homogenous, as there are clearly "positive" and "negative" cells, meaning cells stained and unstained for GFP, respectively. This is observable in the MDCK M2 and RPE 5HT6-GECO polyclonal cell lines and in the MDCK M2 SMO-GECO cell line, on which generation of a clone was attempted, although it is still constituted by a mix of transfected and non-transfected cells. Additionally, only a few RPE cells show GFP staining and it does not overlap with the acetylated tubulin staining.

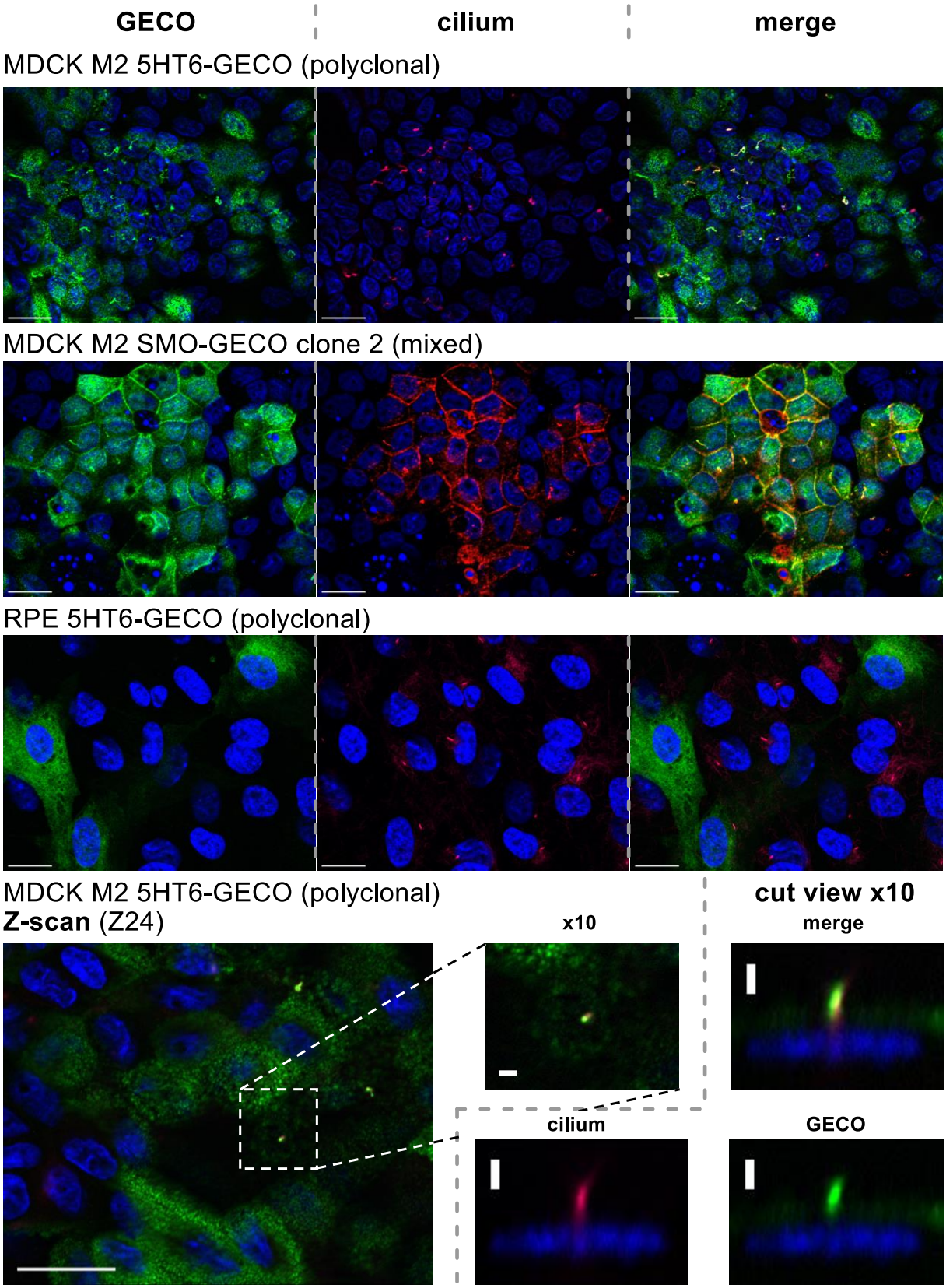

Figure 4.6 – Immunostaining of stable transfected MDCK M2 and RPE cells after ciliogenesis. Both cell lines are stably overexpressing either SMO- or 5HT6-GECO and were serum starved for 4d prior to cell fixation, for cilium formation. The primary cilium (red/magenta) is visualized using an anti-acetylated tubulin antibody, and GECO (green) with an anti-GFP antibody. Co-localization of the primary cilium with SMO- or 5HT6-GECO is shown by yellow colour in the overlay picture. Nuclei are shown in blue (DAPI staining). Z-scan of MDCK M2 5HT6-GECO cells enabled the generation of a 3D picture from which a cut view from a single cell shows an upward primary cilium. Bars indicate 20 µm or 2 µm for x10 amplification.

In the lower panels, a picture of a Z-scan of MDCK M2 5HT6-GECO (MDCK 5HT6) cells is shown. A Z-scan allows reconstruction of a 3D image by taking a series of pictures along the Z plane from a determined section. Afterwards, it is possible to generate a cut view from a region of interest out of the superimposed pictures. In this case, a primary cilium from a single cell was chosen as the region of interest and the respective cut view shows that it is positioned upwards. Moreover, these results also show co-localization of acetylated tubulin and GECO.

4.2.2. ATP-induced [Ca^{2+}] increase in the primary cilium

The primary cilium responds to a series of stimuli, allowing for its great signalling capacity. In addition, it is known that Ca^{2+} ions are important second messengers for signalling pathways in this region[36,38,42], making it interesting to investigate the ciliary [Ca^{2+}] changes upon different kinds of stimulation.

Therefore, in an initial approach, the Ca^{2+} activation in the primary cilium was tested. MDCK 5HT6 cells were measured after purinergic stimulation with 100 µM ATP, which induced a [Ca^{2+}] increase (Figure 4.7).

As the sensor is expressed not only in the primary cilium, it is possible to measure [Ca^{2+}] from the cilium ([Ca^{2+}]$_{cilium}$) simultaneously with [Ca^{2+}] from the cytosol ([Ca^{2+}]$_{cyt}$). The results show that it is possible

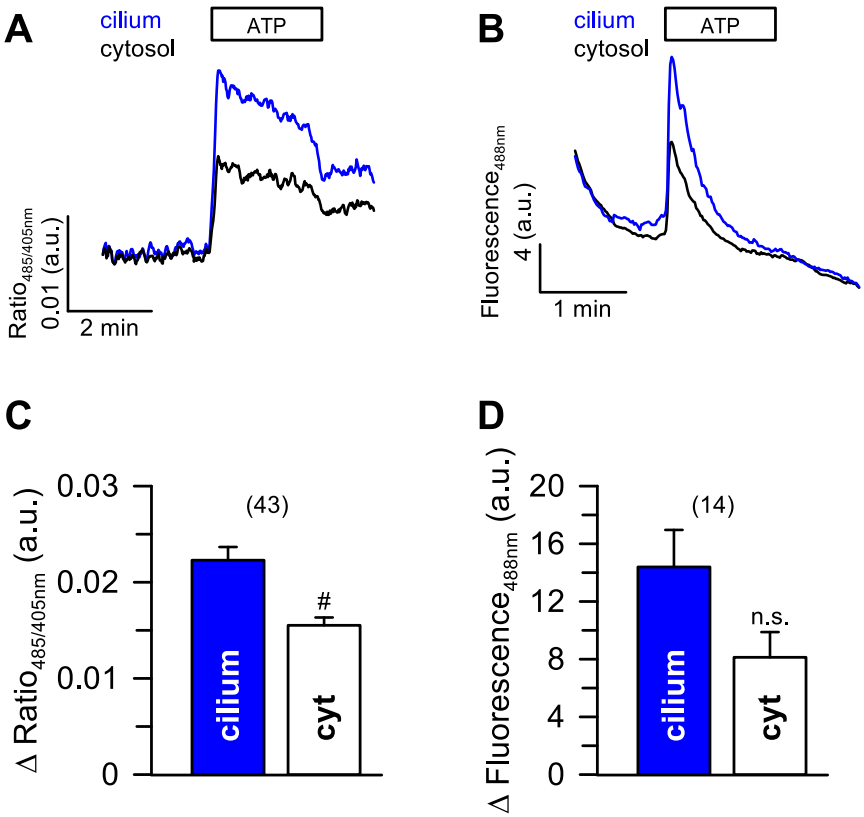

Figure 4.7 – Ca^{2+} signalling activation in the primary cilium through purinergic stimulation by ATP. MDCK 5HT6 cells were previously serum starved for 4-6d for ciliogenesis induction. Original mean tracings of [Ca^{2+}]$_{cilium}$ and [Ca^{2+}]$_{cyt}$ measurements after stimulation with 100 µM ATP, recorded with **(A)** Axiovert S100 x40 magnification, 200 ms exposure time and with **(B)** Axiovert 200M, x63 magnification, 600 ms exposure time. Summary of 100 µM ATP-induced changes of [Ca^{2+}]$_{cilium}$ and [Ca^{2+}]$_{cyt}$, showing a greater Ca^{2+} increase in the primary cilium compared to the cytosol, as obtained with **(C)** Axiovert S100 and **(D)** with Axiovert 200M. Values represent the **(C)** mean ratio or **(D)** mean fluorescence ± SEM; # significant differences with unpaired *t*-test to cyt, $p < 0.05$; n.s. = not significant; (n) = number of cells.

to induce Ca^{2+} signalling in these cells through ATP stimulation, and that the Ca^{2+} increase in the primary cilium is significantly higher than in the cytosol.

For this experiment, two different microscopes were used to assess the best way to perform the measurements. Axiovert 200M fluorescence microscope allows to take high quality pictures and record them in a determined period of time. On the other hand, Axiovert S100 allows high speed measurements that are very important to understand the Ca^{2+} signalling processes in the primary cilium. Also, two different exposure times were tested because the GFP intensity of the sensor was quite low. Therefore, it was necessary to create a compromise between quality and speed of the measurements. The best conditions were achieved using Axiovert S100 with 600 ms exposure time and were used in the subsequent measurements.

4.2.3. Serotonin (5-HT)-induced [Ca^{2+}] increase in the primary cilium

It is known that primary cilia have an accumulation of serotonin 5HT6 receptors[34], therefore it is speculated that 5-HT[77] stimulation would lead to a more specific response than ATP. Once 5HT6 receptors localize almost exclusively to cilia, it is possible that these receptors can sense the amount of 5-HT in the extracellular space in nearby areas[86]. Therefore, MDCK 5HT6 cells were stimulated with 100 µM 5-HT (Figure 4.8).

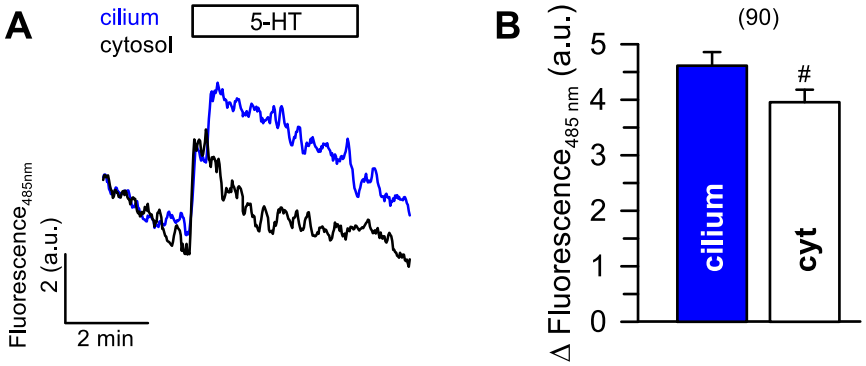

Figure 4.8 – 5-HT-induced [Ca^{2+}] increase in MDCK 5HT6 primary cilia. (A) Original mean tracings of $[Ca^{2+}]_{cilium}$ and $[Ca^{2+}]_{cyt}$ from MDCK 5HT6 cells (4-6d Ø FBS) after stimulation with 100 µM 5-HT. **(B)** Summary 100 µM 5-HT-induced changes of $[Ca^{2+}]_{cilium}$ and $[Ca^{2+}]_{cyt}$, showing a greater Ca^{2+} increase in the primary cilium compared to the cytosol. Values represent the mean fluorescence ± SEM; # significant differences with unpaired *t*-test to cyt, $p < 0.05$; (n) = number of cells.

The results show a significantly higher increase in $[Ca^{2+}]_{cilium}$, however $[Ca^{2+}]_{cyt}$ still follows the same pattern as $[Ca^{2+}]_{cilium}$. This may be explained because the 5HT6 sensor is also expressed in the PM.

4.2.4. Origin of the Ca^{2+} signals

To study the Ca^{2+} signalling mechanisms in the primary cilium, several inhibitors were used to determine whether the Ca^{2+} signals originate from the ER or from the extracellular environment.

Initially, store depletion experiments were performed (Figure 4.9). Surprisingly, blocking of the SERCA pump with 10 µM CPA under Ca^{2+} free condition, did not induce a Ca^{2+} rise as expected due to the leak of Ca^{2+} from the ER. Conversely, subsequent restitution of extracellular Ca^{2+} while CPA is still present resulted in Ca^{2+} increase, which can be interpreted as Ca^{2+} influx by SOCE (Figure 4.9 A, B). In addition, the effect of CPA in the presence of extracellular Ca^{2+} was measured, revealing a Ca^{2+} increase which

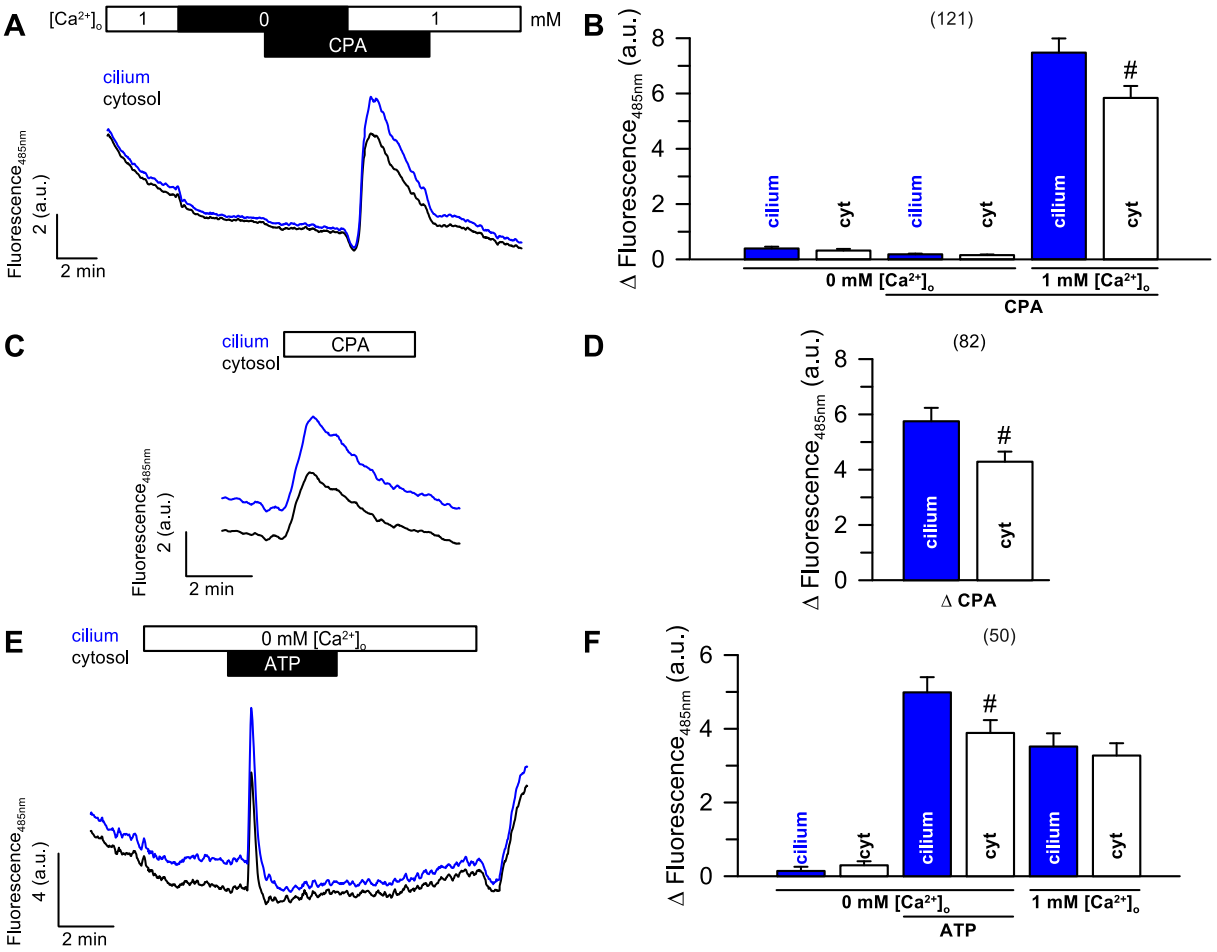

Figure 4.9 – Store depletion effect on ciliary Ca^{2+} signalling. Original mean tracings of $[Ca^{2+}]_{cilium}$ and $[Ca^{2+}]_{cyt}$ from MDCK 5HT6 cells (4-6 d Ø FBS) when 10 µM CPA is added in the **(A)** absence or **(C)** presence of extracellular Ca^{2+} and **(E)** 100 µM ATP stimulation under Ca^{2+} free condition. **(B, D, F)** Corresponding summaries of $[Ca^{2+}]_{cilium}$ and $[Ca^{2+}]_{cyt}$ changes upon CPA or ATP treatment with and without extracellular Ca^{2+}. Values represent mean ± SEM; # significant differences with unpaired *t*-test to cyt, $p < 0.05$; (n) = number of cells.

also indicates that this may correspond to an influx of Ca^{2+} (Figure 4.9 C, D). On the other hand, ATP stimulation under Ca^{2+} free condition revealed an increase of Ca^{2+} in the cilium, as well as the cytosol (Figure 4.9 E, F). In short, these results indicate that the sensor is unable to measure the Ca^{2+} leakage from the stores, although it can measure Ca^{2+} influx induced by SOCE, as well as store release induced by ATP.

For a better understanding of the Ca^{2+} signalling mechanisms upon store depletion of MDCK 5HT6 cells, cytosolic Ca^{2+} changes were measured with Fura-2 (Figure 4.10). Stimulation with 100 µM ATP reveals a $[Ca^{2+}]_i$ increase with a typical peak and plateau response (Figure 4.10 A, B). Moreover, some batches of cells showed a high basal Ca^{2+} (Figure 4.10 C, D, F, G) that decreases to ~50 nM under Ca^{2+} free. In these cells, treatment with 10 µM CPA or 100 µM ATP in the absence of extracellular Ca^{2+} caused only a small $[Ca^{2+}]_i$ increase (Figure 4.10).

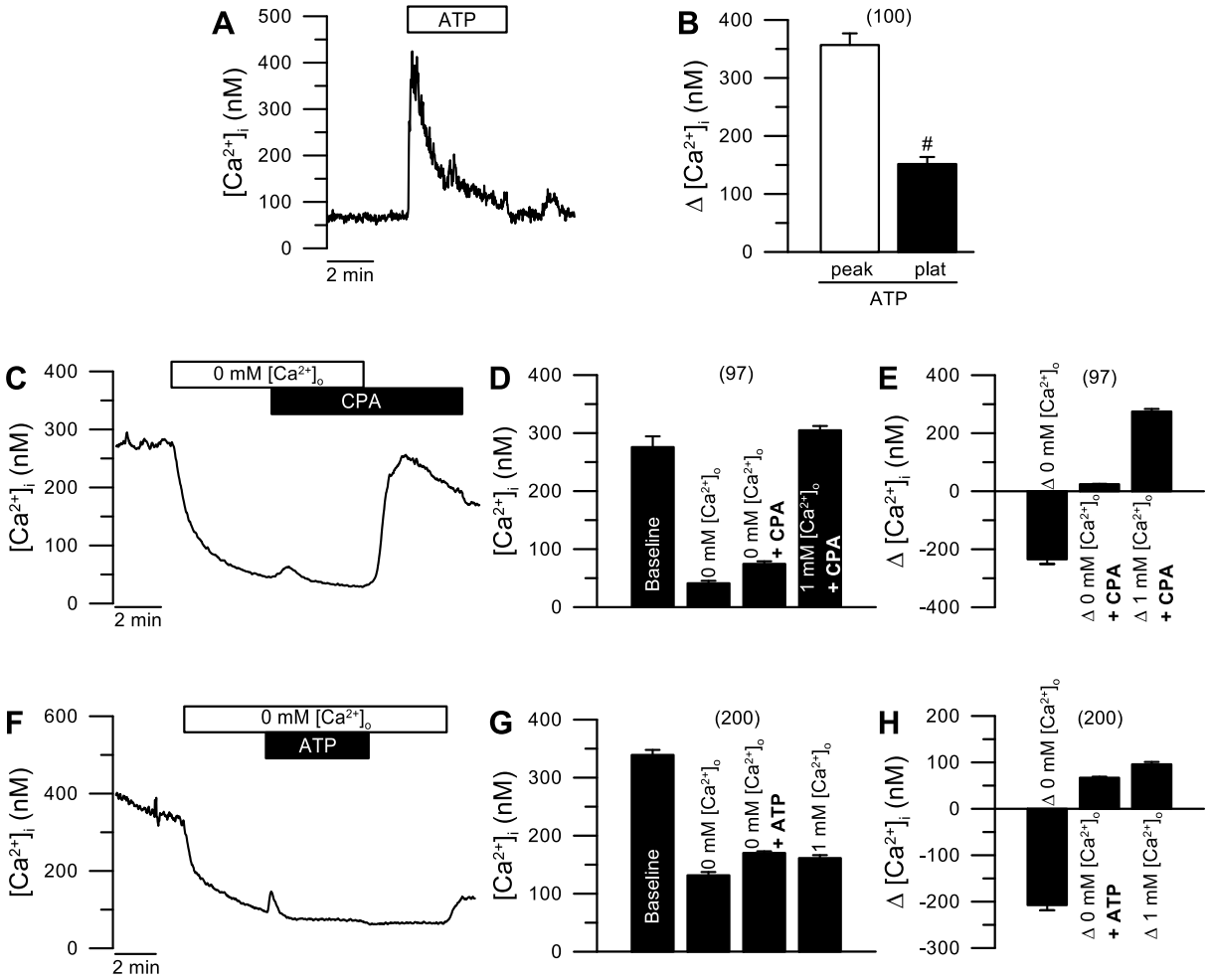

Figure 4.10 – Store depletion effect on $[Ca^{2+}]_i$ from MDCK 5HT6 cells. Original tracings of $[Ca^{2+}]_i$ from MDCK 5HT6 cells (4-6d Ø FBS) treated with **(A)** 100 µM ATP, **(C)** 10 µM CPA in the presence or absence of extracellular Ca^{2+} and **(F)** 100 µM ATP in the absence of extracellular Ca^{2+}. The results show that this cells have a high basal $[Ca^{2+}]_i$ and that ATP and CPA under Ca^{2+} free have a small effect. Corresponding summaries of **(D, G)** $[Ca^{2+}]_i$ in absolute values and **(B, E, H)** $[Ca^{2+}]_i$ changes upon CPA or ATP treatment with and without extracellular Ca^{2+}. Values represent mean ± SEM; # significant differences with paired *t*-test to peak, $p < 0.05$; (n) = number of cells.

TRP channels are known to mediate Ca^{2+} influx in primary cilia, however it is not certain if these channels are involved in purinergic Ca^{2+} signalling in this organelle[34]. Therefore, two different TRP channel inhibitors were used to investigate the effect of influx blockade on MDCK 5HT6 cells: SKF, a non-selective SOCE inhibitor that inhibits TRP channels[78]; and ACA, a phospholipase A2 (PLA_2) inhibitor that also inhibits TRP channels[80].

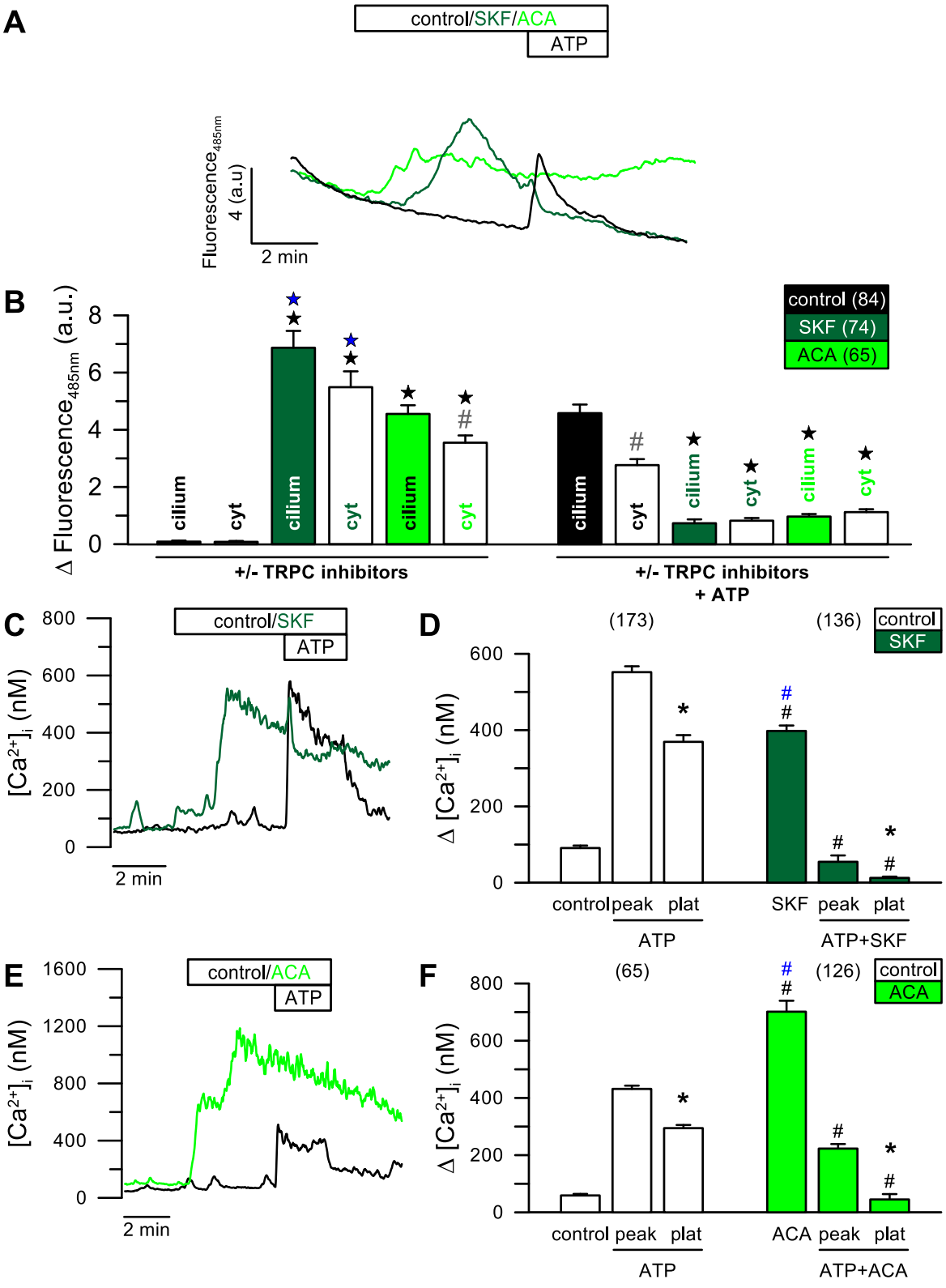

Figure 4.11 - Effect of TRPC inhibitors on ATP-induced Ca^{2+} response in the primary cilium. Original mean tracings of **(A)** $[Ca^{2+}]_{cilium}$ and **(C, E)** $[Ca^{2+}]_i$ from MDCK 5HT6 cells (4-6d Ø FBS) treated with 20 µM SKF or ACA in the presence of 100 µM ATP, compared to cells stimulated only with ATP. The data show an increase of $[Ca^{2+}]_{cilium}$ and $[Ca^{2+}]_i$ with both inhibitors, that resulted in the absence of ATP-induced Ca^{2+} increase. Summary of the effect of TRP channel (TRPC) inhibitors and subsequent purinergic response in **(B)** $[Ca^{2+}]_{cilium}$, $[Ca^{2+}]_{cyt}$, and **(D, F)** $[Ca^{2+}]_i$ showing that the inhibitors cause significant $[Ca^{2+}]$ increases by an unknown mechanism when the influx is blocked. Values represent mean ± SEM; # significant differences with unpaired t-test to cyt (grey), inhibitors to control (black; D, F) or inhibitors to ATP control (blue; D, F); * paired *t*-test peak to plat; ★ ANOVA inhibitors to control (black) or to ATP control (blue), $p < 0.05$; (n) = number of cells.

MDCK 5HT6 cells were treated with either 20 µM of SKF or ACA, followed by stimulation with 100 µM of ATP in the presence of the inhibitors (Figure 4.11). Unexpectedly, these compounds alone led to an increase of $[Ca^{2+}]_{cilium}$ and $[Ca^{2+}]_{cyt}$, and inhibited the ATP response (Figure 4.11 A, B). Indeed, Fura-2 measurements of cytosolic Ca^{2+} in cells treated with SKF or ACA in the same conditions revealed that the inhibitors itself cause a Ca^{2+} increase by an unknown mechanism (Figure 4.11 C-F). Because of this side effect, this results do not allow to take conclusions about the involvement of TRP channels. Nonetheless, absorbance measurements of the inhibitors revealed that they do not absorb at the wavelengths of the Ca^{2+} measurements, excluding possible fluorescence effects (Appendix IV – Absorbance measurements of the inhibitors Figure A VII and VIII).

As referred above, the ER constitutes one of the intracellular Ca^{2+} stores and ER Ca^{2+} store release is a well-known mechanism responsible for numerous cell processes[2]. To assess if the Ca^{2+} signal in the primary cilium originates in the ER, an IP_3R and a RyR inhibitor were used, Xestosopongin C (XeC)[81] and dantrolene[82], respectively.

Inhibition of RyR was explored by continuous perfusion of MDCK 5HT6 cells with 10 µM dantrolene, followed by stimulation with 100 µM ATP in the presence of the inhibitor (Figure 4.12 A, C). The results show that dantrolene alone causes a transient increase of $[Ca^{2+}]_{cilium}$ and $[Ca^{2+}]_{cyt}$, which led to the absence of ATP-induced response. This is a peculiar result, because it was not expected that Ca^{2+} would rise upon RyR inhibition. Inhibition of ATP-induced Ca^{2+} increase is consistent with ER Ca^{2+} store release blocking, however the initial Ca^{2+} rise caused by dantrolene prevents a clear interpretation

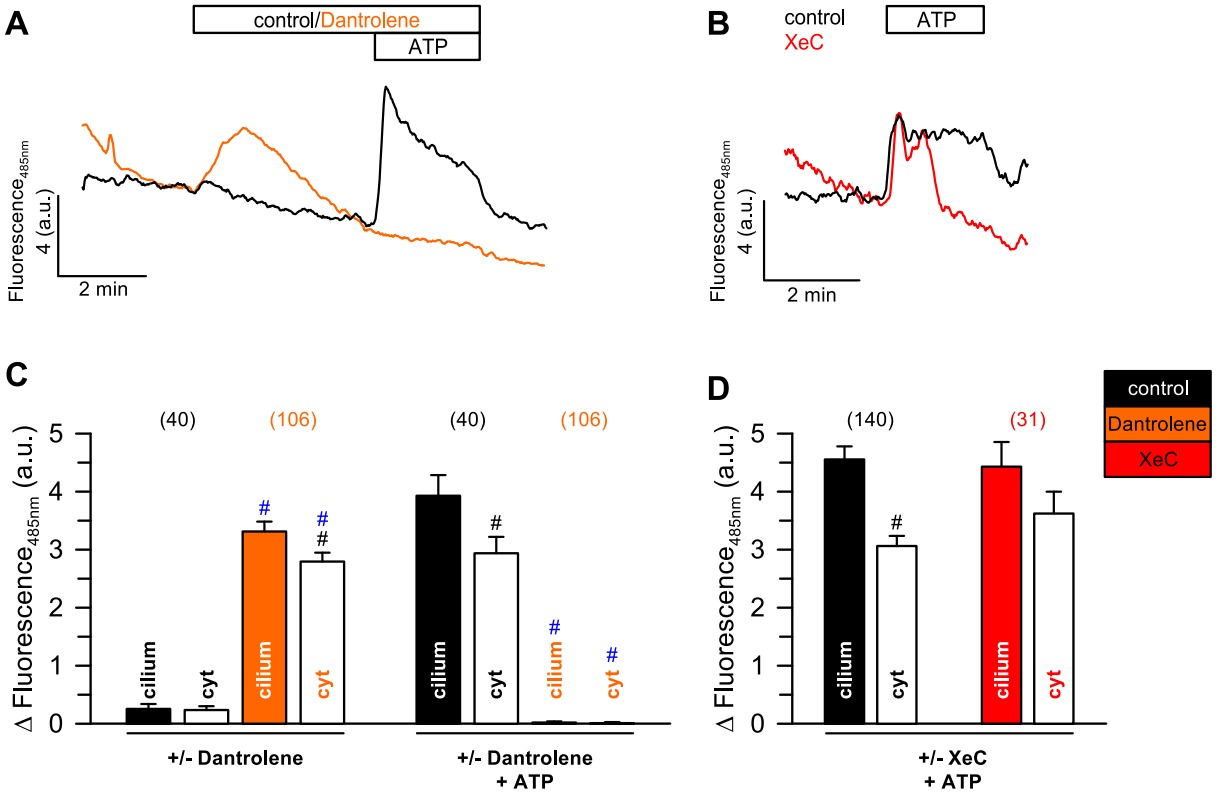

Figure 4.12 – Effect of RyR and IP_3R inhibitors on ATP-induced $[Ca^{2+}]$ increase in the primary cilium. Original tracings of $[Ca^{2+}]_{cilium}$ from MDCK 5HT6 cells (4-6d Ø FBS) treated with **(A)** 10 µM dantrolene in the presence of 100 µM ATP or **(B)** pre-incubated with 1 µM XeC for 2h and stimulated with 100 µM ATP. The data show an increase of $[Ca^{2+}]_{cilium}$ and $[Ca^{2+}]_{cyt}$ with dantrolene alone, that resulted in the absence of ATP-induced Ca^{2+} increase, while XeC did not cause differences in the ATP response. Summary of $[Ca^{2+}]_{cilium}$ and $[Ca^{2+}]_{cyt}$ changes upon treatment with **(C)** dantrolene and subsequent purinergic stimulation and **(D)** ATP-induced response with and without XeC pre-incubation. Values represent mean ± SEM; # significant differences with unpaired *t*-test to cyt (black) and dantrolene to control (blue), $p < 0.05$; (n) = number of cells.

of the results. Nevertheless, this inhibitor was also tested for possible fluorescence interferences, revealing no absorbance peak at the excitation wavelengths of the Ca^{2+} measurements (Appendix IV – Absorbance measurements of the inhibitors Figure A IX).

On the other hand, inhibition of IP_3R was performed by pre-incubation with 1 µM XeC for 2h before stimulation with 100 µM ATP, although it was not observable an inhibition of the ATP-induced response (Figure 4.12 B, D).

4.2.5. Influence of ANOs in ciliary Ca^{2+} signalling

There is growing evidence that ANOs are capable of modulating Ca^{2+} signalling and as some of these proteins are present in the primary cilium[56–58], it was of interest to study their effect in this region. For this purpose, different ANO inhibitors were used.

CaCC-A01 inhibitor is a specific ANO inhibitor[83,84] that caused a transient Ca^{2+} peak in the cilium, when perfused for ~5 min before ATP stimulation (Figure 4.13). Afterwards, purinergic stimulation with 100 µM ATP in the presence of this inhibitor did not induce a Ca^{2+} increase. The CaCC-A01 effect was tested for possible fluorescence interferences as well, which revealed that this inhibitor does not absorb at the wavelengths used for the Ca^{2+} measurements (Appendix IV – Absorbance measurements of the inhibitors, Figure A X). Although CaCC-A01 inhibited the ATP-induced response, these results are not conclusive, because the inhibitor caused an initial Ca^{2+} store release, which might be the reason why ATP has no effect.

Two additional ANO inhibitors were tested, NFA and TA, although they did not cause any effect on the ATP-induced Ca^{2+} response in cilia. This discrepancy may be explained by reduced accession of these compounds to ANOs in microdomains.

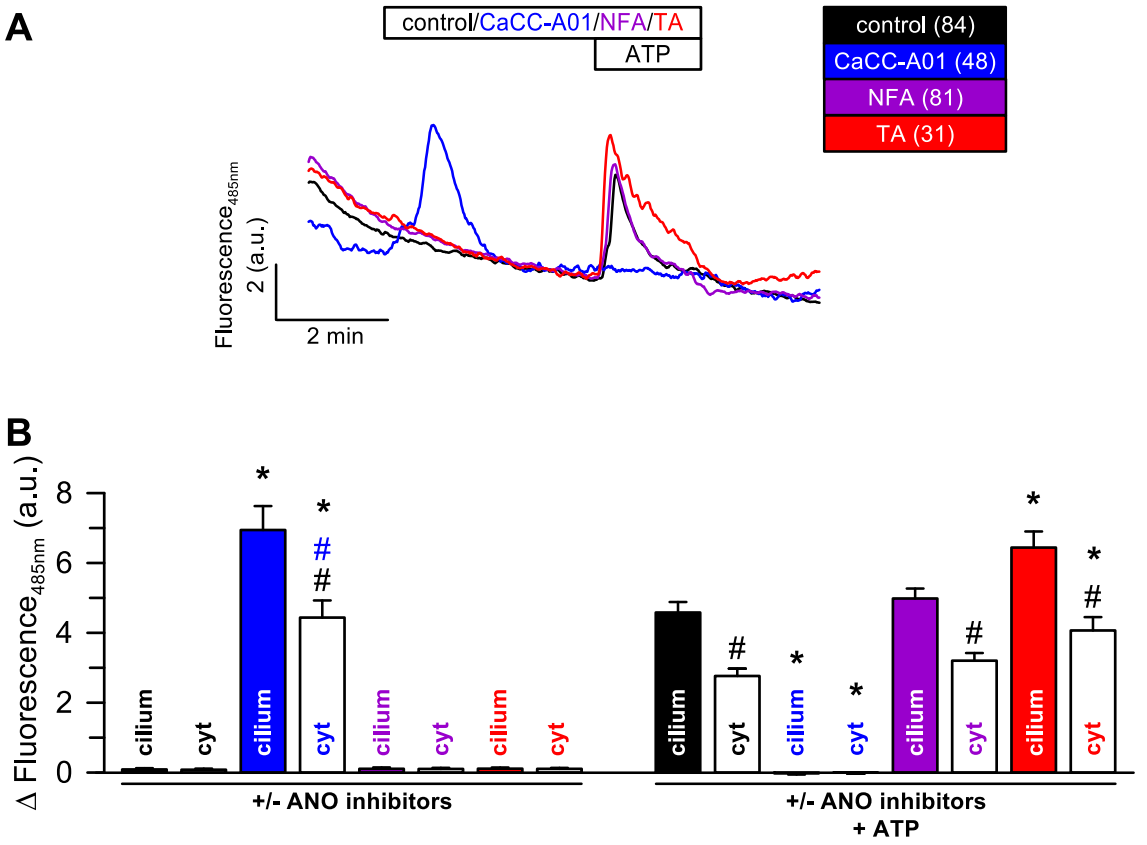

Figure 4.13 - Effect of ANO inhibitors on Ca^{2+} signalling in the primary cilium. (A) Original mean tracings of $[Ca^{2+}]_{cilium}$ from MDCK 5HT6 cells (4-6 Ø FBS) showing the ANO inhibitors (μM: 20 CaCC-A01, 20 NFA, 10 TA) effect. **(B)** Summary of $[Ca^{2+}]_{cilium}$ and $[Ca^{2+}]_{cyt}$ showing that CaCC-A01 alone causes a $[Ca^{2+}]$ increase, while NFA and TA do not cause the same effect nor affect the ATP-induced response. Values represent mean ± SEM; # significant differences with unpaired *t*-test to cyt (black) or CaCC-A01 to ATP control (blue); * ANOVA inhibitors to control; $p < 0.05$; (n) = number of cells.

5. DISCUSSION

Anoctamins play important physiological functions inside cells[15] and have been proposed to regulate Ca^{2+} signalling[27], which is a central mechanism for numerous cellular processes[2]. Thus, this work reports the importance of these Ca^{2+}-activated Cl^- channels for Ca^{2+} modulation in different microdomains.

Particularly, ANO1 and ANO4 were studied for their roles in Ca^{2+} regulation in the PM and ER, while compartmentalized Ca^{2+} signals in the primary cilium were also investigated, giving an initial insight concerning a possible role for Ca^{2+} modulation by ANOs in this sensory organelle.

5.1. GECOs constitute superior tools for localized Ca^{2+} signalling measurements

Fura-2 measurements are broadly used for biochemical studies of the physiological role of intracellular Ca^{2+} concentrations ($[Ca^{2+}]_i$)[73]. However, since the physiologically relevant Ca^{2+} signalling occurs in shielded compartments disconnected from the global cytosolic Ca^{2+}, this might not be the best suited tool to detect possible effects of anoctamins on local Ca^{2+} signalling[27]. Indeed, ANO1 is proposed to have similar properties as its yeast homologue Ist2, tethering the ER to the PM[30] and possibly modulating Ca^{2+} signalling in close proximity to the PM[27].

The PM targeted Ca^{2+}-sensitive protein (PM-GCaMP2) consists of a N-terminal signal peptide from neuromodulin fused to GCaMP2, which is later palmitoylated and anchors the sensor to the PM[61–63]. Thus, this probe is more appropriate to measure Ca^{2+} changes close to the PM ($[Ca^{2+}]_P$) because it allows a better spatial resolution of Ca^{2+} signals[27] near the PM that might be masked when using Fura-2.

The primary cilium constitutes another specialized compartment for Ca^{2+} signalling, but given its small dimensions the interpretation of the signals is difficult. Measurements with Fura-2 or similar indicator dyes result in signal saturation of the entire cytosol and cannot detect local Ca^{2+} transients in primary cilia[34,49]. To overcome this problems, several cilium-targeting genetically encoded Ca^{2+} indicators for optical imaging (GECOs) were previously developed[41,49] and are formed by a CTS fused to the indicator protein GECO, which are similar to GCaMPs. The CTS enables the sensor to be connected to the cilium and consists of proteins expressed in this region[34,49]. In the case reported the CTS corresponds to the 5HT6 receptor or the Smo protein, in the sensors 5HT6-mCherry-GECO1.0 (5HT6-GECO) and SMO-Cherry-GECO (SMO-GECO), respectively[41,49]. These sensors are also connected to a mCherry protein, which functions as primary cilium marker independent of $[Ca^{2+}]$. GECO has a K_d of 749 nM, however this is of sufficient sensitivity to detect changes in $[Ca^{2+}]_{cilia}$ upon ATP stimulation[49], which can induce increases of Ca^{2+} up to a thousand nM[2].

Utilization of cilium-targeting Ca^{2+} indicators allows the monitoring of Ca^{2+} signals that are not diluted in the global cytosolic $[Ca^{2+}]$, consisting of a better approach to measure changes of Ca^{2+} in primary cilia. Indeed, using SMO-mCherry-GCaMP3 (a ciliary-GECO), Delling and co-workers were able to determine the resting ciliary Ca^{2+} concentration ($[Ca^{2+}]_{cilium}$) that is 580 nM[41], which is about five times higher than the cytosolic resting concentration[2].

5.2. [Ca^{2+}] modulation by ANOs in different subcellular domains

The anoctamin family of Ca^{2+}-activated Cl^- channels have possible functions as Ca^{2+} regulators in specific cellular domains, since they induce different Ca^{2+} responses upon cell stimulation. This was suggested recently in studies from our group[27,28,87] and confirmed through this work, using different Ca^{2+} indicators.

Recently, Schreiber *et al.*[28] showed that ANO1 is able to support Cl^- secretion in mouse intestine by facilitating Ca^{2+} signalling. In addition, last year, Inês Cabrita demonstrated in her Master thesis that different overexpressed anoctamins led to distinct purinergic-induced Ca^{2+} responses, of which ANO4 was shown to decrease intracellular Ca^{2+} signalling, while ANO1 enhanced Ca^{2+} signals near the PM. The effect of ANO4 was then thought to be due to a decreased [Ca^{2+}] inside the stores. Thus, to evaluate this question, global cytosolic Ca^{2+} ($[Ca^{2+}]_i$) changes were measured in HeLa cells overexpressing ANO1 or ANO4 and store depletion protocols using ATP, CPA or ionomycin under extracellular free Ca^{2+} conditions were performed.

ATP stimulation induces the ER store release[7], typically represented by a Ca^{2+} peak, followed by a plateau corresponding to Ca^{2+} influx, which in this case was not observed due to the absence of extracellular Ca^{2+} (Figure 5.1). The cells were subsequently treated with CPA, a SERCA pump inhibitor[76], that induces the complete depletion of the ER store through a slow leak of Ca^{2+} to the cytosol. This experiment revealed that ANO4 overexpressing cells had diminished $[Ca^{2+}]_i$ peaks upon ATP and CPA stimulation, while ANO1 overexpressing cells did not show significant differences to control. However, considering that ANO4 depletes the Ca^{2+} stored in the ER, it was expected a stronger influx through SOCE after restoring the extracellular Ca^{2+} or a higher baseline in ANO4 overexpressing cells.

Therefore, an additional model was used to prove this hypothesis, using the ionophore ionomycin in the absence of extracellular Ca^{2+} in a second store depletion experiment. This revealed once more that ANO4 overexpressing cells had smaller $[Ca^{2+}]_i$ peaks, while ANO1 did not show an effect on $[Ca^{2+}]_i$. For this reason, together these results suggest that ANO4 might decrease the Ca^{2+} content inside the ER store. In addition, $P2Y_2$ expression HEK293 cells were used to assess the effect of ANO4 overexpression in the [Ca^{2+}] inside the intracellular stores. Reduction of the [Ca^{2+}] in the stores should activate Orai1 by SOCE. This was evaluated using the specific Orai1 inhitior YM-58483, which is a potent CRAC channel inhibitor that blocks SOCE[75]. Indeed basal $[Ca^{2+}]_i$ was enhanced and YM-58483 action demonstrated a greater drop in ANO4 overexpressing cells.

Overexpression of the $P2Y_2$ receptors resulted in a higher ATP-induced response that was significantly reduced by overexpression of ANO4 in $P2Y_2$ transfected cells. The HEK293 $[Ca^{2+}]_i$ data corroborates the previous HeLa results, suggesting a reduced [Ca^{2+}] inside the ER store in ANO4 overexpressing cells, that can be due to inhibition of SERCA, causing an impaired store refilling, or due to extra leakage of Ca^{2+} to the cytoplasm, both resulting in the higher basal Ca^{2+} (Figure 5.1). This increased $[Ca^{2+}]_i$ was sensitive to the Orai1-inhibitor that caused a pronounced drop in the basal Ca^{2+} from ANO4 and $P2Y_2$ co-expressing cells, suggesting that the ANO4 action results in activation of Orai1 by SOCE.

Interestingly, ANO4 was identified as a Ca^{2+}-dependent lipid scramblase that shares 40,7% sequence similarity with ANO6, having a comparable degree of phosphatidylserine (PS) exposure. Curiously, the endogenous Ca^{2+} level was sufficient to activate the ANO4 scramblase activity[88]. Also, ANO6 was

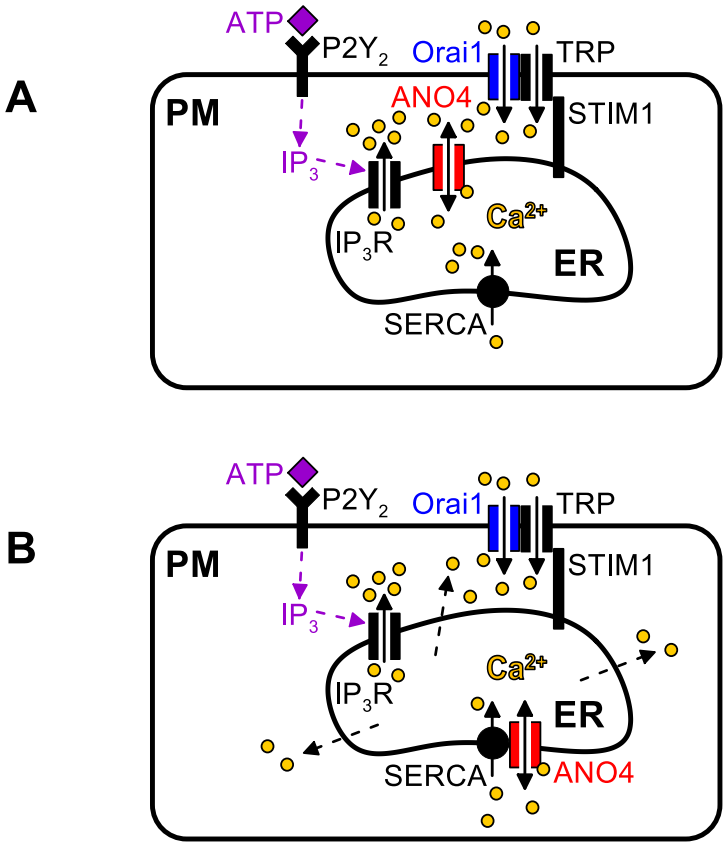

Figure 5.1 – ANO4 decreases intracellular Ca^{2+} signalling by induction of Ca^{2+} leakage or inhibition of SERCA pump. Simplified representation of the Ca^{2+} signalling mechanisms involving ANO4. ATP triggers the IP_3 pathway, promoting Ca^{2+} release through IP_3R. **(A)** ANO4 might conduct Ca^{2+} through SCAN, similarly to ANO6; or **(B)** it may inhibit the SERCA pump, causing Ca^{2+} to diffuse out of the ER to the cytoplasm.

found to produce a small-conductance Ca^{2+}-activated nonselective cation (SCAN) current, with a high permeability to Ca^{2+} ions[22]. This channel is located in the PM, therefore other ANO members are likely to be in the membrane as well. On the other hand, it is also possible that they form scramblases in intracellular membranes, in the manner of ANO5, which is present in intracellular vesicles[88]. Therefore, given the similarity between ANO4 and ANO6, it is possible that ANO4 conducts Ca^{2+} in a comparable way, supporting its role in decreasing Ca^{2+} in the ER (Figure 5.1).

It had already been proposed that activation of endogenous anoctamins requires the triggering of specific Ca^{2+} release and/or influx pathways[16]. Therefore, PM-GCaMP2 was used to study the ATP-induced $[Ca^{2+}]$ changes in PM microdomains ($[Ca^{2+}]_P$) where transient $[Ca^{2+}]_P$ peaks corresponding to ER store release were obtained. HeLa cells co-expressing the PM-GCaMP2 sensor with ANO1 or ANO4 were stimulated with ATP under extracellular Ca^{2+} free condition, demonstrating an enhanced $[Ca^{2+}]_P$ peak when ANO1 is overexpressed, whereas ANO4 overexpression resulted in a decreased $[Ca^{2+}]_P$ peak. This data suggest that ANO1 might modulate Ca^{2+} in close proximity to the PM, increasing its concentration in this location. On the other hand, considering that ANO4 decreases the Ca^{2+} content in the ER, it is likely that the ATP-induced $[Ca^{2+}]_P$ response is lower in ANO4 overexpressing cells.

With the discovery of the ANO yeast homologue Ist2 as a tethering protein that is able to make ER and PM contacts[30,31], a possible connection between Ist2 and the function of ANO1 in microdomains was suggested. Therefore, the $[Ca^{2+}]_P$ upon ATP stimulation was measured in Ist2 overexpressing cells as well as in nhTMEM16 overexpressing cells, the ANO fungal homologue, and was compared to the

ANO1 overexpression effect in the $[Ca^{2+}]_P$. Overexpression of these two homologues induced enhanced $[Ca^{2+}]_P$ peaks, an effect similar to overexpression of ANO1.

The localized Ca^{2+} increase close to the PM in ANO1 overexpressing cells is supported by the findings of Jin *et al.*, that claim that ANO1 is activated by Ca^{2+} transients that are channeled towards ANO1, in dorsal root ganglia. They hypothesized that ANO1 is preferentially activated by Ca^{2+} released from the ER, independently of Ca^{2+} influx through voltage-gated Ca^{2+} channels (VGCCs), due to juxtaposition of ANO1 with IP_3R that are separated from VGCCs[32]. Similarly, the Ist2 protein was also shown to make ER-PM interactions, tethering the ER to the PM through a C-terminus polybasic domain[31,32]. However, ANO1 does not possess such a domain and the human anoctamin that shares the highest degree of similarity with Ist2 is ANO10[32]. These constitute very interesting findings, but more information is needed in order to make clear assumptions.

5.3. Cell lines overexpressing ciliary GECOs

The primary cilium is a specialized sensory organelle that is tightly related to Ca^{2+} signalling[41]. Therefore, it was interesting to develop cell lines expressing ciliary-targeting GECOs, which constitute sensitive Ca^{2+} sensors.

MDCK M2 and RPE cells constitute suitable cell lines to study the primary cilium, since they can develop cilia easily in the absence of proliferative stimuli[38]. However, transient transfection is often difficult and expression can be lost while culturing cells in serum free media. Typically, cells take around 4d to develop primary cilia, hence the need for a stably expressing cell line. Thus, it was attempted to develop cell lines stably expressing the sensors 5HT6-GECO and SMO-GECO.

Expression of the ciliary Ca^{2+} sensors in the stably transfected cells was confirmed by immunolocalization of acetylated tubulin with GFP. Tubulin acetylation is a dynamic process that occurs inside microtubules[89] and since they constitute the primary cilium cytoskeleton[37], acetylated tubulin is widely used as a ciliary marker. On the other hand, GFP was used as a marker to detect the GECO sensor.

This subcellular localization study demonstrated that both cell lines express the sensors not only in the primary cilium but also in the PM or even other internal membranes (Figure 5.2). It also showed that the expression of the sensor is not homogeneous, being present a mixture of transfected and non-transfected cells. In the case of the RPE 5HT6-GECO cell line, only a few cells expressed the sensor but it did not co-localized with acetylated tubulin.

These problems can be explained by random integration of the plasmid in the cells during cell replication[90]. In this process, the circular plasmid is randomly opened by endogenous enzymes and is inserted in the chromosome. If, by chance, when the plasmid is cut it loses or is separated from the CTS but maintains the GECO and/or mCherry genes, the cells can express these proteins elsewhere apart from the cilium. Nevertheless, in MDCK 5HT6-GECO cells, it was possible to create a superimposed image from a set of pictures of a cut view of a single primary cilium pointing upwards, showing co-localization of acetylated tubulin with the sensor. Subsequent Ca^{2+} measurements from the primary cilium were performed using these cells after ciliogenesis induction by serum starvation for 4-6d.

Initially, the activation of the Ca^{2+} signalling in the primary cilium was tested stimulating cells with ATP, which induced a $[Ca^{2+}]$ increase in both the cilium ($[Ca^{2+}]_{cilium}$) and the cytosol ($[Ca^{2+}]_{cyt}$), because of the localization of the sensor in both regions (Figure 5.2). Still, the increase in $[Ca^{2+}]_{cilium}$ was significantly higher than in $[Ca^{2+}]_{cyt}$, proving that this cell line can be very useful since it allows the monitoring of distinct $[Ca^{2+}]$ changes in two different regions at the same time.

This can be compared to Delling *et al.* findings, that using a similar ciliary-targeting Ca^{2+} indicator (SMO-GCaMP3) were also able to detect $[Ca^{2+}]$ changes in primary cilia and cytosol simultaneously. With this sensor, the investigators discovered that rupture of the ciliary tip with a laser pulse caused a fast increase in $[Ca^{2+}]_{cilium}$, whereas $[Ca^{2+}]_{cyt}$ had a small increase seconds later[41].

Additionally, MDCK 5HT6-GECO cells were stimulated with serotonin (5-HT)[77] to evaluate if this would induce a more specific response, once 5HT6 receptors are a subtype of serotonin receptors that localize to primary cilia[91]. However, 5-HT stimulation lead to a response similar to purinergic ATP stimulation, with a higher increase in $[Ca^{2+}]_{cilium}$ than in $[Ca^{2+}]_{cyt}$, which is explained by the expression of the 5HT6 sensor in the PM besides the cilium.

Following this, it was studied whether the Ca^{2+} signals in the primary cilium originate from the ER or from the extracellular environment using several inhibitors. To do so, $[Ca^{2+}]_{cilium}$ and $[Ca^{2+}]_{cyt}$ measurements from MDCK 5HT6-GECO cells were compared to $[Ca^{2+}]_i$ measurements from the same cell line, using the SERCA pump blocker CPA and ATP in the presence and absence of extracellular free Ca^{2+} (Figure 5.2).

When measuring $[Ca^{2+}]_{cilium}$ and $[Ca^{2+}]_{cyt}$ it was not observed a Ca^{2+} increase due to leakage from the ER upon blocking of SERCA by CPA under Ca^{2+} free condition (Figure 5.2). It was only observed when Ca^{2+} was restored in the continuous presence of CPA, or when CPA was applied in the presence of extracellular Ca^{2+}. In these conditions, the response might correspond to Ca^{2+} influx through SOCE. This could be explained by the finding that some batches of cells have a high basal $[Ca^{2+}]_i$ (~280 nM), that is due to extracellular Ca^{2+} influx, supported by the reduction to ~50 nM under Ca^{2+} free condition. This influx is most likely required to fill the stores, since CPA and ATP caused only small $[Ca^{2+}]_i$ increases in the absence of extracellular Ca^{2+}. However, this could not be detected by 5HT6-GECO.

The effect of ATP under Ca^{2+} free in $[Ca^{2+}]_i$ from MDCK 5HT6-GECO cells was small, but in contrast the ATP-induced response in $[Ca^{2+}]_{cilium}$ and $[Ca^{2+}]_{cyt}$ was not affected by the removal of extracellular Ca^{2+}. This indicates that the 5HT6-GECO sensor is able to measure $[Ca^{2+}]$ in microdomains close to the plasma and ciliary membranes. In other words, this means that the Ca^{2+} release from the ER store measured by the sensor is not diluted in the whole cytosol. This Ca^{2+} increase in microdomains is indeed due to Ca^{2+} store release, because the ATP-induced $[Ca^{2+}]_{cilium}$ and $[Ca^{2+}]_{cyt}$ changes are transient without a plateau phase, unlike the $[Ca^{2+}]_i$ measurements which show clear peak and plateau phases.

Experiments from MDCK 5HT6-GECO cells using the RyR inhibitor dantrolene[82] and the IP3R inhibitor XeC[81], as well as experiments with TRP channel inhibitors (SKF[78,79] and ACA[80]) were performed in order to understand how Ca^{2+} signalling in the cilium is processed. XeC was not able to block the ATP-induced Ca^{2+} response, whereas dantrolene inhibited the ATP effect. This could be due to Ca^{2+}-induced Ca^{2+} release (CICR), however dantrolene alone led to a Ca^{2+} increase by an unknown mechanism, which precludes a clear statement. It is possible that the Ca^{2+} influx that fills the stores is

dependent on TRP channel activation, but a similar secondary effect occurred with the TRP channel inhibitors, hindering plausible conclusions.

Considering the growing evidences on Ca^{2+} modulation by ANOs[27,32] and given that some of them were shown to be present in the primary cilium[56,57], initial experiments using ANO inhibitors were performed in MDCK 5HT6-GECO cells to access their role in this small sensitive organelle. Three different inhibitors were used (CaCC-A01[83,84], NFA[18] and TA[85]), from which only CaCC-A01 reduced the ATP-induced response in the $[Ca^{2+}]_{cilium}$ and $[Ca^{2+}]_{cyt}$ (Figure 5.2). These differences might be explained because CaCC-A01 is a more specific ANO inhibitor or because the other inhibitors have no access to ANOs in the microdomains. In fact, NFA and TA are relatively big organic molecules, that may not be able to enter the narrow intraciliary space. But then again, the compound itself increased the $[Ca^{2+}]$ in the microdomains by an unknown mechanism, during the pre-incubation prior to ATP stimulation, making the interpretation of the processes unclear.

There was the possibility that these strange Ca^{2+} increases caused by some of the inhibitors used (dantrolene, SKF, ACA and CaCC-A01) were due to fluorescence interference, although this was excluded given that these compounds do not absorb at the wavelengths used for the Ca^{2+} measurements (Appendix IV – Absorbance measurements of the inhibitors, Figure A VII-X).

It is speculated that the unknown mechanisms referred might include alterations in the intracellular pH or metabolites caused by the inhibitors that then lead to the Ca^{2+} increases. Some authors refer that indeed SKF can cause a transient Ca^{2+} increase at high concentrations of the inhibitor, which they observe in intracellular Ca^{2+} measurements from platelets[78]. Similarly, other investigators indicate that this inhibitor blocks SOCE and TRP channels, although it elevates intracellular Ca^{2+} [92]. A different group was able to detect the SKF effect without a secondary Ca^{2+} rise effect by pre-incubating cells with the inhibitor for 50 min. This led to the complete blocking of SOCE in DGR neurons[93]. Given this observations, maybe similar effects occur with the remaining inhibitors.

Nevertheless, it is of note that there are publications suggesting the involvement of anoctamins in the primary cilium. Particularly, the work from Ruppersburg and Hartzell, who showed that ANO1 is present in the primary cilium from cultured collecting duct cells and that the Cl^- transport mediated by this channel is required for ciliogenesis[57]. Considering this, it is speculated that ANO1 might play a role in Ca^{2+} signalling in the primary cilium in a similar fashion as epithelial and dorsal root ganglia cells. In another study, Forschbach *et al.*, discovered that ANO6 is localized in the primary cilium of the renal epithelium from MDCK cells and is functionally relevant for cyst formation *in vitro* and *in vivo*[56]. This channel was also found in the primary cilium from RPE cells, along with ANO10, but their function in these cells is still under examination[87]. Therefore, according to these discoveries, evidence points out towards a function of anoctamins in the regulation of Ca^{2+} signals inside the primary cilium.

In conclusion, it seems that the anoctamin family has exciting new functions besides Cl^- transport, particularly its involvement in Ca^{2+} modulation in several microdomains, which can be studied using diverse Ca^{2+} indicators targeted to specific subcellular localizations.

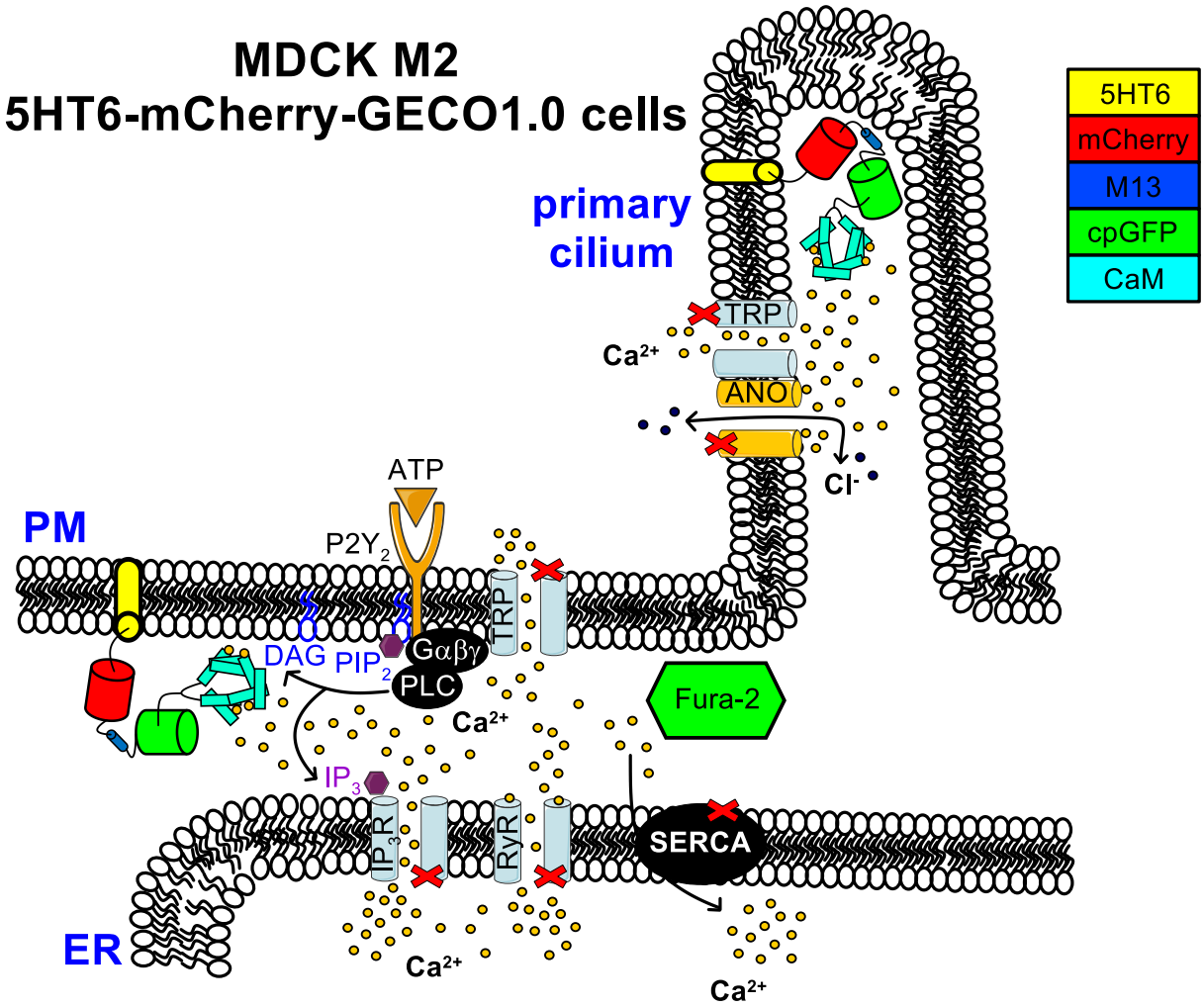

Figure 5.2 – Schematic representation of the possible Ca^{2+} mechanisms occurring in ciliated MDCK 5HT6-GECO cells. MDCK M2 cells were stably transfected with the 5HT6-mCherry-GECO1.0 (5HT6-GECO) sensor that is localized in the primary cilium, but also in the PM. It possesses a CTS, the 5HT6 receptor, targeting the protein preferentially to the primary cilium. It is fused to a mCherry protein, used as a ciliary marker independent of the [Ca^{2+}]. The Ca^{2+} sensitive part consists of a myosin light chain kinase (M13) connected to a circularly permuted GFP protein (cpGFP) and to calmodulin (CaM), that binds Ca^{2+} ions. Studies with this sensor were addressed in parallel with $[Ca^{2+}]_i$ measurements using Fura-2 and purinergic stimulation with ATP was combined with several inhibitors. ATP binds the purinergic receptor $P2Y_2$, triggering PLC activation through G proteins, resulting in PIP_2 cleavage in DAG and IP_3. The second messenger IP_3 then binds to IP_3R inducing Ca^{2+} release from the ER. The components blocked are marked with a cross and include the SERCA pump, which drives Ca^{2+} back into the ER; TRP channels, Ca^{2+} influx channels present in the primary cilium as well as the PM; IP_3R and RyR, responsible for Ca^{2+} release from the internal stores; and ANOs, that were recently identified in the primary cilium.

6. FUTURE PERSPECTIVES

The functional properties of anoctamins begin to be disclosed, with evidences pointing towards a new role in Ca^{2+} signalling modulation in different microdomains. Their proposed function in regulating Ca^{2+} signals in specific regions might be on the verge to explain the great diversity of anoctamin related diseases. Therefore, it is of utmost importance to pursue investigations that can lead to a better understanding of the underlying Ca^{2+} mechanisms controlled by ANOs.

Throughout this work, several proteins were overexpressed, for instance ANOs and their homologues. In spite of that, it would also be useful to couple the study of endogenous proteins by silencing their expression, because overexpression systems often lead to heterogeneous plasmid uptake.

Regarding the cell lines expressing the ciliary targeting Ca^{2+} indicators, several procedures might be done to improve the expression of the protein and targeting efficacy. First of all, to prevent complications caused by random integration of the plasmid in the cell chromosome, a better transfection system could be used, for example a lentivirus infection system combined with linearization of the circular plasmid. Also, to obtain a homogeneous population of stably transfected cells, they should be repeatedly subcloned until a monoclonal cell line is achieved, or alternatively, since the sensor is constituted by fluorescent proteins, the expression of the indicator could be enriched by fluorescence-activated cell sorting.

Another interesting topic that deserves more attention is the optimization of the spatial and temporal resolution of the Ca^{2+} measurements in the primary cilium, which could be decisive to determine the sequence of events of the Ca^{2+} signal in this region. More specifically, how is the Ca^{2+} signalling processed, does it occur first in the cytosol or in the cilium?

The inhibitors used to study the Ca^{2+} mechanisms in the primary cilium sometimes resulted in unexpected increases on the intracellular Ca^{2+}. On that account, to fully understand the Ca^{2+} signalling in this petite sensory organelle, experiments using inhibitors that do not lead to undesired effects on the Ca^{2+} levels are needed.

Finally, a great asset would be the generation of cell lines or even animal models that express the microdomain targeting Ca^{2+} probes endogenously, for example PM-GCaMP2 or 5HT6-GECO. Afterwards, using these tools ANO knockdowns could be further performed, which would give a much better insight about the function of these Ca^{2+}-activated Cl^- channels for Ca^{2+} signalling.

7. REFERENCES

1. Clapham, D. E. Calcium Signaling. *Cell* **131,** 1047–1058 (2007).

2. Berridge, M. J., Lipp, P. & Bootman, M. D. The versatility and universality of calcium signalling. *Nat. Rev. Mol. Cell Biol.* **1,** 11–21 (2000).

3. Mikoshiba, K. IP3 receptor/Ca2+ channel: From discovery to new signaling concepts. *J. Neurochem.* **102,** 1426–1446 (2007).

4. Pozzan, T., Rizzuto, R., Volpe, P. & Meldolesi, J. Molecular and cellular physiology of intracellular calcium stores. *Physiol. Rev.* **74,** 595–636 (1994).

5. Schreiber, R. Ca2+ signaling, intracellular pH and cell volume in cell proliferation. *J. Membr. Biol.* **205,** 129–137 (2005).

6. Salter, M. W. & Hicks, J. L. ATP causes release of intracellular Ca2+ via the phospholipase C beta/IP3 pathway in astrocytes from the dorsal spinal cord. *J. Neurosci.* **15,** 2961–2971 (1995).

7. Viana, F., De Smedt, H., Droogmans, G. & Nilius, B. Calcium signalling through nucleotide receptor P(2Y2) in cultured human vascular endothelium. *Cell Calcium* **24,** 117–127 (1998).

8. Boron, W. F. & Boulpaep, E. L. *Medical Physiology*. *Physiology* (2012). doi:10.1136/pgmj.51.599.683-c

9. Wang, Y., Deng, X., Hewavitharana, T., Soboloff, J. & Gill, D. L. STIM, ORAI and TRPC channels in the control of calcium entry signals in smooth muscle. *Clin. Exp. Pharmacol. Physiol.* **35,** 1127–1133 (2008).

10. Feske, S. *et al.* A mutation in Orai1 causes immune deficiency by abrogating CRAC channel function. *Nature* **441,** 179–185 (2006).

11. Putney, J. W. Capacitative calcium entry: From concept to molecules. *Immunol. Rev.* **231,** 10–22 (2009).

12. Blaustein, M. P., Blaustein, M. P., Lederer, W. J. & Lederer, W. J. Sodium/calcium exchange: its physiological implications. *Physiol. Rev.* **79,** 763–854 (1999).

13. Hartzell, C., Putzier, I. & Arreola, J. Calcium-Activated Chloride Channels. *Annu. Rev. Physiol.* **67,** 719–758 (2005).

14. Eggermont, J. Calcium-activated Chloride Channels: (Un)known, (Un)loved? *Proc. Am. Thorac. Soc.* **1,** 22–27 (2004).

15. Kunzelmann, K. *et al.* Anoctamins. *Pflugers Arch. Eur. J. Physiol.* **462,** 195–208 (2011).

16. Tian, Y., Schreiber, R. & Kunzelmann, K. Anoctamins are a family of Ca2+-activated Cl-channels. *J. Cell Sci.* **125,** 4991–4998 (2012).

17. Duran, C. & Hartzell, H. C. Physiological roles and diseases of Tmem16/Anoctamin proteins: are they all chloride channels? *Acta Pharmacol. Sin.* **32,** 685–92 (2011).

18. Pedemonte, N. & Galietta, L. J. V. Structure and function of TMEM16 proteins (anoctamins). *Physiol. Rev.* **94,** 419–59 (2014).

19. Yang, H., Jin, T., Cheng, T., Jan, Y. N. & Jan, L. Y. Scan: A Novel Small-Conductance Ca2+-Activated Non-Selective Cation Channel Encoded by TMEM16F. *Biophys. J.* **100,** 259a (2011).

20. Schroeder, B. C., Cheng, T., Jan, Y. N. & Jan, L. Y. Expression Cloning of TMEM16A as a Calcium-Activated Chloride Channel Subunit. *Cell* **134,** 1019–1029 (2008).

21. Billig, G. M., Pál, B., Fidzinski, P. & Jentsch, T. J. Ca2+-activated Cl− currents are dispensable for olfaction. *Nat. Neurosci.* **14,** 763–769 (2011).

22. Yang, H. *et al.* TMEM16F forms a Ca2+-activated cation channel required for lipid scrambling in platelets during blood coagulation. *Cell* **151,** 111–22 (2012).

23. Caputo, A. *et al.* TMEM16A, a membrane protein associated with calcium-dependent chloride channel activity. *Science* **322,** 590–594 (2008).

24. Yang, Y. D. *et al.* TMEM16A confers receptor-activated calcium-dependent chloride conductance. *Nat. …* **455,** 1210–1215 (2008).

25. Brunner, J. D., Lim, N. K., Schenck, S., Duerst, A. & Dutzler, R. X-ray structure of a calcium-activated TMEM16 lipid scramblase. *Nature* **516,** 207–212 (2014).

26. Whitlock, J. M. & Hartzell, H. C. A Pore Idea: the ion conduction pathway of TMEM16/ANO proteins is composed partly of lipid. *Pflugers Arch. Eur. J. Physiol.* **468,** 455–473 (2016).

27. Kunzelmann, K. *et al.* Modulating Ca2+ signals: a common theme for TMEM16, Ist2, and TMC. *Pflugers Arch. Eur. J. Physiol.* **468,** 475–490 (2016).

28. Schreiber, R. *et al.* Anoctamins support calcium-dependent chloride secretion by facilitating calcium signaling in adult mouse intestine. *Pflugers Arch. Eur. J. Physiol.* **467,** 1203–1213 (2014).

29. Barrett, K. E. & Keely, S. J. Chloride secretion by the intestinal epithelium: molecular basis and regulatory aspects. *Annu. Rev. Physiol.* **62,** 535–572 (2000).

30. Wolf, W. *et al.* Yeast Ist2 recruits the endoplasmic reticulum to the plasma membrane and creates a ribosome-free membrane microcompartment. *PLoS One* **7,** (2012).

31. Manford, A. G., Stefan, C. J., Yuan, H. L., MacGurn, J. A. & Emr, S. D. ER-to-Plasma Membrane Tethering Proteins Regulate Cell Signaling and ER Morphology. *Dev. Cell* **23,** 1129–1140 (2012).

32. Jin, X. *et al.* Activation of the Cl- channel ANO1 by localized calcium signals in nociceptive sensory neurons requires coupling with the IP3 receptor. *Sci. Signal.* **6,** ra73 (2013).

33. Sorokin, S. P. Reconstructions of centriole formation and ciliogenesis in mammalian lungs. *J. Cell Sci.* **3,** 207–30 (1968).

34. Phua, S. C., Lin, Y. C. & Inoue, T. An intelligent nano-antenna: Primary cilium harnesses TRP channels to decode polymodal stimuli. *Cell Calcium* **58,** 415–422 (2015).

35. Satir, P. & Christensen, S. T. Structure and function of mammalian cilia. *Histochem. Cell Biol.* **129,** 687–693 (2008).

36. Alaiwi, W. A. A., Lo, S. T. & Nauli, S. M. Primary cilia: Highly sophisticated biological sensors. *Sensors* **9,** 7003–7020 (2009).

37. Satir, P. & Christensen, S. T. Overview of structure and function of mammalian cilia. *Annu. Rev. Physiol.* **69,** 377–400 (2007).

38. Basten, S. G. & Giles, R. H. Functional aspects of primary cilia in signaling, cell cycle and tumorigenesis. *Cilia* **2,** 6 (2013).

39. Hsiao, Y.-C., Tuz, K. & Ferland, R. J. Trafficking in and to the primary cilium. *Cilia* **1,** 4 (2012).

40. Lee, S. H. & Somlo, S. Cyst growth, polycystins, and primary cilia in autosomal dominant polycystic kidney disease. *Kidney Res. Clin. Pract.* **33,** 73–78 (2014).

41. Delling, M., DeCaen, P. G., Doerner, J. F., Febvay, S. & Clapham, D. E. Primary cilia are specialized calcium signalling organelles. *Nature* **504,** 311–314 (2013).

42. Singla, V. & Reiter, J. F. The primary cilium as the cell's antenna: signaling at a sensory organelle. *Science* **313,** 629–633 (2006).

43. Michaud, E. J. & Yoder, B. K. The primary cilium in cell signaling and cancer. *Cancer Res.* **66,** 6463–6467 (2006).

44. Schwartz, E. A., Leonard, M. L., Bizios, R. & Bowser, S. S. Analysis and modeling of the primary cilium bending response to fluid shear. *J. Physiol* 132–138 (1997).

45. Praetorius, H. A. & Spring, K. R. Bending the MDCK cell primary cilium increases intracellular calcium. *J. Membr. Biol.* **184,** 71–79 (2001).

46. Praetorius, H. A. & Spring, K. R. Removal of the MDCK cell primary cilium abolishes flow

sensing. *J. Membr. Biol.* **191,** 69–76 (2003).

47. Nauli, S. M. *et al.* Polycystins 1 and 2 mediate mechanosensation in the primary cilium of kidney cells. *Nat. Genet.* **33,** 129–37 (2003).

48. Yoder, B. K. The Polycystic Kidney Disease Proteins, Polycystin-1, Polycystin-2, Polaris, and Cystin, Are Co-Localized in Renal Cilia. *J. Am. Soc. Nephrol.* **13,** 2508–2516 (2002).

49. Su, S. *et al.* Genetically encoded calcium indicator illuminates calcium dynamics in primary cilia. *Nat. Methods* **10,** 1105–7 (2013).

50. Praetorius, H. A. & Leipziger, J. Primary cilium-dependent sensing of urinary flow and paracrine purinergic signaling. *Semin. Cell Dev. Biol.* **24,** 3–10 (2013).

51. Delling, M. *et al.* Primary cilia are not calcium-responsive mechanosensors. *Nature* **531,** 656–660 (2016).

52. Berbari, N. F., O'Connor, A. K., Haycraft, C. J. & Yoder, B. K. The Primary Cilium as a Complex Signaling Center. *Curr. Biol.* **19,** R526–R535 (2009).

53. Fliegauf, M., Benzing, T. & Omran, H. When cilia go bad: cilia defects and ciliopathies. *Nat. Rev. Mol. Cell Biol.* **8,** 880–93 (2007).

54. Pazour, G. J. *et al.* Chlamydomonas IFT 88 and Its Mouse Homologue , Polycystic Kidney Disease Gene Tg 737 , Are Required for Assembly of Cilia and Flagella. *J. Cell Biol.* **151,** 709–718 (2000).

55. Lehman, J. M. *et al.* The Oak Ridge Polycystic Kidney Mouse: Modeling Ciliopathies of Mice and Men. **10,** 54–56 (2008).

56. Forschbach, V. *et al.* Anoctamin 6 is localized in the primary cilium of renal tubular cells and is involved in apoptosis-dependent cyst lumen formation. *Cell Death Dis.* **6,** e1899 (2015).

57. Ruppersburg, C. C. & Hartzell, H. C. The Ca2+-activated Cl- channel ANO1/TMEM16A regulates primary ciliogenesis. *Mol. Biol. Cell* **25,** 1793–807 (2014).

58. Faria, D. *et al.* The calcium-activated chloride channel Anoctamin 1 contributes to the regulation of renal function. *Kidney Int.* 1369–1381 (2014). doi:10.1038/ki.2013.535

59. Nakai, J., Ohkura, M. & Imoto, K. A high signal-to-noise Ca(2+) probe composed of a single green fluorescent protein. *Nat. Biotechnol.* **19,** 137–41 (2001).

60. Akerboom, J. *et al.* Optimization of a GCaMP Calcium Indicator for Neural Activity Imaging. *J. Neurosci.* **32,** 13819–13840 (2012).

61. Tallini, Y. N. *et al.* Imaging cellular signals in the heart in vivo: Cardiac expression of the high-

signal Ca2+ indicator GCaMP2. *Proc. Natl. Acad. Sci. U. S. A.* **103,** 4753–4758 (2006).

62. Watts, S. D., Suchland, K. L., Amara, S. G. & Ingram, S. L. A sensitive membrane-targeted biosensor for monitoring changes in intracellular chloride in neuronal processes. *PLoS One* **7,** 1–11 (2012).

63. Liu, Y., Fisher, D. a & Storm, D. R. Intracellular sorting of neuromodulin (GAP-43) mutants modified in the membrane targeting domain. *J. Neurosci.* **14,** 5807–5817 (1994).

64. Kleene, N. K. & Kleene, S. J. A method for measuring electrical signals in a primary cilium. *Cilia* **1,** 1 (2012).

65. Decaen, P. G., Delling, M., Vien, T. N. & Clapham, D. E. Direct recording and molecular identification of the calcium channel of primary cilia. *Nature* **504,** 315–318 (2013).

66. Landry, J. J. M. *et al.* The genomic and transcriptomic landscape of a HeLa cell line. *G3 (Bethesda).* **3,** 1213–24 (2013).

67. Thomas, P. & Smart, T. G. HEK293 cell line: A vehicle for the expression of recombinant proteins. *J. Pharmacol. Toxicol. Methods* **51,** 187–200 (2005).

68. Gaush, C. R., Hard, W. L. & Smith, T. F. Characterization of an established line of canine kidney cells (MDCK). *Proc. Soc. Exp. Biol. Med.* **122,** 931–935 (1966).

69. Bodnar, A. G. *et al.* Extension of Life-Span by Introduction of Telomerase into Normal Human Cells. *Science (80-.).* **279,** 349–352 (1998).

70. Felgner, P. L. *et al.* Lipofection: a highly efficient, lipid-mediated DNA-transfection procedure. *Proc. Natl. Acad. Sci. U. S. A.* **84,** 7413–7 (1987).

71. Manuscript, A. Transfection by electroporation. (2010). doi:10.1002/0471142727.mb0903s62.Transfection

72. Sugar, I. P. & Neumann, E. Stochastic model for electric field-induced membrane pores electroporation. *Biophys. Chem.* **19,** 211–225 (1984).

73. Grynkiewicz, G., Poenie, M. & Tsien, R. Y. A new generation of Ca2+ indicators with greatly impoved fluorescence properties. *J. Biol. Chem.* **260,** 3440–3450 (1985).

74. Chao-min, L. & Theron, H. E. Characterization of ionomycin as a calciun ionophore. *J. Biol. Chem.* **253,** 5892–5894 (1978).

75. Ohga, K., Takezawa, R., Arakida, Y., Shimizu, Y. & Ishikawa, J. Characterization of YM-58483/BTP2, a novel store-operated Ca2+ entry blocker, on T cell-mediated immune responses in vivo. *Int. Immunopharmacol.* **8,** 1787–1792 (2008).

76. Seidler, N. W., Jona, I., Vegh, M. & Martonosi, A. Cyclopiazonic acid is a specific inhibitor of the Ca2+-ATPase of sarcoplasmic reticulum. *J. Biol. Chem.* **264,** 17816–17823 (1989).

77. Nguyen, T., Chin, W. C., O'Brien, J. A., Verdugo, P. & Berger, A. J. Intracellular pathways regulating ciliary beating of rat brain ependymal cells. *J. Physiol.* **531,** 131–140 (2001).

78. Merritt, J. E. *et al.* SK&F 96365, a novel inhibitor of receptor-mediated calcium entry. *Biochem. J.* **271,** 515–22 (1990).

79. Várnai, P., Hunyady, L. & Balla, T. STIM and Orai: the long-awaited constituents of store-operated calcium entry. *Trends Pharmacol. Sci.* **30,** 118–128 (2009).

80. Harteneck, C., Frenzel, H. & Kraft, R. A Phospholipase A 2 Inhibitor and TRP Channel Blocker. **25,** 61–75 (2007).

81. Gafni, J. *et al.* Xestospongins: Potent membrane permeable blockers of the inositol 1,4,5-trisphosphate receptor. *Neuron* **19,** 723–733 (1997).

82. Krause, T., Gerbershagen, M. U., Fiege, M., Weisshorn, R. & Wappler, F. Dantrolene – A review of its pharmacology, therapeutic use and new developments. *Anaesthesia* **59,** 364–373 (2004).

83. Fuente, R. D. La & Namkung, W. Small-molecule screen identifies inhibitors of a human intestinal calcium-activated chloride channel. *Mol. Pharmacol.* **73,** 758–768 (2008).

84. Namkung, W., Phuan, P. W. & Verkman, A. S. TMEM16A inhibitors reveal TMEM16A as a minor component of calcium-activated chloride channel conductance in airway and intestinal epithelial cells. *J. Biol. Chem.* **286,** 2365–2374 (2011).

85. Namkung, W., Thiagarajah, J. R., Phuan, P. W. & Verkman, A. S. Inhibition of Ca2+-activated Cl- channels by gallotannins as a possible molecular basis for health benefits of red wine and green tea. *FASEB J.* **154484,** 355–357 (2010).

86. Brailov, I. *et al.* Localization of 5-HT6 receptors at the plasma membrane of neuronal cilia in the rat brain. *Brain Res.* **872,** 271–275 (2000).

87. Schreiber, R. & Kunzelmann, K. Expression of anoctamins in retinal pigment epithelium (RPE). *Pflügers Arch. - Eur. J. Physiol.* **1,** (2016).

88. Suzuki, J. *et al.* Calcium-dependent phospholipid scramblase activity of TMEM16 protein family members. *J. Biol. Chem.* **288,** 13305–16 (2013).

89. Perdiz, D., Mackeh, R., Poüs, C. & Baillet, A. The ins and outs of tubulin acetylation: More than just a post-translational modification? *Cell. Signal.* **23,** 763–771 (2011).

90. Smith, K. Theoretical mechanisms in targeted and random integration of transgene DNA. *Reprod. Nutr. Dev.* **41,** 465–485 (2002).

91. Berbari, N. F., Johnson, A. D., Lewis, J. S., Askwith, C. C. & Mykytyn, K. Identification of Ciliary Localization Sequences within the Third Intracellular Loop of G Protein-coupled Receptors. *Mol. Biol. Cell* **19,** 308–317 (2007).

92. Song, M., Chen, D. & Yu, S. P. The TRPC channel blocker SKF 96365 inhibits glioblastoma cell growth by enhancing reverse mode of the Na^{+}/Ca^{2+} exchanger and increasing intracellular Ca^{2+}. *Br. J. Pharmacol.* **171,** 3432–3447 (2014).

93. Alkhani, H. *et al.* Contribution of TRPC3 to store-operated calcium entry and inflammatory transductions in primary nociceptors. *Mol. Pain* **10,** 43 (2014).

APPENDICES

Appendix I – Killing curve

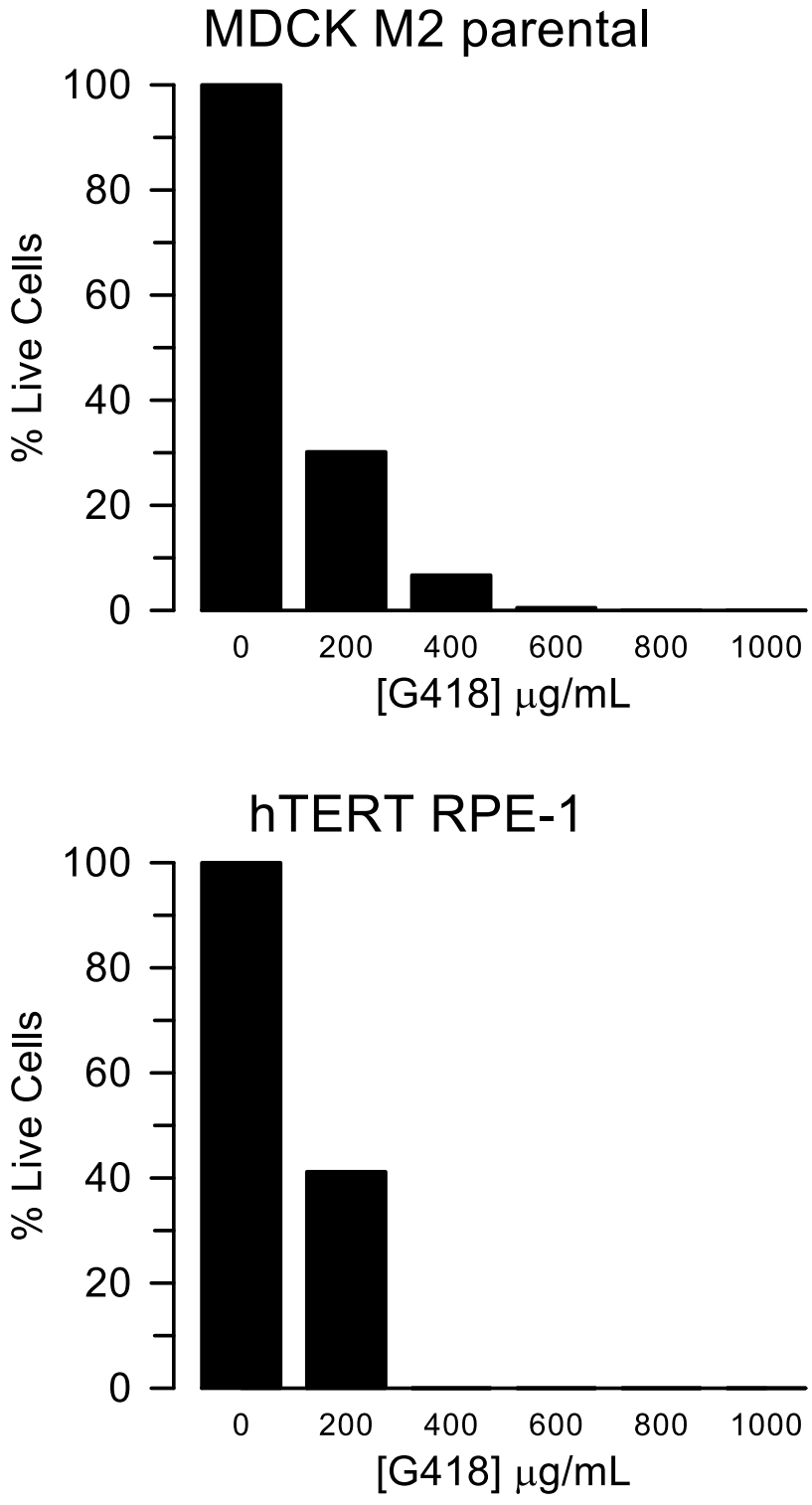

Figure A I – Antibiotic killing curve from MDCK M2 parental and hTERT RPE-1 cells. The concentration of the antibiotic G-418 ([G-418]) was varied from 0 to 1000 μg/mL and the % of live cells was counted with trypan blue exclusion, after ~10d of exposure to selective media.

Appendix II – Transfection Efficiency

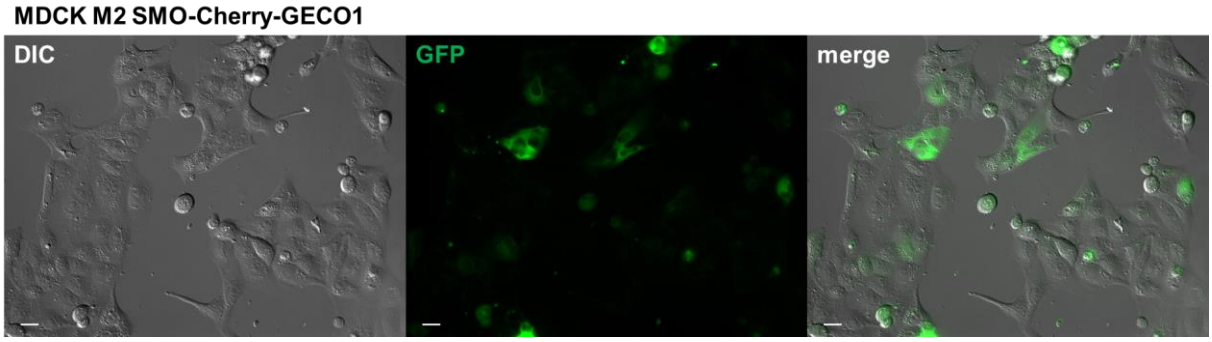

Figure A II – Live cell imaging after 1d of SMO-Cherry-GECO1 transfection on MDCK M2 cells by electroporation. From left to right: Differential Interference Contrast (DIC) image, GFP fluorescence from the GECO sensor and merged pictures. Bars indicate 20 µm.

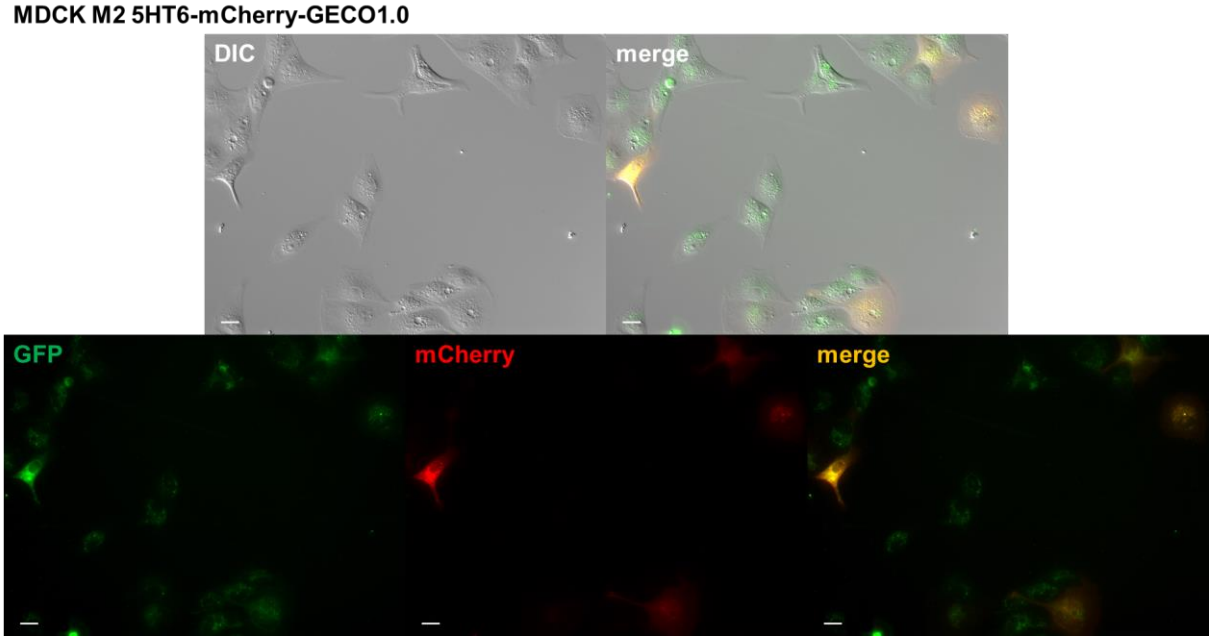

Figure A III – Live cell imaging after 1d of 5HT6-mCherry-GECO1.0 transfection on MDCK M2 cells by electroporation. Upper panels: Differential Interference Contrast (DIC) image and merged images. Lower panels, from left to right: GFP fluorescence from the GECO sensor, fluorescence from mCherry ciliary marker and merged fluorescence channels. Bars indicate 20 µm.

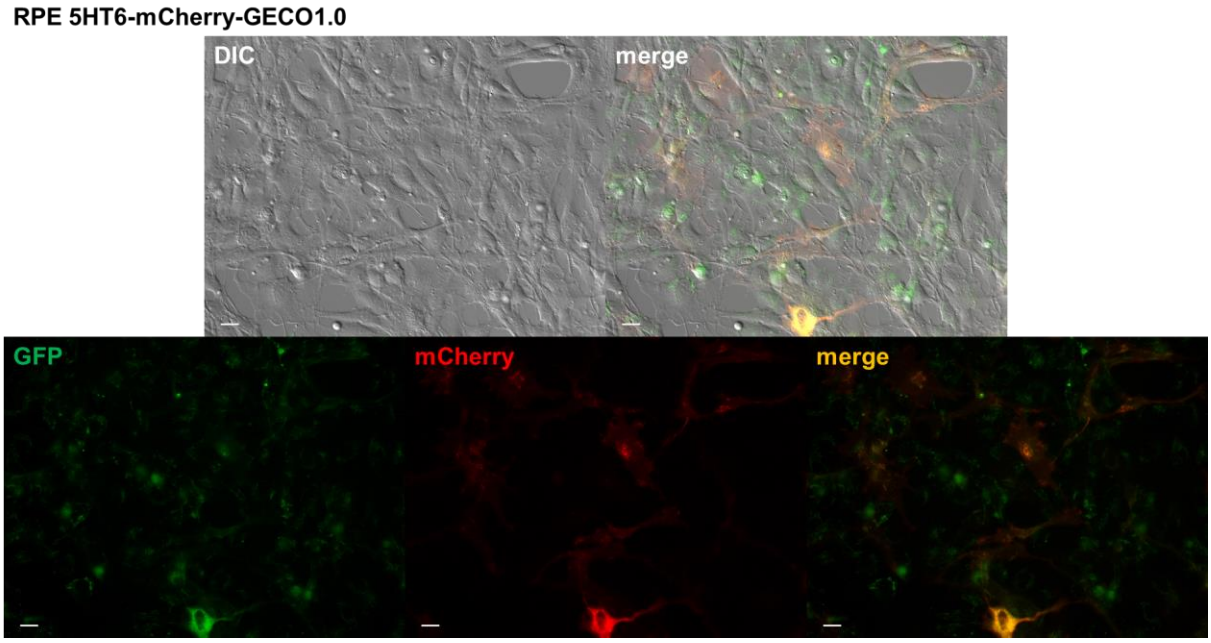

Figure A IV – Live cell imaging after 1d of 5HT6-mCherry-GECO1.0 transfection on RPE cells by electroporation. Upper panels: Differential Interference Contrast (DIC) image and merged images. Lower panels, from left to right: GFP fluorescence from the GECO sensor, fluorescence from mCherry ciliary marker and merged fluorescence channels. Bars indicate 20 µm.

Appendix III – cDNA plasmids

Table A I – List of cDNA plasmids used. Accession number (no.) and plasmid size in base pairs (bp).

Target	Accession no.	Size (bp)
ANO1	NM_018043.5	4811
ANO4	NM_001286615.1	4247
CD8	NM_001145873.1	3177
$P2Y_2$	NM_002564.3	8602
Ist2	NM_001178434.1	2841

Appendix IV – Absorbance measurements of the inhibitors

Fluorescein in -Bic Ringer

#	Sample ID	Date and Time	1 (nm)	1 (Abs)	2 (nm)	2 (Abs)	3 (nm)	3 (Abs)	4 (nm)	4 (Abs)	5 (nm)	5 (Abs)
13	Fluorescein 1	28.07.2016 17:23:44	485	1,032	405	0,592	206	1,779	340	0,793	380	0,553

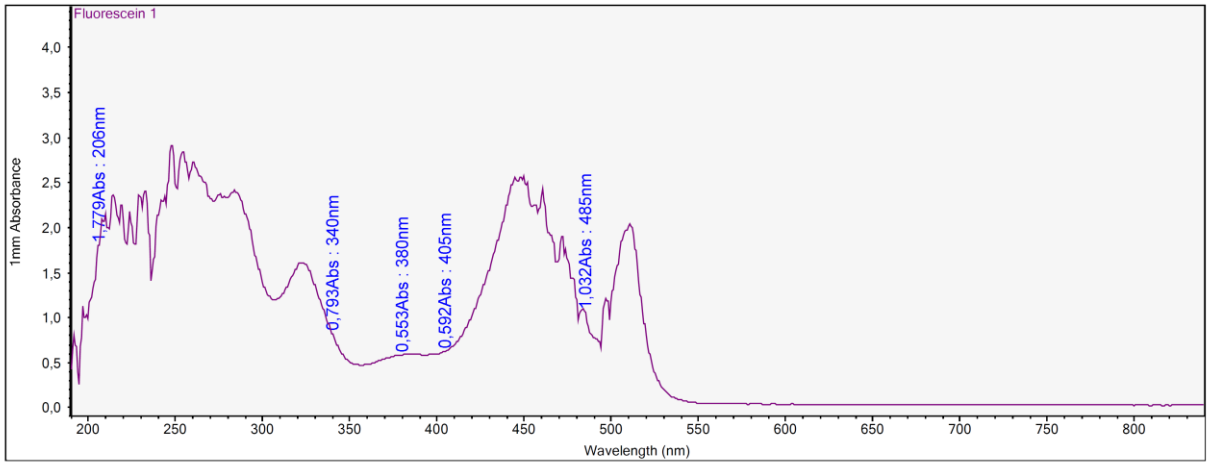

Figure A V – Representative absorbance measurement from fluorescein. This compound has an absorbance peak at ~450 nm, close to the GFP excitation wavelength (485 nm), absorbing at other wavelengths as well. Fluorescein served as a positive control for the absorbance measurements.

- Bic Ringer

#	Sample ID	Date and Time	1 (nm)	1 (Abs)	2 (nm)	2 (Abs)	3 (nm)	3 (Abs)	4 (nm)	4 (Abs)	5 (nm)	5 (Abs)
1	-Bic Ringer 1	21.07.2016 10:21:19	485	0,011	405	0,015	206	0,078				

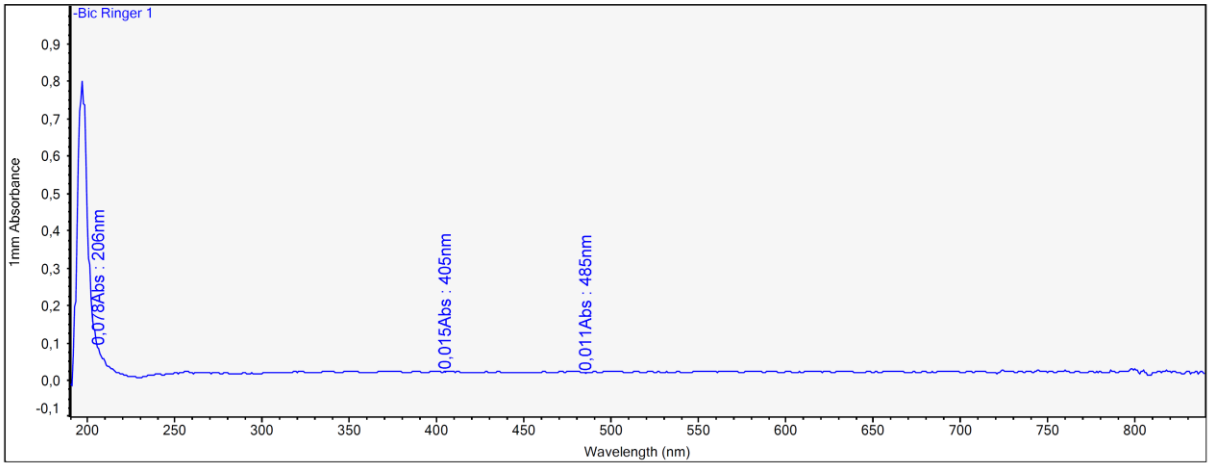

Figure A VI – Representative absorbance measurement from Ringer buffer solution. The buffer does not absorb at any wavelength used in the Ca^{2+} measurements (GFP is excited at 485 nm and Fura-2 at 340/380 nm), functioning as a negative control for the absorbance measurements.

SKF in -Bic Ringer

#	Sample ID	Date and Time	1 (nm)	1 (Abs)	2 (nm)	2 (Abs)	3 (nm)	3 (Abs)	4 (nm)	4 (Abs)	5 (nm)	5 (Abs)
4	SK&F 1	21.07.2016 10:33:13	485	0,015	405	0,017	206	0,107				

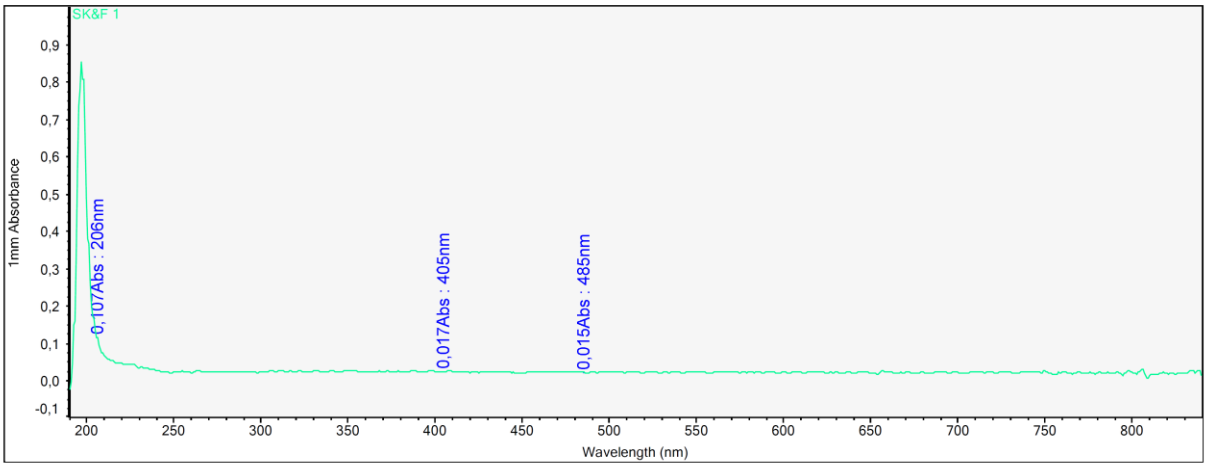

Figure A VII – Representative absorbance measurement from SKF. The inhibitor does not absorb at any wavelength used in the Ca^{2+} measurements (GFP is excited at 485 nm and Fura-2 at 340/380 nm).

ACA in -Bic Ringer

#	Sample ID	Date and Time	1 (nm)	1 (Abs)	2 (nm)	2 (Abs)	3 (nm)	3 (Abs)	4 (nm)	4 (Abs)	5 (nm)	5 (Abs)
8	ACA 1	21.07.2016 10:36:09	485	0,005	405	0,008	206	1,379				

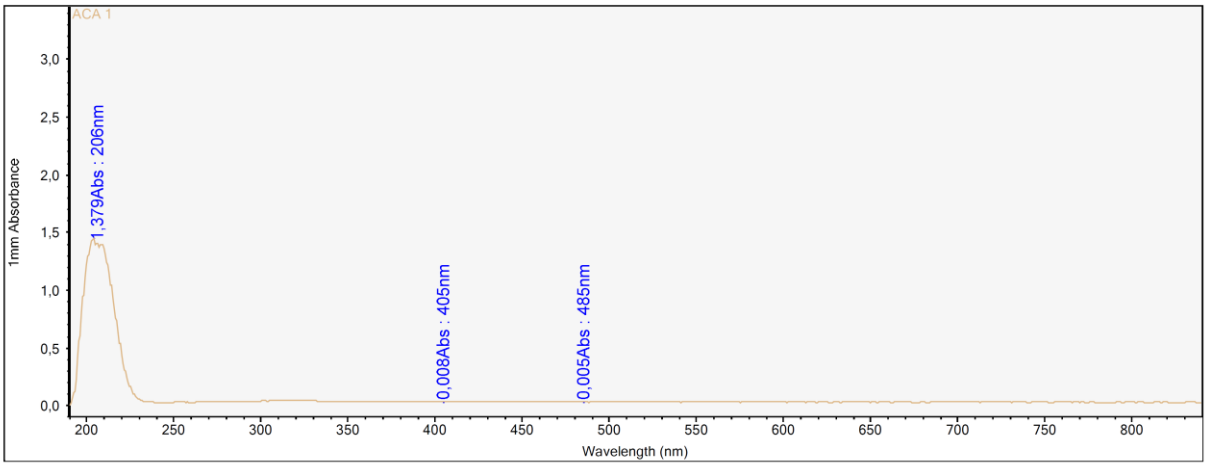

Figure A VIII – Representative absorbance measurement from ACA. The inhibitor does not absorb at any wavelength used in the Ca^{2+} measurements (GFP is excited at 485 nm and Fura-2 at 340/380 nm).

Dantrolene in -Bic Ringer

#	Sample ID	Date and Time	1 (nm)	1 (Abs)	2 (nm)	2 (Abs)	3 (nm)	3 (Abs)	4 (nm)	4 (Abs)	5 (nm)	5 (Abs)
16	Dantrolene 1	04.08.2016 17:47:14	485	0,012	405	0,028	206	1,364	340	0,021	380	0,030

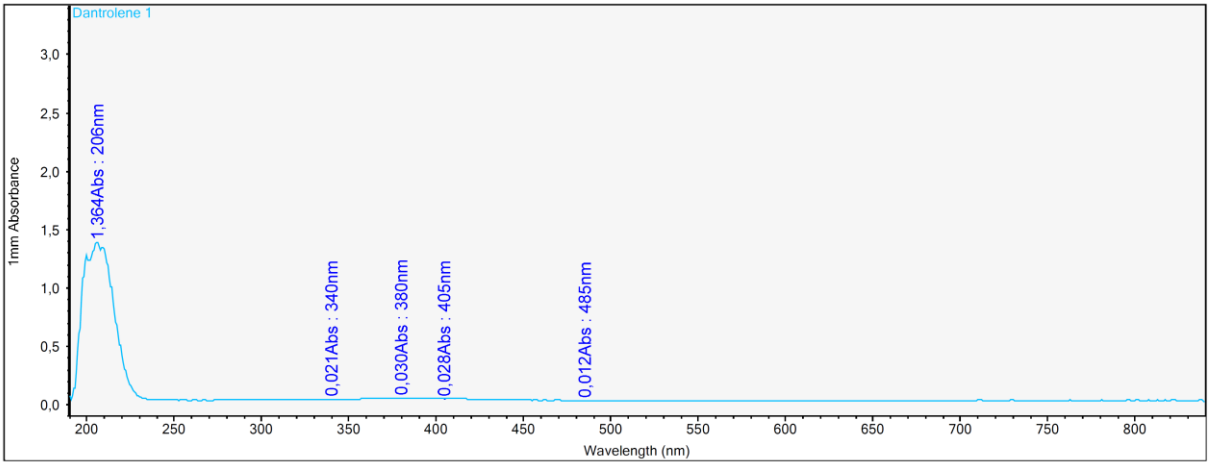

Figure A IX – Representative absorbance measurement from dantrolene. The inhibitor does not absorb at any wavelength used in the Ca^{2+} measurements (GFP is excited at 485 nm and Fura-2 at 340/380 nm).

CaCC-AO1 in -Bic Ringer

#	Sample ID	Date and Time	1 (nm)	1 (Abs)	2 (nm)	2 (Abs)	3 (nm)	3 (Abs)	4 (nm)	4 (Abs)
13	CaCC-AO1	11.05.2016 10:48:01	485	0,001	405	0,001	206	0,280		

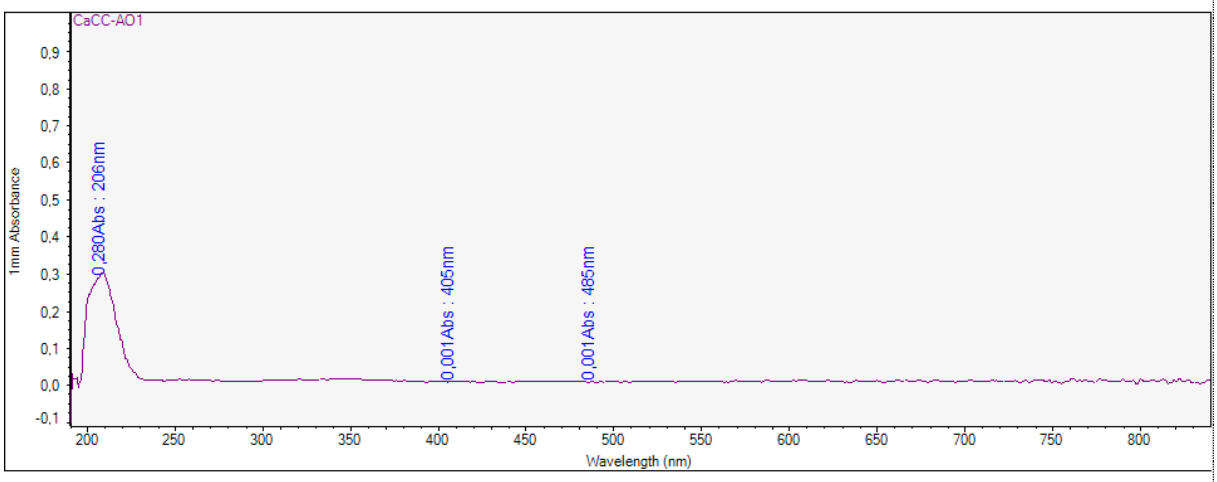

Figure A X – Representative absorbance measurement from CaCC-A01. The inhibitor does not absorb at any wavelength used in the Ca^{2+} measurements (GFP is excited at 485 nm and Fura-2 at 340/380 nm).